A Prototype Diamond Amplified Photocathode

A Thesis Presented

by

Jacob T. Grimes

to

The Graduate School

in Partial Fulfillment of the Requirements

for the Degree of

Master of Science

in

Physics & Astronomy

(Scientific Instrumentation)

Stony Brook University

May 2007

Stony Brook University

The Graduate School

Jacob T. Grimes

We, the Thesis committee for the above candidate for the Master of Science degree, hereby recommend acceptance of the Thesis.

Ilan Ben-Zvi

Adjunct Professor, Department of Physics & Astronomy, Stony Brook University

---

Peter Paul

Professor, Department of Physics & Astronomy, Stony Brook University

---

Vladimir J. Goldman

Professor, Department of Physics & Astronomy, Stony Brook University

---

Robert L. McCarthy

Professor, Department of Physics & Astronomy, Stony Brook University

This Thesis is accepted by the Graduate School.

Dean of the Graduate School

Abstract of the Thesis

A Prototype Diamond Amplified Photocathode

by

Jacob T. Grimes

Master of Science

in

Physics & Astronomy

Stony Brook University

2007

The purpose of this report is to detail the steps involved in the construction and testing as well as the theoretical underpinnings of a Diamond Amplified Photocapsule. The DAP Injector is intended as a high brightness low emittance electron source. The version discussed here is the direct current prototype of a device that will eventually be the electron source for the new 703.75 MHz Superconducting Energy Recovering LINAC(ERL) at Brookhaven National Lab. While this device does not incorporate all of the design requirements of later injectors, it does act as a stage on which many of the construction steps, and the order in which they must occur, may be tested.

The basic concept behind the DAP injector is that we construct a self contained, ultra-high-vacuum capsule that uses a low average power laser or other light source to generate a high brightness low emittance electron pulse beam. A diagram showing the major components and describing the operation of the DAP is shown in Fig. 1.1. There are two stages in this capsule. The first stage is a photocathode that is stimulated by a light source to emit electrons. The electrons are accelerated by a high

voltage potential to the second stage. This stage is where the amplification occurs via secondary emission. The electron-hole pairs are separated by an electric field of approximately 1 MV/m, or greater, and the electrons are induced to drift through the second stage and are emitted into vacuum. These two stages are the faces of the vacuum capsule. This new type of compound photo-injector introduces the use of a diamond window that will act as the amplifier. Depending on the type of diamond used and the input or primary current energy, as well as other mitigating factors, the capsule output can be hundreds of times greater than the primary current generated at the photo cathode.

To Allison, Ayden & Preston

Contents

List of Figures

List of Tables

Acknowledgements

First, I would like to thank the members of the e-cooling group; Ilan, Triveni, Chang, John, Qiong Wu, Ranjan, Rob, Andrew, and lasts but certainly not least Dave. Through council and direction each of you have made this project possible. I would not have completed it with out your help.

To my advisor, Ilan Ben-Zvi, thank you for giving me such an incredible opportunity. Your patience and guidance has been instrumental in my education. Thank you for spending hours answering my questions, setting straight my misperceptions, and helping me see deeper into the world around us. Most importantly, thank you for giving me the time and freedom to be both a father and a graduate student.

To Chang and Qiong Wu, thank you for helping me to see the system and results for what they were. Especially to Chang, many thanks for your thoughtful analysis of the data and help in making sense of the results. You have both shown me that there is a lot more to learn.

To Dave Pate, truly, without you I would have never finished. Thank you for filling all of my last minute orders, teaching me how to navigate the system (sort of), and most of all reminding me that I need to keep focused. It has been a pleasure working closely with you, one that I shall miss greatly. Keep flying.

I would also like to thank everyone at the Stony Brook University Physics Department. To all of 'The First Years (04)', you have made it a memorable experience. To Eman, Glen, Jim, Kevin, Steve, Jason, Jet, Katy, Luigi, Doug, Rob, Jen, Sue, Jan, Itai, Stewie, and others; I'll see you at the Ice Bar.

Pat Peiliker, thanks for being a 'Momma Bear' to all the grads. Your guidance and sometime stern hand has helped many through. I will miss our little visits.

Finally, I would like to thank my family. To my lovely and talented wife, you diverted your dream for a year to let me carry on with mine. When I did not finish in time, you gave me more, and took on an even greater burden, raising our son and

attending medical school simultaneously. I am awed by your strength and honored to call you wife. Thank you so much for standing by and supporting me through this trial.

To Noni and Mimi, thank you for helping Alley carry her burden. Without you she would not have made it, and neither would I. The debt of gratitude that I owe you both is deep. Because of you, Ayden has gotten all the love he needs, and then some, in this stressful time. You are both amazing, and I cannot say how thankful I am that you are in my life.

To my mom, thank you for your kind words and support through these last years. I'm glad that we are becoming closer again. It has been too long coming. It's really nice to know that I make you proud.

Dad and Cynthia, thank you for pushing me and providing support through undergrad and beyond. I would not have made it this far with out you. Thank your for helping me come home to Texas on numerous occasions. I might have lost my mind otherwise. Dad, lets go surfing.

To all the others I have neglected to mention, it is impossible to list all the many hands that have carried me on this journey in such a small space. Know that you are remembered with gratitude. Thank you for your support and kindness.

Two of the graphs, Fig. 2.3 and Fig. 2.4, presented in this thesis are used under permission from Newport Oriel Corporation. Permission to use these images was specifically granted by Chris Ball and Nancy Fernandes as representatives of Newport.

Jacob Grimes, Stony Brook University, May 2007

Chapter 1

Introduction

The purpose of this report is to detail the steps involved in the construction and testing, as well as the theoretical underpinnings, of a Diamond Amplified Photocapsule. The DAP Injector is intended as a high brightness low emittance electron source. The version discussed here is the direct current prototype of a device that will eventually be the electron source for the new 703.75 MHz Superconducting Energy Recovering LINAC(ERL) at Brookhaven National Lab. While this device does not incorporate all of the design requirements of later injectors, it does act as a stage on which many of the construction steps, and the order in which they must occur, may be tested.

The basic concept behind the DAP injector is that we construct a self contained, ultra-high-vacuum capsule that uses a low average power laser or other light source to generate a high brightness low emittance electron pulse beam. A diagram showing the major components and describing the operation of the DAP is shown in Fig. 1.1. There are two stages in this capsule. The first stage is a photocathode that is stimulated by a light source to emit electrons. The electrons are accelerated by a high voltage potential to the second stage. This stage is where the amplification occurs via secondary emission. The electron-hole pairs are separated by an electric field of approximately 1 MV/m, or greater, and the electrons are induced to drift through the second stage and are emitted into vacuum. These two stages are the faces of the vacuum capsule. This new type of compound photo-injector introduces the use of

a diamond window that will act as the amplifier. The mechanism of its operation will be discussed in greater detail later. Depending on the type of diamond used and the input or primary current energy, as well as other mitigating factors, the capsule output can be hundreds of times greater than the primary current generated at the photo cathode.

1.1 Organization

The remainder of this report will be broken into four chapters. Each of the chapters encompasses a major part of the capsule development. The following is a brief description of what each chapter covers.

1.1.1 Chapter 2: Theoretical Details

The major concepts underlying the capsule functioning are discussed in this chapter. First, the functioning of the diamond as an amplifier is explored along with the hydrogenated surface and its relationship to negative electron affinity and how that influences emission into vacuum. Next, the capsule design is discussed. This area covers the specific elements involved as well as the choice of materials and relevant dimensions. Then, the light source used to stimulate photoemission is introduced. This leads to a discussion of the photocathode quantum efficiency and how it may be improved, as well as an approximation of the capsule quantum yield. Finally, the space charge limitations of the DAP are calculated for various configurations as well as inside the diamond and between the diamond and anode.

1.1.2 Chapter 3: Experiment/Procedure

In this chapter the apparatus and methodology will be examined. First, the two vacuum chambers that are used to assemble the various parts of the DAP are described. Following this is a detailed look at the Diamond Electrical Contact Assembly. This

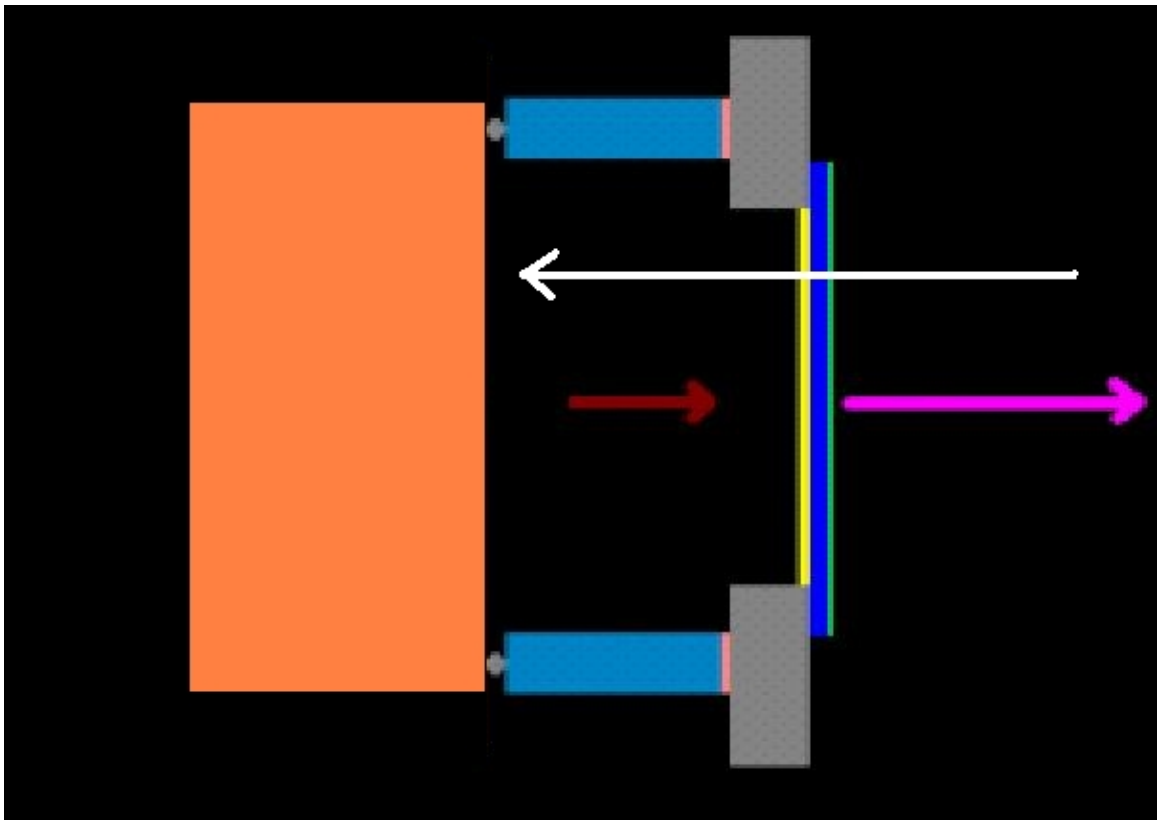

Figure 1.1: Diagram of DAP Injector Functioning - Light(white arrow) passes through a diamond window and into the DAP where it is incident on the photocathode(orange) surface. The incident light stimulates photoemission of electrons from the PC surface. The photoemitted primary electrons(red arrow) are accelerated by an electric field and pass through a metal coating on the diamond(blue). Inside the diamond the primary electrons lose their energy to the creation of secondary electrons. The secondaries drift through the diamond and are emitted into vacuum(pink arrow) where they are accelerated.

includes descriptions of all the mechanical and chemical procedures used in the manufacture and preparation of each of the DECA elements. Next, the preparation of a photocathode for photoemission will be discussed. Lastly, the specific testing and assembly procedure for the DAP injector will be described. This includes surface cleaning and photoemission measurement of the PC, as well as the final assembly and emission testing of the capsule in both open and closed configurations.

1.1.3 Chapter 4: Characterization of DAP Injector

The focus of this chapter is the emission testing of the photocathode and capsule. The first section covers the collection and handling of data. Of specific importance are methods for dealing with the integration and conversion of pulses. Additional methods for smoothing and noise reduction are covered. Several sections are given to a discussion of background noise and the effects of EMI in the system. Once all issues with noise and EMI are resolved, possible sources of pressure increases in Capsule Assembly Chamber are discussed. Next, the emission signature from an unobscured photocathode is measured across the range of pulse energies and anode voltages. These data will serve to verify the correct, uniform operation of the photocathode. Following the photoemission measurements, the preparation of the specific DECA used for measurement will be discussed. Insertion of the DECA into the CAC brings the need for a reduction of Diamond Photo-Emission and an investigation of the residual DPE to be subtracted from the gain emission signal. With the residual DPE characterized, we move on to test the secondary emission properties of the DAP. This includes an examination of the gain profile as function of field in diamond. Finally, the amplified emission from a closed DAP injector is measured.

1.1.4 Chapter 5: Conclusion

In this final chapter the results of the experiment are discussed. The primary focus will be the successful construction and operation of a prototype DAP injector. There

will also be some discussion of error and anomalies that were observed in the system. Finally, suggestions for improvements in the DAP and CAC are presented.

Chapter 2

Theoretical Details

The DAP injector is a device that takes a low power laser input and converts it into a high brightness, high average power electron beam. In this chapter the physical concepts that govern the inner workings of the capsule are discussed, as well as the design features and the materials of which it is comprised.

2.1 Diamond as an Amplifier

The DAP injector utilizes a diamond wafer as a secondary amplification stage, as in Fig. 2.1. Amplification occurs when electrons that have many times the 5.5 eV diamond band gap energy are incident on the surface of a high purity sample. The energetic electrons pass into the diamond and in approximately the first thirty nanometers lose the majority of their energy through scattering interactions and the formation of many electron hole pairs.[1] An electric field of approximately 1 MV/m is maintained in the diamond by a high voltage potential between an external anode and a metalization layer that has been deposited on the side of the diamond on which the energetic electrons are incident. The newly formed electron hole pairs are separated by the field and the holes recombine with electrons from the metalization layer. The extra electrons are induced to drift through the diamond toward the other surface of the diamond, where the crystal lattice has been hydrogen terminated.

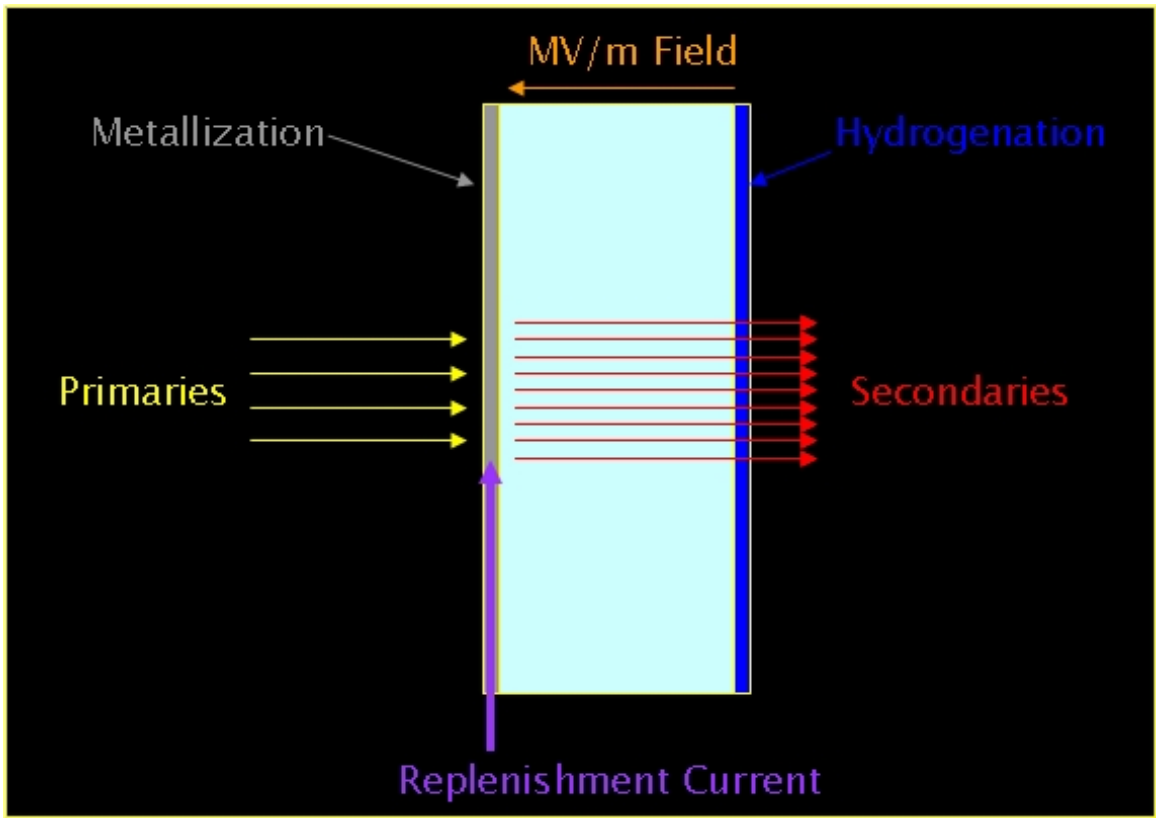

Figure 2.1: Mechanism of Amplification in Diamond - Energetic primary electrons are incident on the diamond surface. They pass into the diamond and generate many electron hole pairs. The e-h pairs are separated by an electric field maintained in the diamond. The electrons are induced to drift through the diamond toward the other surface, which is hydrogen terminated, where they are emitted into vacuum.

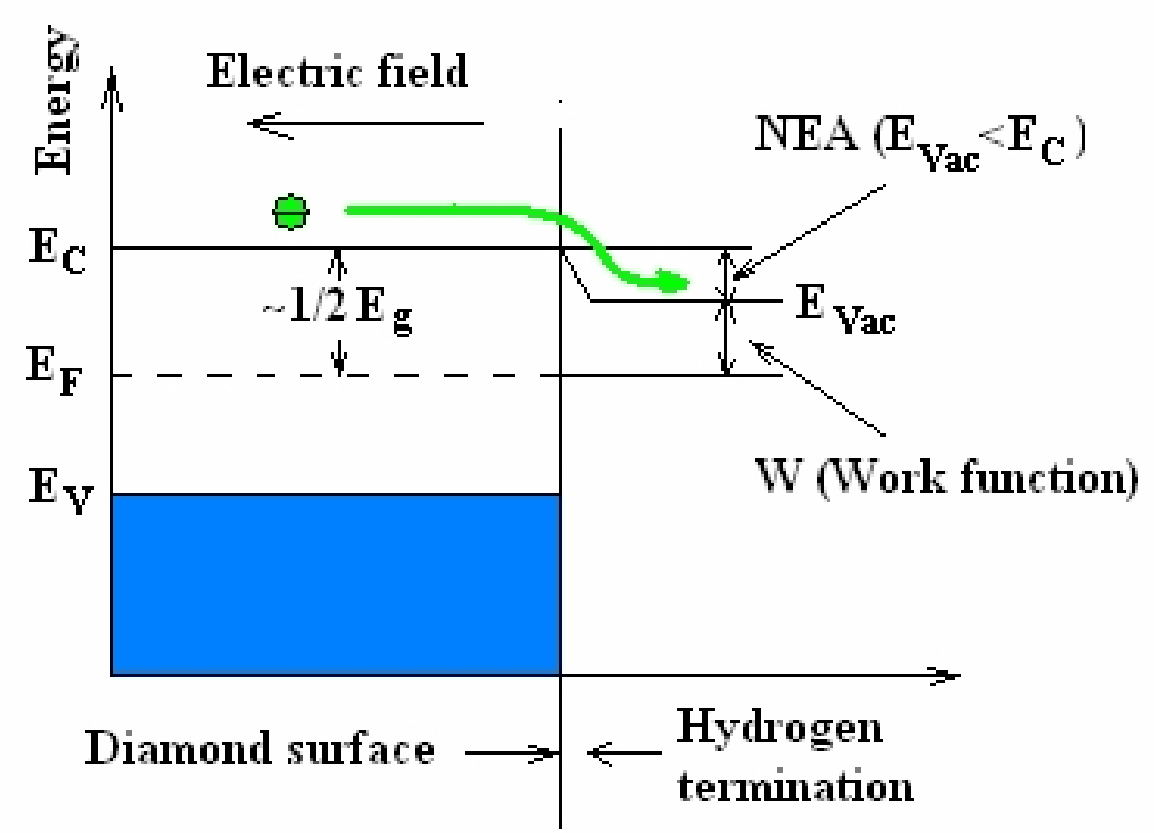

Figure 2.2: Negative Electron Affinity in a Hydrogen Terminated Diamond[14]

2.2 The Hydrogenated Diamond Surface and Negative Electron Affinity

The hydrogen termination of the diamond surface serves two purposes. First it allows the electrons to flow more freely into the vacuum. This is accomplished by lowering the surface energy level so that is closer to the vacuum level. The conduction band of a hydrogen terminated diamond sits ~0.7eV above the vacuum level. This allows electrons to flow more easily into the vacuum, Fig. 2.2. Secondly, it creates a stable surface that does not readily degrade when exposed to atmosphere. The hydrogen terminated surface can withstand annealing up to 1000℃ before desorption and relaxation occur.[5][12]

2.3 Capsule Design

The photo-injector capsule design is highly influenced by the choice of materials involved and how they may be machined or formed. The particular materials used will be discussed in the next section. There are, however, other characteristics that will determine, in a more general fashion, the elements that are necessary in the capsule.

Since the construction of the capsule is but one facet of a much larger project, it is necessary to mesh this research with both previous and on-going work. For instance, in work conducted by Chang et al.[2], the diamond types and dimensions have varied greatly, but there is a general push toward standardization of the diamond samples. For initial experiments the less expensive 1cm diameter electronic grade diamond is used. This allows for a large central diameter of minimum 7mm to be used as the target for primary electrons. This central diameter will be extended to the rest of the capsule and become the minimum inner diameter of other components. In later experiments the inner diameter will be as large as 1.2cm, but the same handling techniques will be applied.

The diamond amplification layer properties determine other necessary elements of the capsule. In order to replace the electrons used in amplification, there is a current replenishment layer that consists of a metal film deposited on one of the diamond faces. Current must be supplied to this metal film by a conduction layer with which it will be in direct contact. Additionally, the diamond will need some form of structure that will hold it in place and act as a rigid support during polishing and manipulation. The capsule inner diameter will be a required dimension in this conduction and support layer. Therefore, it must be in the form of a washer.

In previous experiments the primary electrons were supplied by a DC mode electron gun[2]. Since we are interested in producing a self contained capsule, it is necessary to incorporate an emission source. This work represents the first instance of a photocathode, which is one required item, being used to supply electrons. In order

to accelerate the electrons emitted by this photocathode there must be a high electrical potential between the photocathode and the metal layer. To support this high potential, an electrical insulating layer is necessary to act as a standoff between the two metal layers. This layer will also be subject to the inner diameter dimension of 7mm, necessarily making this layer also a washer.

2.4 Materials Selection

As has been shown, there are four major components to the photocapsule. They are the diamond that acts as the secondary amplification layer, a conduction and support layer, an insulation layer, and the photocathode. The materials selected to be used for each layer must meet specific criteria particular to their functioning. Additional layers are employed for the joining of these materials.

2.4.1 Diamond Dimensions

Diamond is the material of primary importance that informs the selection of all other materials. The diamond samples to be used are of two outer diameter sizes 5mm and 10mm. For the purposes of this report, the 10mm sample will be the focus of the discussion to avoid any confusion in dimensioning. The 5mm samples are handled in the same fashion but generate smaller dimensions for other capsule elements. For this particular device, which uses greater than 1μs pulse durations and is effectively a DC emitter, the wafer is much thicker than what will be used in later pulsed mode applications. Samples come in a range of thicknesses between 150μm and 300μm, with the largest portion of those used being approximately 160μm thick.

2.4.2 Conduction and Support Layer

Since the capsule is to be the source for a superconducting gun, it will need to withstand being cryo-cycled at least once. Additionally, it will be subjected, in part or

whole, to extreme thermal cycling during manufacture. Therefore, any material that is to be joined to the diamond must have a coefficient of thermal expansion that is close to that of diamond and will therefore introduce a minimum of stress into the system. Furthermore, any material directly joined to the diamond must have good thermal and electrical conductivity as it will be both the path by which current is delivered and heat is removed. Table 2.1 shows the thermal and electrical properties of various materials that were considered. While silicon and sapphire have thermal expansion values that are closer to that of diamond than other materials, they are poor electrical conductors and are not able to provide the necessary replenishment current. Gold and copper have similar flaws in that they are excellent conductors of both heat and current but poor matches in thermal expansion. After reviewing the properties of several materials, we find that high purity RRR niobium, having a thermal expansion coefficient of 7.3μm/K compared to diamonds 1.8μm/K (@300 K), is the closest match among the electrically conducting materials. This will warrant extra care in the preparation of samples to ensure that diamond samples are not cracked or excessively stressed. In addition to the afore mentioned properties, niobium has superior corrosion resistance. It is also the best choice for joining to the gun as it is made from niobium.

Material	Electrical Conductivity $\Omega^{-1} \cdot m^{-1}$	Thermal Conductivity $\frac{W}{m \cdot K}$	Thermal Expansion $\frac{\mu m}{K}$
Diamond	N/A	2000-2500	1.8
Niobium	$6.57 \cdot 10^6$	53.7	7.3
Copper	$5.95 \cdot 10^7$	401	16.5
Titanium	$2.38 \cdot 10^6$	21.9	8.6
Gold	$4.55 \cdot 10^6$	318	14.2
Silicon	$1.56 \cdot 10^{-3}$	149	2.6
Sapphire	$1 \cdot 10^{-14}$	40	5.8

Table 2.1: Properties of Possible Conduction and Support Layer Materials

2.4.3 Insulation Layer

The insulation layer acts as both a thermal pathway and an electrical standoff. Therefore, an appropriate insulating material must be able to conduct heat away from the conduction and support layer. Since a potential of approximately 5 KV is required to accelerate electrons, the dielectric strength must be high. Additionally, the insulating material must be machinable or formable into a washer shape to allow a clear path for electrons through the chamber. Sapphire meets all of the above criterion. It has a dielectric strength of 480 KV/cm, so even a millimeter thick wafer will easily standoff the necessary 5 KV. Sapphire will also effectively conduct heat from the niobium and diamond layers. It has a thermal conductivity of approximately 40 W/m·K averaged across both the c-axis and a-axis. The thermal expansion of sapphire also closely matches that of niobium(Table 2.1), to which it will be directly joined.

2.4.4 Photocathode

There are a variety of materials that would serve well as the photocathode in this system. There are several criteria that are used to determine exactly which material is used. Of the main considerations, ease of surface preparation and machineability stand out. It is also important that the material be available in a high purity form and that it is a well characterized photo-emitter.

Of the many options, Oxygen Free Copper is the candidate that will be used as the photocathode in this system. OFC is a high purity material that is easily machinable. It also is easily polished to a mirror-like finish. Additionally, it is one of the most often used photocathode materials; therefore, there is ample data on it's photoemission characteristics and detailed information on how the quantum efficiency of a sample may be increased.

2.4.5 Joining Materials

The properties of the specific joining materials used to construct the capsule are defined by the layers they form joints between. To create a vacuum tight bond between a diamond and a refractory metal such as niobium, an active metal braze alloy is required. The results of a previous investigation[4] show that Ticusil® is an appropriate material for creating vacuum tight joints at both the Nb/diamond and Nb/sapphire interfaces.

2.5 Light Source

Photoemission of electrons from a copper photocathode requires a light source that operates in the UV. In order to generate the amount of charge that will result in the production of sufficient numbers of primary and secondary electrons as to be easily measurable, the light source must have a significant amount of power in the UV. A pulsed laser operating at 266nm would be ideal, allowing for study of the temporal response profile. Unfortunately, safety constraints place limits on the types of lasers that may be used in this experiment to class III-A or less. Lasers of this classification do not deliver the power required to stimulate sufficient photoemission to generate observable secondary emission. Therefore, another option must be considered.

The Oriel Xe flash lamp, depending on configuration, provides up to 5 Joules of light energy per pulse with an average power output of 60W. The pulse frequency, which is variable from 1Hz to 75Hz, is related to the pulse energy such that $PulseEnergy(J) \cdot PulseFrequency(Hz) \leq 60W$. The Xe flash lamp has an extremely broad spectral distribution, as is evident in Fig. 2.3. This reduces the amount of power available in the UV, making it a small fraction of the total power of the lamp. Still there is a significant amount of power available for photoemission. This is even a benefit as the total amount of light energy in the UV requires only limited safety measures, in the form of shielding and UV blocking goggles, when compared to lasers

that generate similar power. The flash lamp also produces significantly more power in the UV than similar Xe light sources that operate continuously. Additionally, the pulse shape generated by the flash lamp, Figure 2.4 will serve as a marker by which to identify the primary photoemission and secondary emission signals.

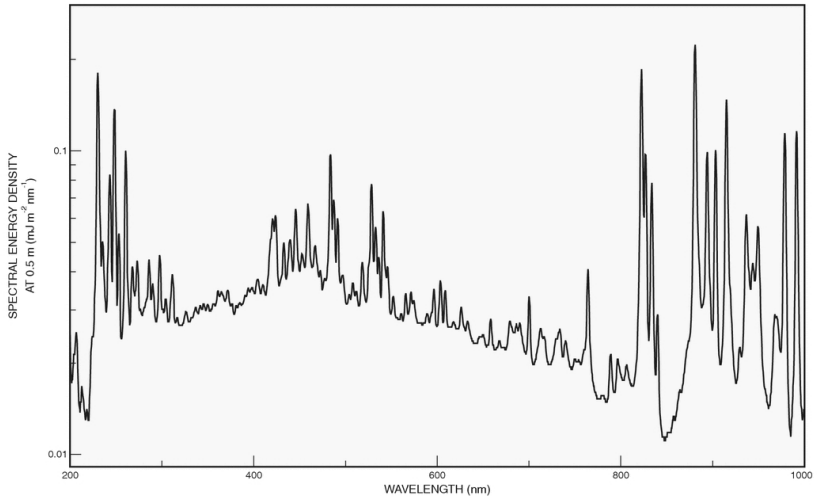

Figure 2.3: Xe Light Source Spectral Irradiance - The energy output for each wavelength is approximated from this graph[9]. The wavelengths of interest are between 200nm and 300nm, at the far left of the graph.

2.6 Photocathode Quantum Efficiency

The quantum efficiency(η) of a photocathode is a ratio of the number of electrons emitted to the number of incident photons. This idea can be used to determine the potential output of the photocathode based on the amount of energy delivered form the light source chosen. It can also be extended, by taking into account various other parameters of the system, to provide a predicted pulse charge yield from the capsule. In this section the Q.E. of the photocathode, and how it can be improved, will be discussed.

According to the literature, the Q.E. of a polished copper photocathode is in the

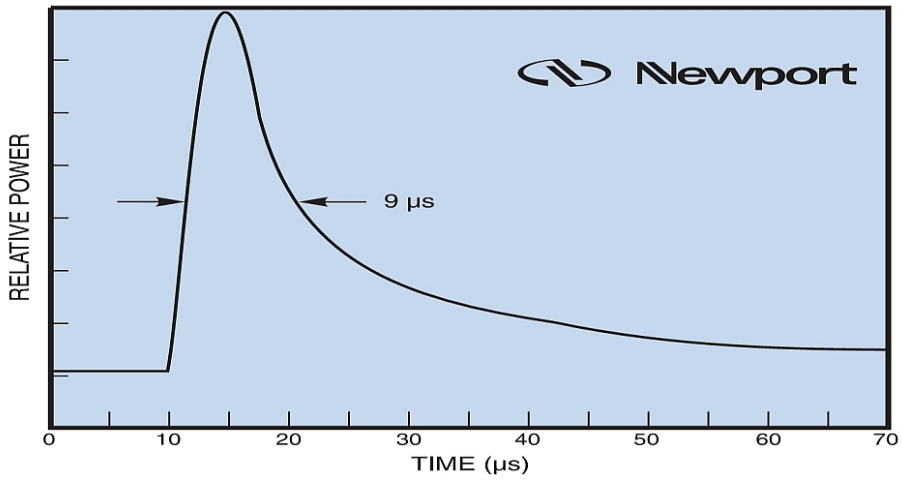

Figure 2.4: Xe Light Source Pulse Shape - This is the characteristic Pulse Shape generated by the Oriel Xe Flash Lamp with a 5 Joule Bulb. This pulse shape will serve as a marker by which to identify the primary and secondary output of the photo-injector capsule.[9]

range of 10^{-6}. This can be improved by up to two orders of magnitude through various cleaning procedures, such as argon ion bombardment, hydrogen etching, or laser cleaning. All of these are effective, and can increase the Q.E. of a copper photocathode by up to two orders of magnitude. While these methods are useful, they require complicated systems of their own, are difficult to integrate, and suffer from various safety requirements. A far simpler method is suggested by Palmer et. al.[8] By heating the photocathode and annealing it at approximately 230℃ for 1.5 hours, quantum efficiencies of up to $1.6\text{x}10^{-4}$ can be obtained. This is one of the methods that will be the method attempted to increase the Q.E. of the photocathode.

2.7 Capsule Quantum Yield

Drawing on the two sections above(§2.5 and §2.6), the output of the photocathode is approximated by summing the photoelectron yield over all relevant wavelengths generated by the light source. The range of relevant wavelengths is delimited by

two factors, the work function of copper and the UV transmission of metal coated diamond. Polycrystalline copper begins to emit electrons at about 290nm, while the transmission of UV through a TiPt coated diamond rapidly falls off below 220nm. Although, the decrease in UV transmission is more closely related to the fact that 220nm light has equivalent energy to the band gap of the diamond($\sim$5.5eV) which is beginning to act as a primary emitter[12]. Within this range there are other factors that serve to amplify or diminish the intensity of each wavelength.

The pulsed Xe light source used in this experiment includes a reflector and collimating optics. The reflector increases the amount of light emitted by 60%($C_R = 1.6$). The collimating optics, despite focusing the output into a beam, reduce the total emitted light by 89%($T_{op} = .11$). As the light passes through the sapphire window into the vacuum chamber there is a reduction in intensity, signified by the coefficient of transmission (T_s) that varies with the wavelength. Figure 2.5 is an approximation, modeled from the ISI documentation[7], of how the sapphire window transmission changes over the region of interest. Figure 2.6 is the measured percent transmission in the UV of a diamond coated with an optically transparent 50Å thick TiPt thin film when compared to the raw UV beam output from a monochromator. The slope between points is taken to approximate for a smaller bin size when the integration is performed to provide a more accurate estimate of the photocathode output.

The estimated photoelectron yield is calculated summing the approximate photoelectron yield from Eq. 2.1 with $\lambda_i = 220nm$ and $\lambda_f = 290nm$. Figure 2.7 displays the estimated energy incident at the photocatode surface taking into account the afore mentioned transmission factors. The beam energy output at the light source is represented by E_λ in Eq. 2.2. After the integration, the total charge resulting from a pulse is given by Eq. 2.4. Dividing the charge by the pulse length of 40μs yields the pulse current which can be multiplied by the desired system impedance, according to Ohm's law to obtain a measurable voltage.

The results of the photocathode emission approximations are shown in Tables 2.2

and 2.3. These results indicate that the photocathode will emit between 1.29 and 34.1 nC per pulse while the DECA is in the beam-line. These values are converted into a voltage, by multiplying by a 5KΩ effective system resistance, to provide an estimate of what will be measured at the oscilloscope.

To approximate the values for a bare photocathode, the calculations are made as if there were no metalized diamond in the beam line to reduce the amount of light incident on the photocathode. For a bare photocathode the emitted pulse charge will be in the range from from 5.5 to 145nC as seen in Table 2.4 and Table 2.5.

$$N_e = \sum_{\lambda_i}^{\lambda_f} \eta(\lambda) N_p(\lambda) \tag{2.1}$$

where

$$N_p(\lambda) \cong C_{trans} T_s(\lambda) T_d(\lambda) E_{beam}(\lambda) \tag{2.2}$$

and

$$C_{trans} = T_{op} \cdot T_m \cdot C_R \cong 0.158 \tag{2.3}$$

$$Q_{pulse} = eN_e, \;\; I_{pulse} = Q_{pulse}/t, \;\; V = IR \tag{2.4}$$

The accuracy of this estimation will be judged later. Regardless of its success or failure to predict the pulse charge, the real value in this calculation is demonstrating that the photoemission generated by a capsule, using the selected light source, will be large enough to measure with an oscilloscope. This is certainly the case. In fact, should the charge increase or decrease by up to 2 orders of magnitude the signal will still be measurable by changing the systems effective resistance.

Pulse Energy	0.32 Joule	1.2 Joule	5 Joule
N_e	$2.39 \cdot 10^{10}$	$5.30 \cdot 10^{10}$	$2.13 \cdot 10^{11}$
Q_{pulse}(nC)	3.83	8.49	34.13
$I_{pulse}(\mu A)$	95.6	212	853
Scope Voltage (V)	.478	1.06	4.27

Table 2.2: High QE Approximation of the Photoelectron Yield from a Copper Photocathode with a DECA in-line

Pulse Energy	0.32 Joule	1.2 Joule	5 Joule
N_e	$8.06 \cdot 10^{9}$	$1.79 \cdot 10^{10}$	$7.19 \cdot 10^{11}$
Q_{pulse}(nC)	1.29	2.87	11.51
$I_{pulse}(\mu A)$	32.5	71.7	288
Scope Voltage (V)	.161	.358	1.44

Table 2.3: Low QE Approximation of the Photoelectron Yield from a Copper Photocathode with a DECA in-line

Pulse Energy	0.32 Joule	1.2 Joule	5 Joule
N_e	$1.01 \cdot 10^{11}$	$2.26 \cdot 10^{11}$	$9.09 \cdot 10^{11}$
Q_{pulse}(nC)	16.3	36.3	145
$I_{pulse}(\mu A)$	408	906	3643
Scope Voltage (V)	2.04	4.53	18.2

Table 2.4: High QE Approximation of the Photoelectron Yield from an Unobscured Copper Photocathode

Pulse Energy	0.32 Joule	1.2 Joule	5 Joule
N_e	$3.44 \cdot 10^{10}$	$7.63 \cdot 10^{10}$	$3.07 \cdot 10^{11}$
Q_{pulse}(nC)	5.51	12.2	49.2
$I_{pulse}(\mu A)$	138	306	1229
Scope Voltage (V)	.689	1.53	6.14

Table 2.5: Low QE Approximation of the Photoelectron Yield from an Unobscured Copper Photocathode

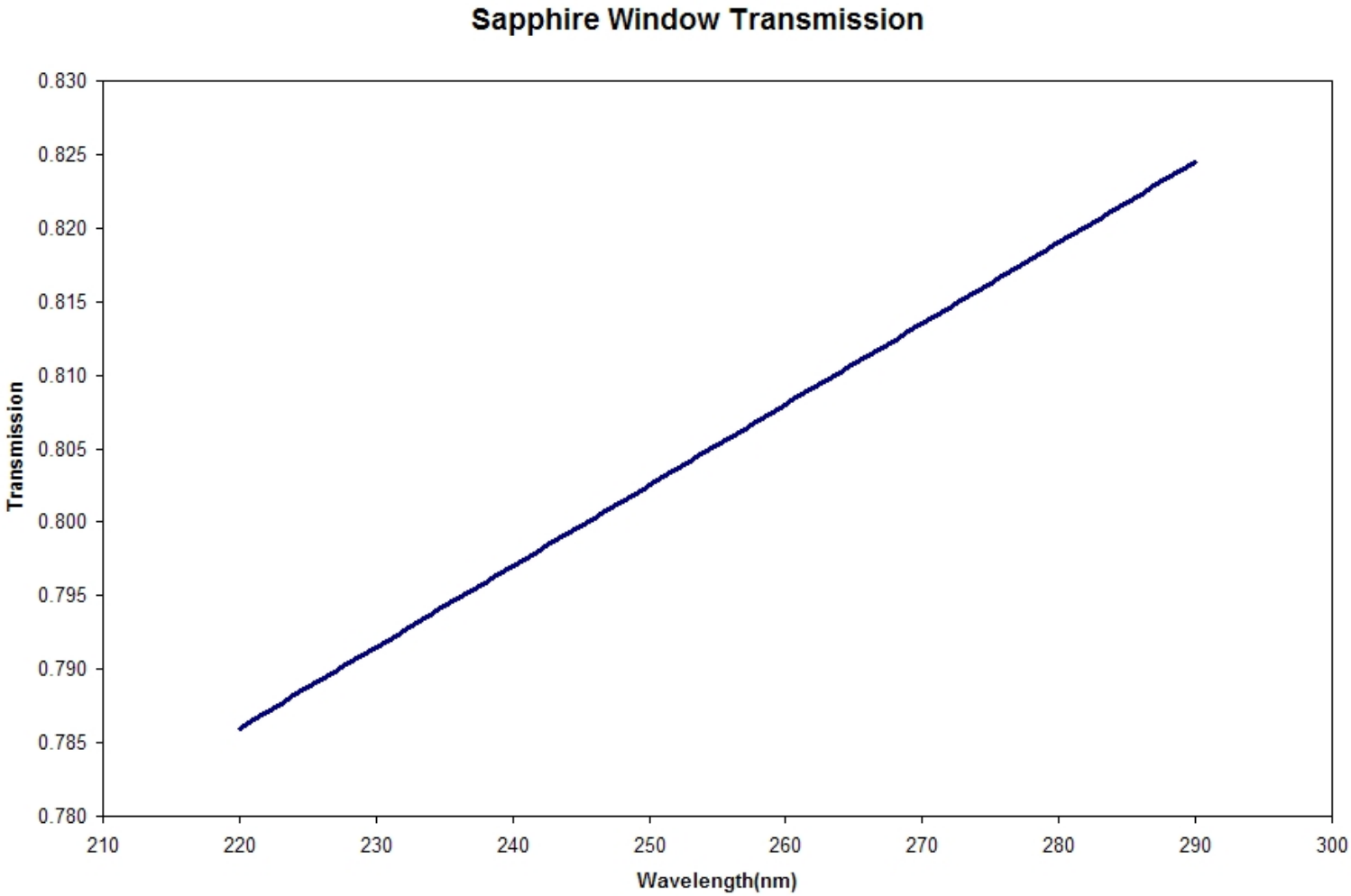

Figure 2.5: UV Light Transmission Through a Sapphire Window - Approximate light transmitted into the Capsule Assembly Chamber. These values are estimated from ISI documentation.

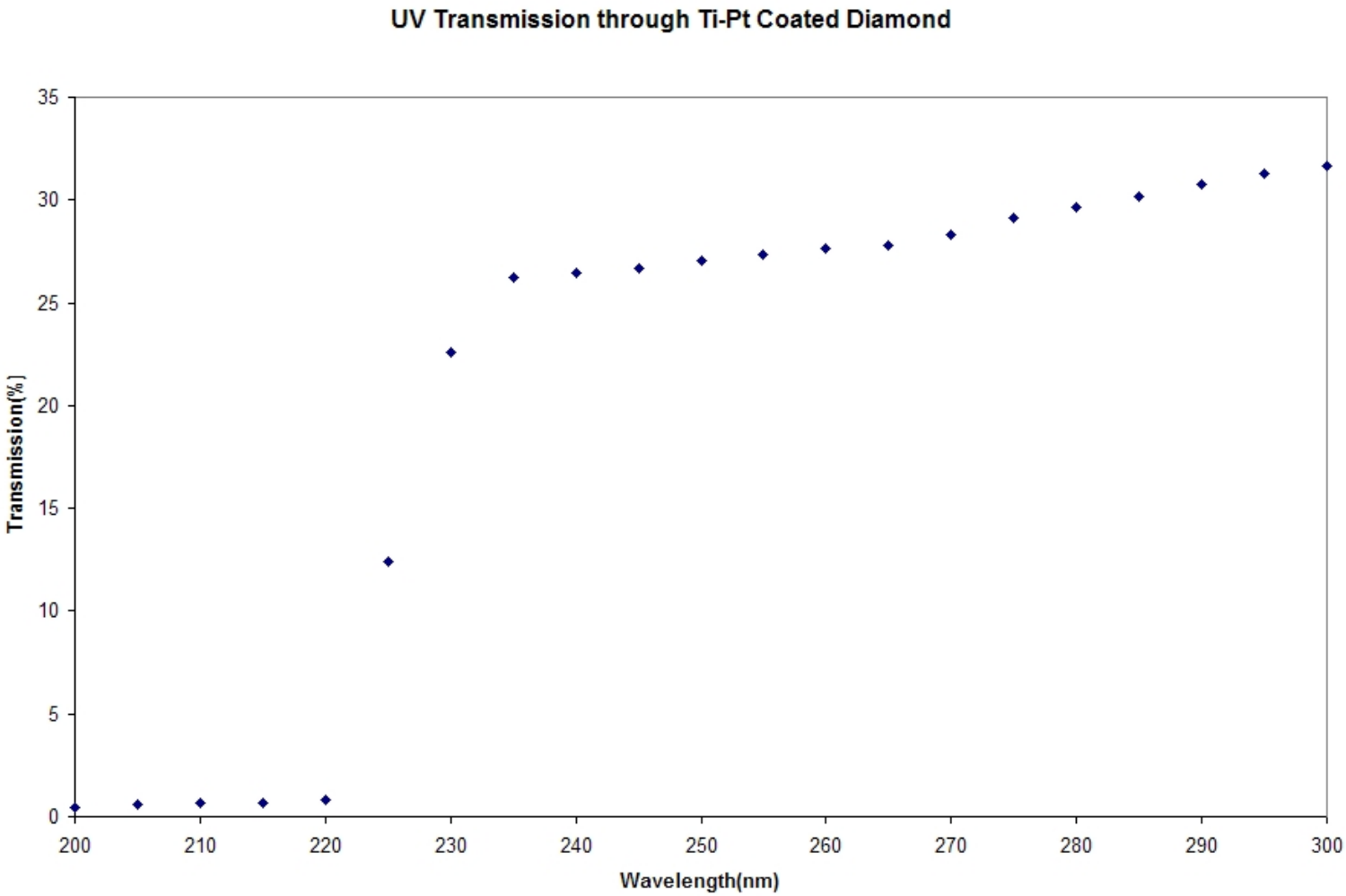

Figure 2.6: UV Transmission Through TiPt Coated Diamond - Measured percent transmission in the UVC spectrum as measured through a TiPt coated optical grade diamond.

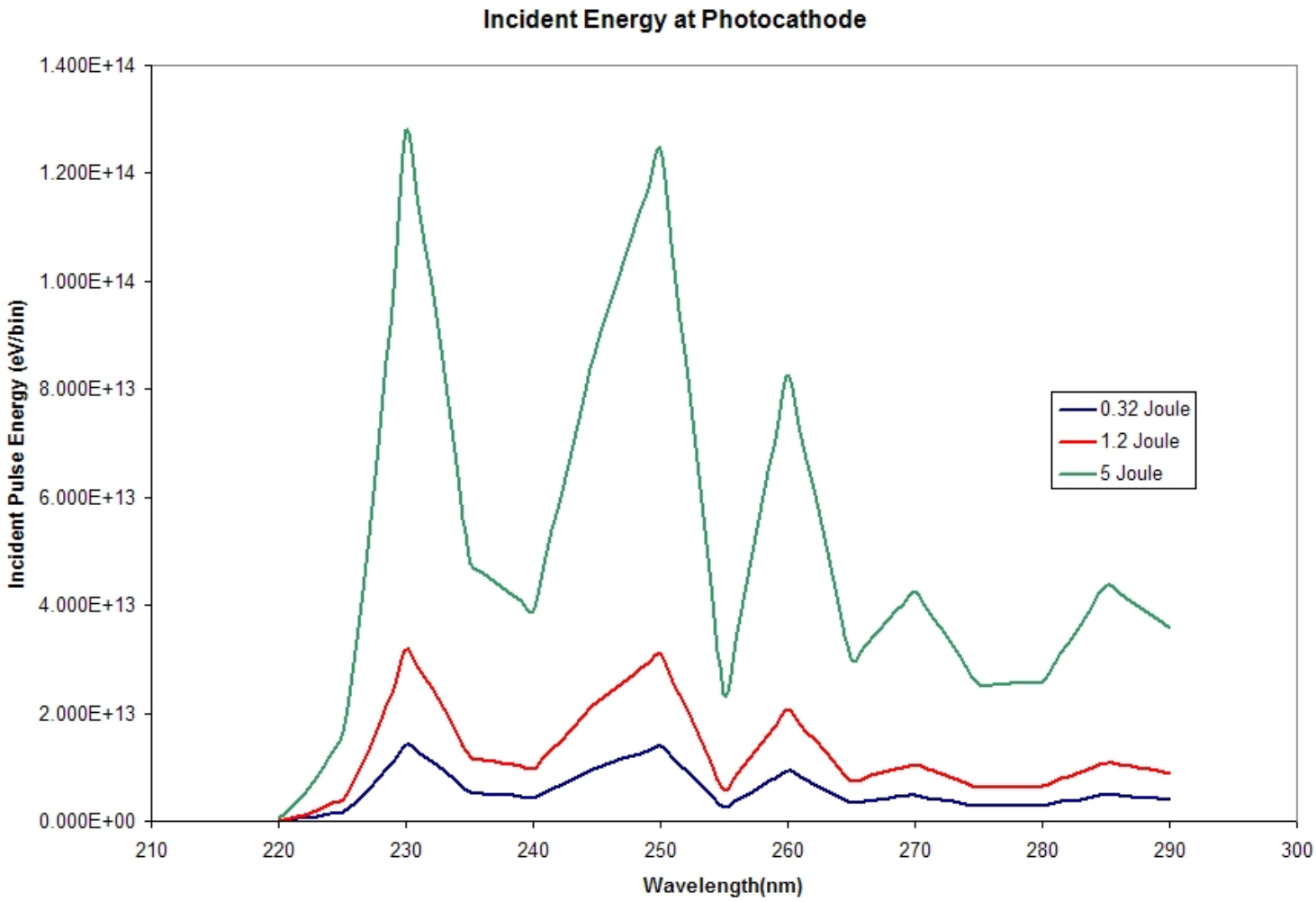

Figure 2.7: Incident Light Energy at Photocathode - This is an approximation of the light energy per pulse incident on the photocathode. This estimate incorporates losses as the beam passes through each of the optical elements.

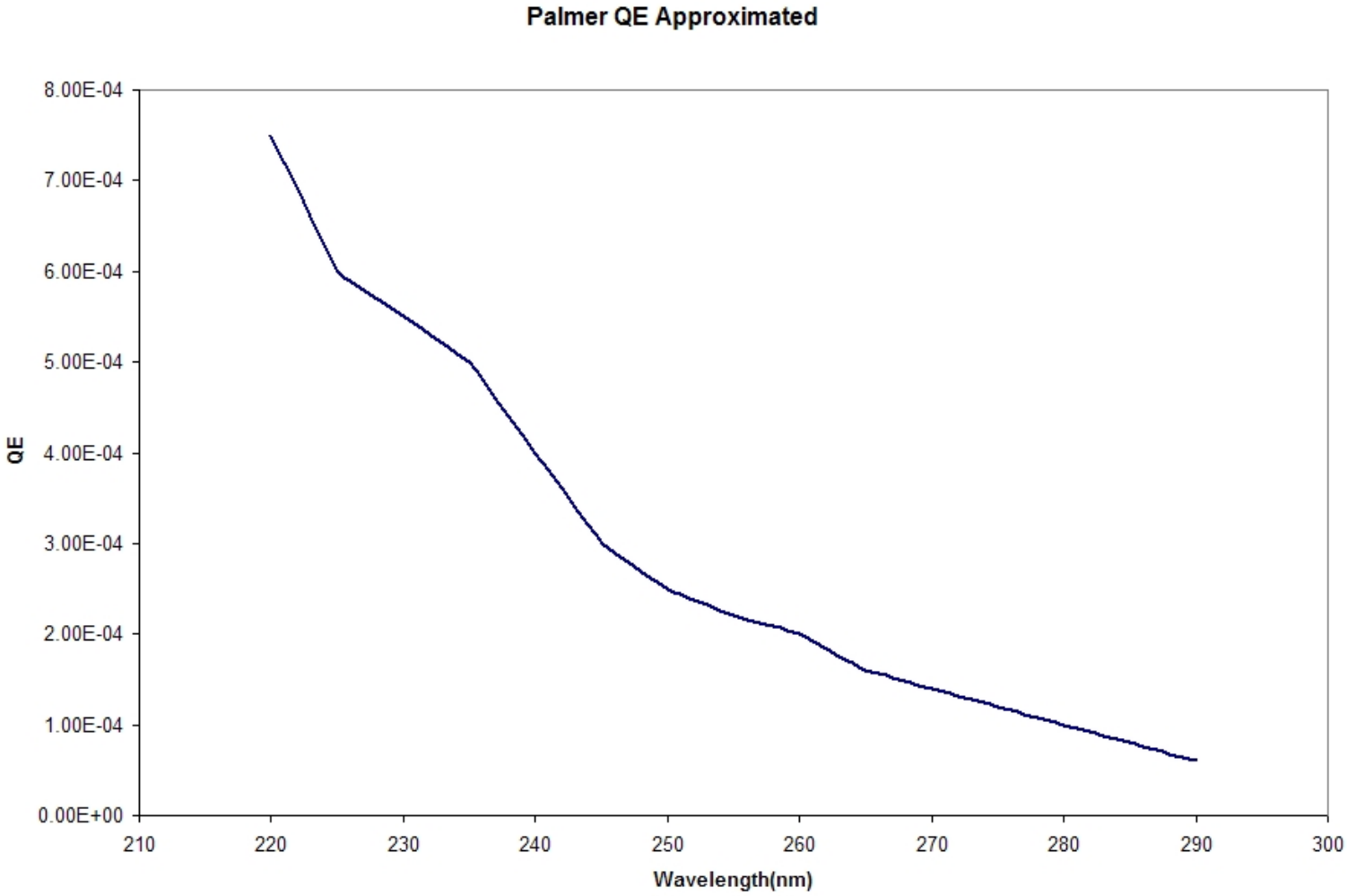

Figure 2.8: QE of Copper Photocathode Approximated from Palmer Data

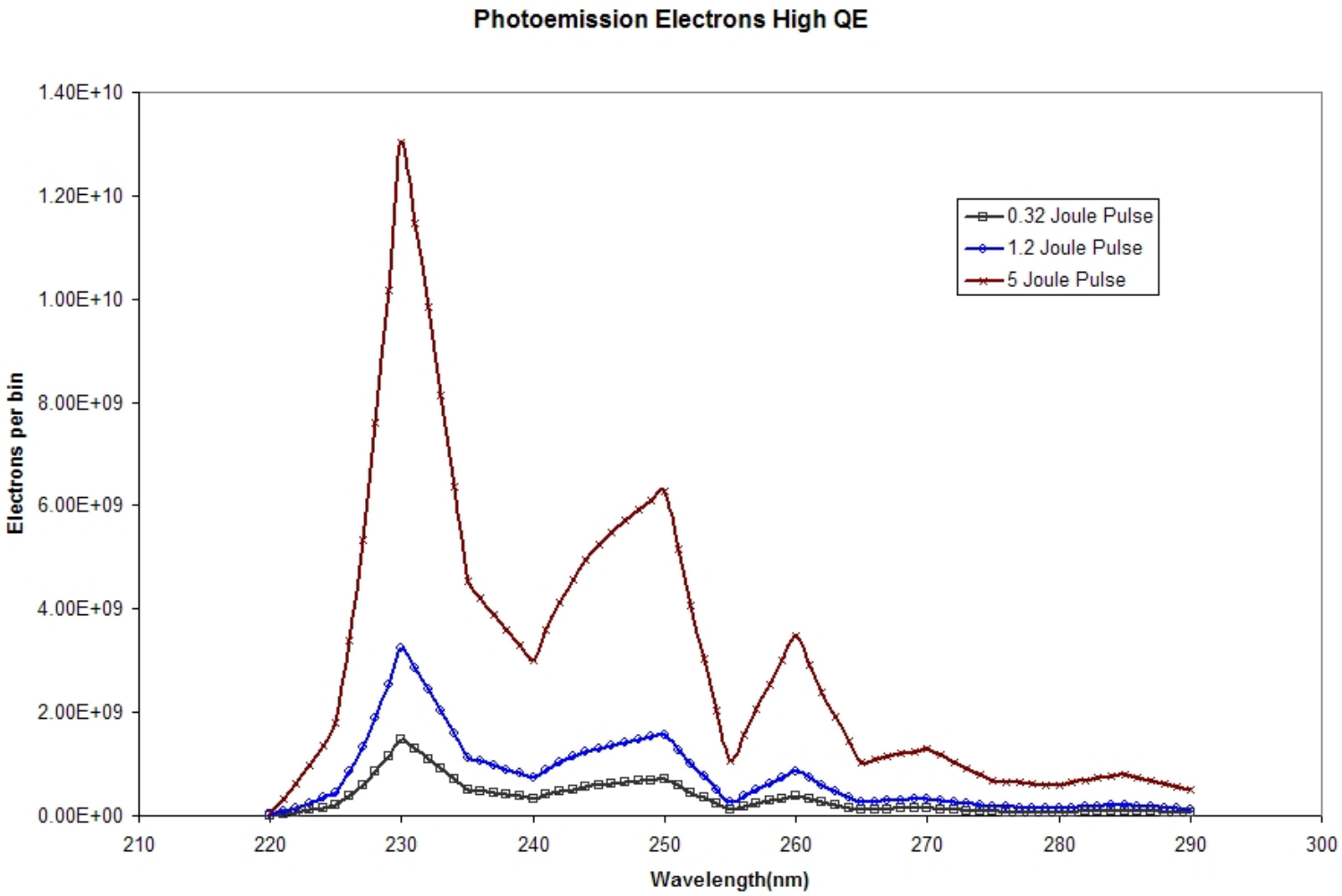

Figure 2.9: Predicted Photoemission from a High QE Photocathode Surface - An identical result occurs for the lower QE estimate. the total photoelectron yield is computed from the data presented in this figure.

2.8 Space Charge Limitations

One of the determining factors in the design of the capsule and assembly chamber is the possibility of space charge effects. To determine whether space charge will be an issue the, Langmuir-Child equation for a plane diode (Eq. 2.5) is used to calculate the space-charge-limit (SCL) for a variety of capsule configurations[6].

$$J_L = K \cdot \frac{V^{3/2}}{d^2} \tag{2.5}$$

where

$$K = \frac{4}{9}\epsilon_0(2e/m)^{1/2} \tag{2.6}$$

The quantity e/m is the charge to mass ratio for the electron and ϵ_0 is the well known permittivity of free space. In this equation the photocathode and anode are considered as parallel plates with a separation d. The fields involved limit the final group velocity of the electrons. Therefore, the entire system is operating in the non-relativistic regime.

Figures 2.10 and 2.11 show J_L for increasing voltage between the photocathode and the anode. It is visible from these graphs of the Langmuir-Child equation that, in the range of voltages that will be applied to this system, both capsule configurations are operating well below the SCL, when compared to the predicted photoemission in Sec. 2.7.

From the definition of K in Eq. (2.6), we see that the SCL is linearly related to ϵ_0. Therefore, it is only necessary to multiply by the relative permittivity of diamond to calculate the SCL in the amplification layer. The results of this calculation (Fig. 2.12) show that given the predicted photoemission yield and a projected gain of 100 secondary electrons per incident photoemitted electron, the total pulse charge in the diamond is still well below the SCL.

The SCL between the hydrogenated diamond (Fig.2.13) surface and the anode is also of importance to the operation of the capsule. If the total pulse charge exiting

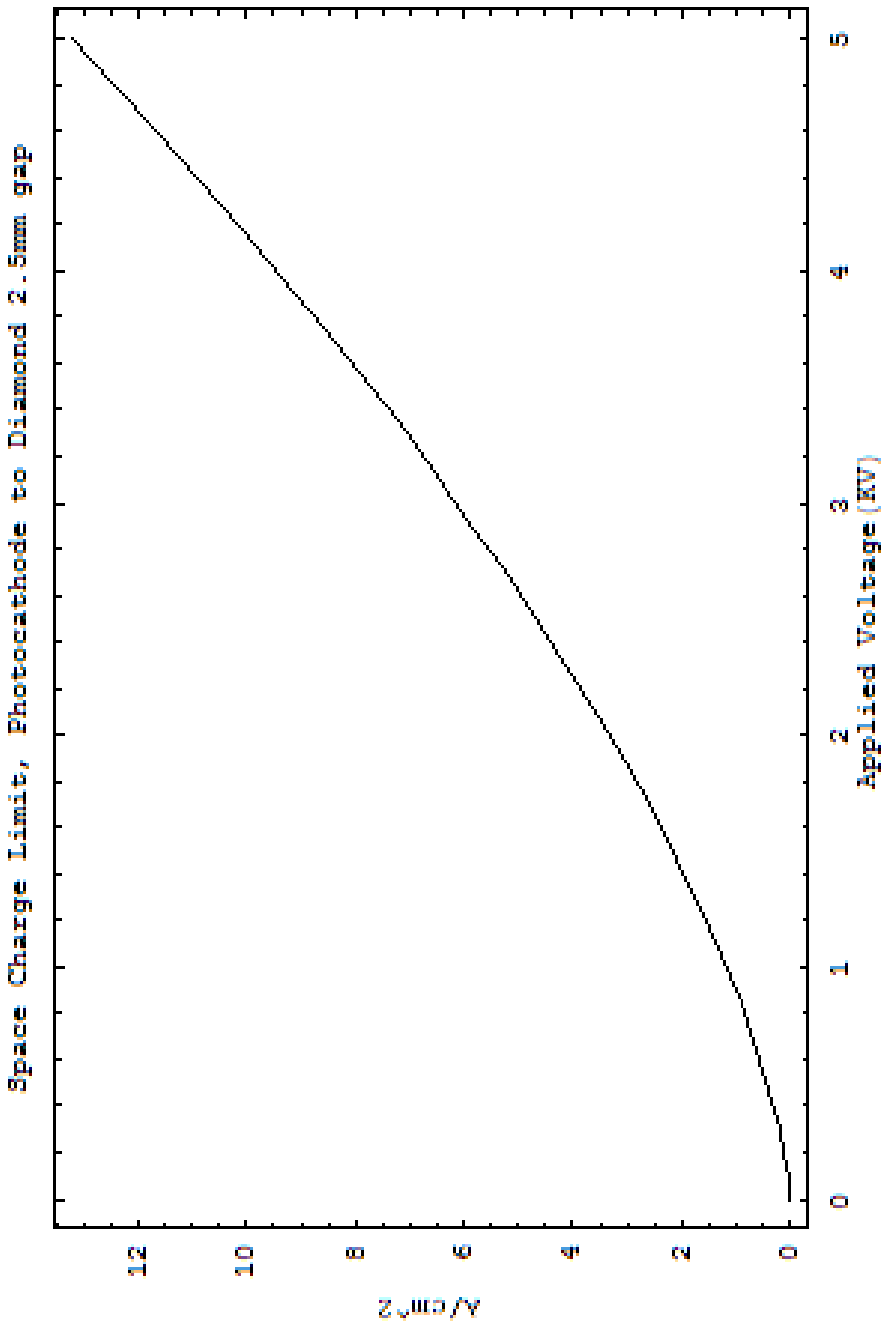

Figure 2.10: SCL in a 2.5mm Separation Between the Photocathode and Ground

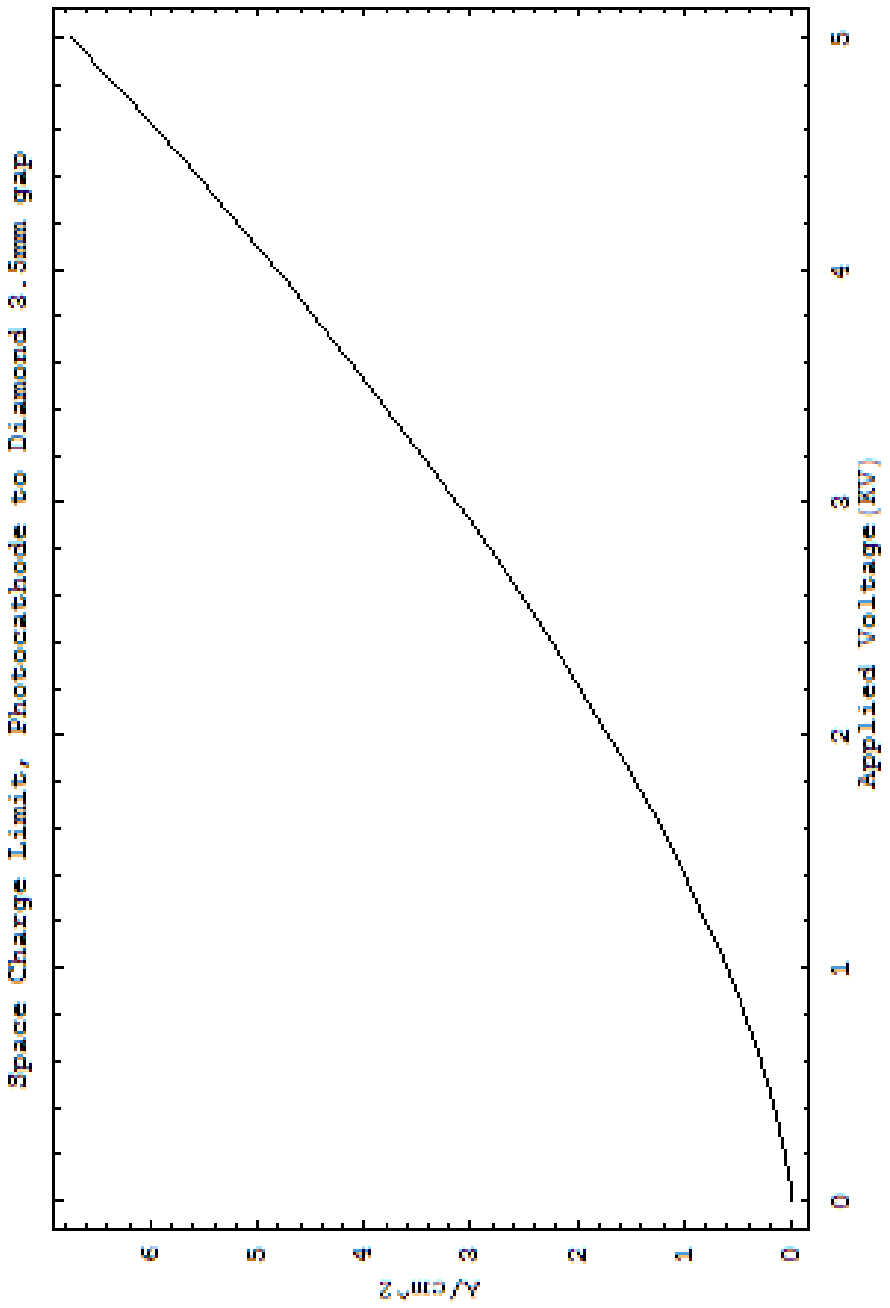

Figure 2.11: SCL in a 3.5mm Separation Between the Photocathode and Ground

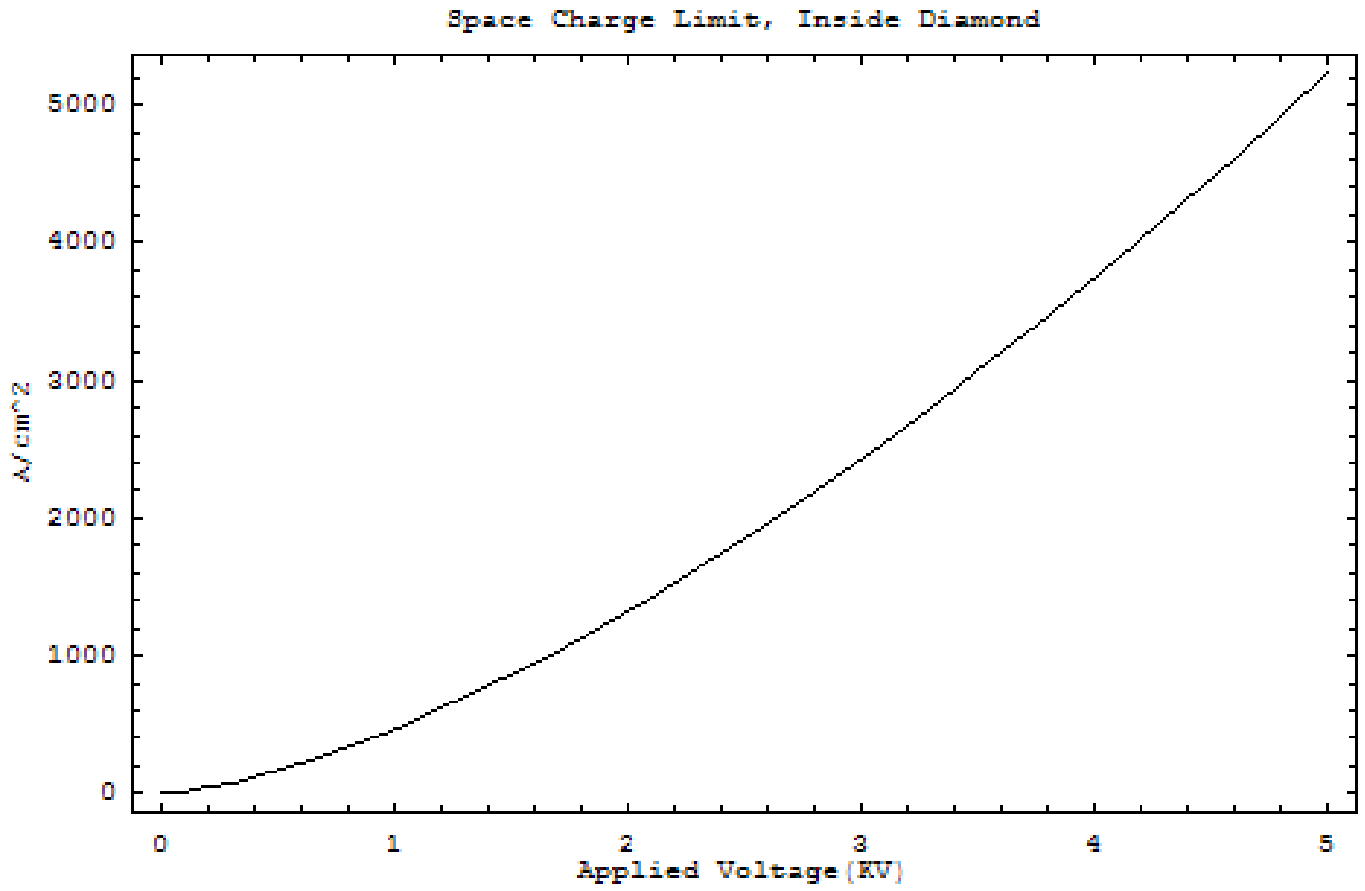

Figure 2.12: SCL Inside a 300μm Thick Diamond

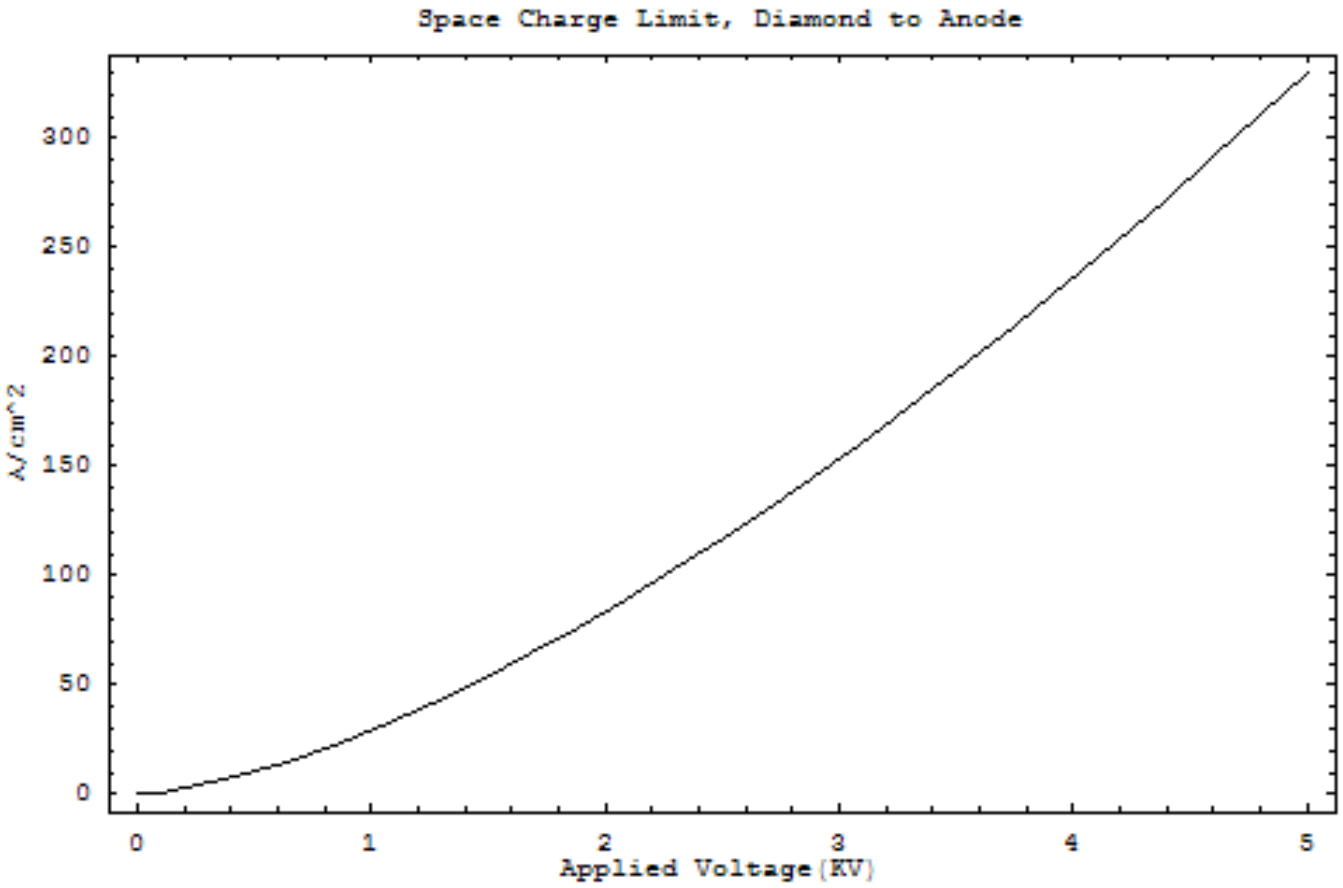

Figure 2.13: SCL between the Hydrogenated Diamond Surface and a Wire Mesh Anode

the diamond is above the SCL, then not all of the secondary electrons will exit the diamond. This increases the total amount of charge inside the diamond. This residual charge reduces the field in the diamond causing a reduction in the number of secondary electrons that are accelerated out of the recombination zone.

Chapter 3

Experiment/Procedure

3.1 Brazing Chamber

Brazing occurs in a Mellen MT1300 furnace that is capable of reaching temperatures up to 1300℃Fig. 3.1. The furnace has a 3" bore in which a mullite tube sits to shield the brazing chamber from direct contact with the electrical heating filaments. During operation it is controlled by a programmable Omega controller. The brazing chamber is a long 304SS tube with an ID of approximately 1.5" that has been capped on one end and welded to a 2.75" conflat flange on the other. Samples to be brazed are mounted on a stainless steel tongue attached to a cross. The cross and tube are suspended from a metal cage with a track that allows the cross to advance and retract, bringing the sample into and out of the furnace core. Samples are held in a stainless steel cup during brazing to ensure proper alignment of the elements. Temperature at the furnace core is measured with a type K thermocouple. Pumping is provided by a 20L/s Pfeiffer turbo-cube which brings the system into the HV regime, as measured at the pump before the brazing program begins. Pressures as low as $5 \cdot 10^{-9}$ have been observed after brazing.

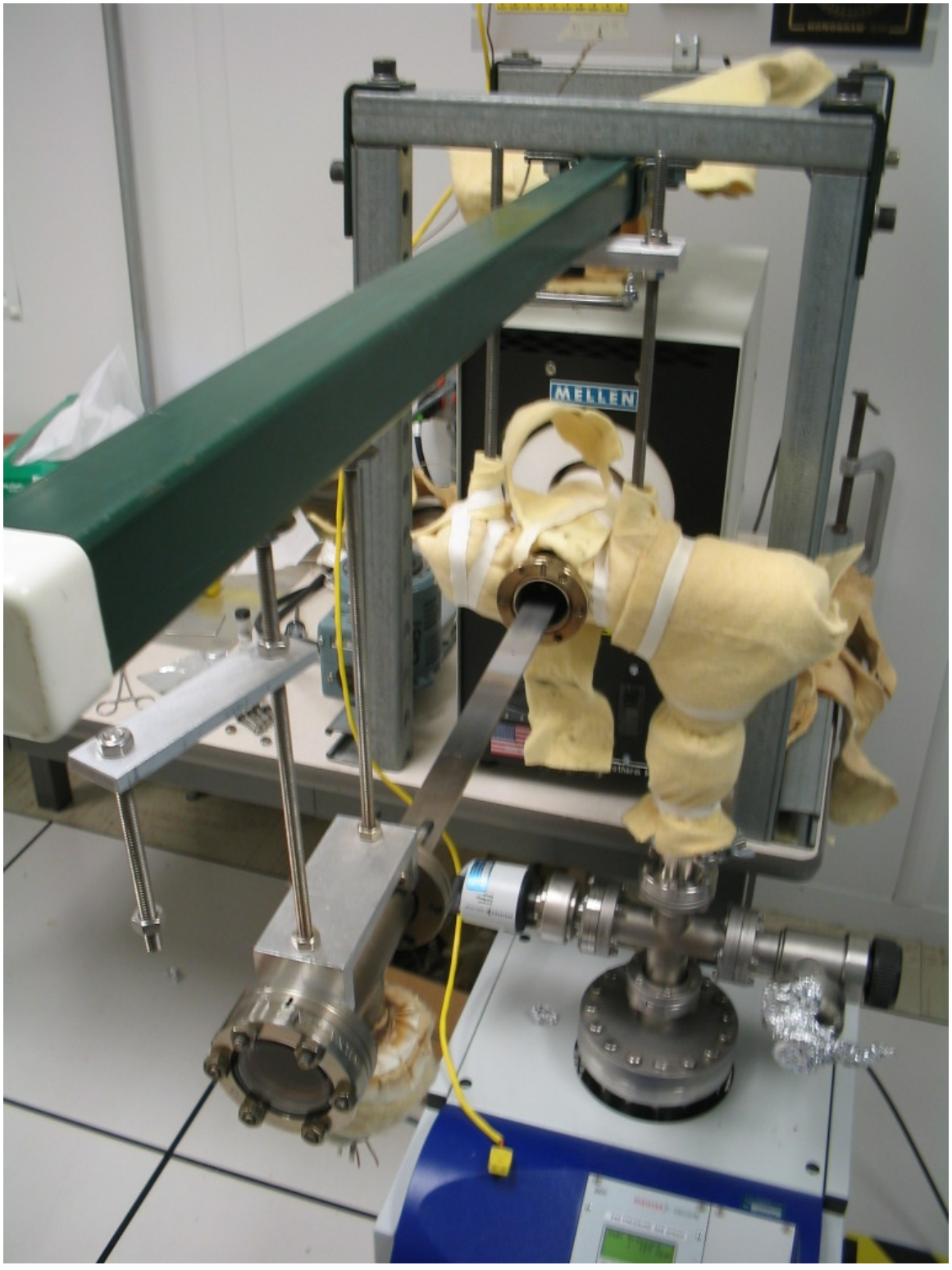

Figure 3.1: Vacuum Braze Furnace - The Mellen MT1300 furnace with a vacuum chamber insert is used for high temperature brazing applications

3.2 Capsule Assembly Chamber

The Capsule Assembly Chamber(CAC), Fig. 3.2, is where the final construction of the capsule and emission testing occur. It is designed to hold the diamond and its relevant assembly firmly in place while the photocathode, mounted on a manipulator arm, is lowered onto it from above. The CAC is designed to provide stability to both pieces of the capsule during alignment and assembly. The CAC also hosts the electrical contacts necessary to provide the required high voltage inputs and grounded output for measurement.

The design of the CAC is centered around a 2.75" conflat cube. Four of the six available ports are used for electronics and instrumentation. Mounted vertically to the top of the cube is a linear actuator that passes through a 2.75" cross and a gate valve into the center of the chamber. Attached to the one of the remaining cross ports is a 20 L/s ion pump that will bring the CAC into UHV range during operation. The other port is occupied by a cold cathode gauge used to measure vacuum. On the end of the linear arm is a cylindrical Macor electrical standoff to which a photocathode will be attached with a M3 set screw. The linear actuator fully retracts to bring the photocathode behind the gate-valve to keep it under vacuum during instances in which it is necessary to reconfigure the chamber.

Opposite the linear actuator is a sapphire window for admitting UV light pulses, mounted on a 1.33" to 2.75" reducing flange, which is connected to the long axis of a conflat T. Mounted to the vacuum side of the reducing flange via three 5" stainless steel posts is the centering assembly. The length of the posts places the centering assembly into the chamber core when the T is attached to the bottom of the cube. The remaining T port is occupied by a 4-pin SHV feed-through which provides electrical contact between the centering assembly and the outside. The centering assembly consists of an alignment guide, a wire mesh anode, and the photocathode electrical contact.

The alignment guide, Fig. 3.3, is machined from a single piece of stainless steel and

has a triangular base with posts that extend from the vertices. Atop the posts is a chamfered ring that mates with and aligns the macor standoff on the linear actuator. In the center of the triangular base is an aperture that holds the diamond assembly. The alignment guide stands at the very top of the mounting posts and is attached to them with 2-56 screws.

Below the alignment guide is the anode. The anode is formed out of 70 line/inch nickel mesh. It is mounted on a hollow cylindrical copper holding piece that is inserted into the central aperture of a triangular copper mounting plate. The mesh and holding piece are secured by conductive silver paint. The copper mounting plate has a hole at each vertex through which a pair of male and female mating insulators is inserted to provide electrical insulation. The 2-56 screws fit through the central diameter these insulators to mount the anode plate to the three posts.

The photocatode electrical contact sits below the aforementioned insulators and is connected to only two of the posts. It consists of a steel mount, a macor standoff, and a beryllium-copper spring finger. The macor standoff is attached to the steel mount and has a hole in it for the spring finger. The spring finger sets in the hole so that it is elevated above the base of the alignment guide and bends out over it. Electrical contact is made when the photocathode is driven down into the alignment guide.

3.3 Diamond Electrical Contact Assembly

The Diamond Electrical Contact Assembly(DECA) is a multilayer assembly that contains most of the capsule components. The DECA is comprised of a diamond disk – the amplifier, a niobium washer – provides electrical contact, a sapphire washer – for electrical insulation, and a niobium washer – mates with the photocathode. These layers are assembled in a two step braze process. It provides electrical contact to the metallization layer and thereby, the diamond.

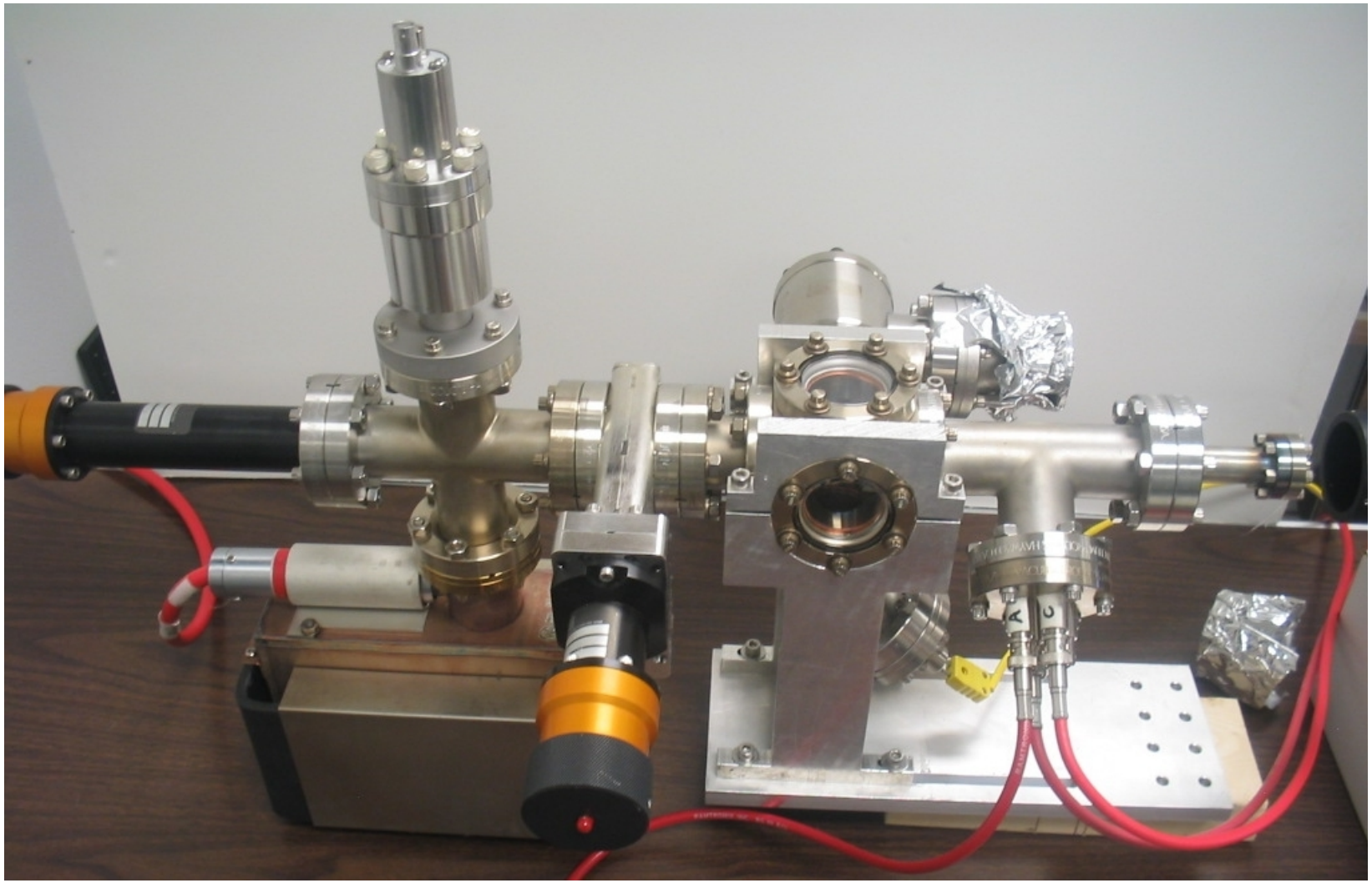

Figure 3.2: Capsule Assembly Chamber - used for testing and assembly of Diamond Amplified Photocathodes.

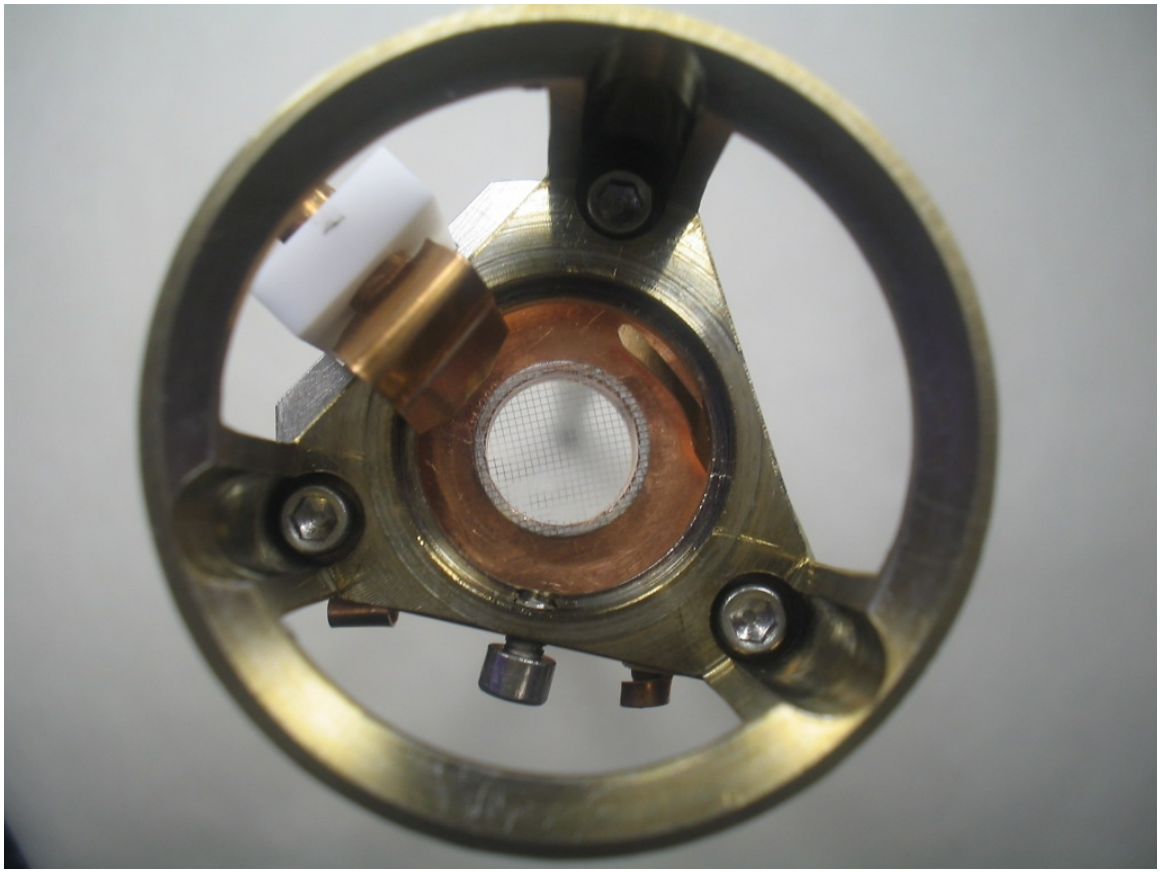

Figure 3.3: Alignment guide as seen from above - Visible in this image are the alignment guide(outer ring), the wire-mesh anode(center), the DECA electrical contact(upper-right center), and the photocathode electrical contact with Macor® standoff(upper-left center). The alignment guide outer diameter is 1.3in.

Each of the elements in the assembly must be handled to ensure cleanliness and surface integrity. Specifically, they are each subjected to cleaning processes to remove contaminants. Some repetition will be noticed, as the cleaning of each sample may contain identical steps.

3.3.1 Diamond preparation

Diamond samples are initially subjected to a battery of tests(Raman scattering, and X-ray absorption spectra) that serve as a backdrop against which to track any possible changes in integrity and physical impurities, either internal or surface. This provides a window into the physical state of the diamond. The tests can be repeated after any of the later steps to see what changes have occurred.

After initial characterization, the diamond is etched in a chemical process (Fig. 3.4) that involves a hot saturated chromic acid in sulfuric acid solution, boiling sulfuric acid in water and boiling ammonium hydroxide. This process removes any surface impurities, free carbon, or graphite and then attaches oxygen to the dangling carbon bonds on the surface. The etched sample is then inserted into high vacuum and heated to break the oxygen bonds. Once the oxygen is freed from the surface, a stream of cracked hydrogen is introduced to the system. The hydrogen bonds with the dangling carbons and forms a stable surface that can be exposed to atmosphere. The hydrogenated diamond is then removed to another chamber where the amplified emission is measured as background for comparison to later measurements after the capsule assembly.

Diamonds that are not etched are treated to a multi-step washing procedure to remove oils and other impurities. Samples are first washed in acetone and ethyl alcohol. Then they are ultrasonically cleaned in a hexane bath for 20 minutes. Finally, they are blown dry with dry nitrogen or a heat-gun to prevent residues from forming.

Recipe for Diamond Etching

1. 15 minutes in saturated CrO_3 in H_2SO_4 (solution heated until vapors are visible) followed by DI water rinse
2. 2 minutes in NH_4:H_2O (1:10) solution agitated ultrasonically followed by DI water rinse
3. 2 minutes in HCl:H_2O (1:10) solution agitated ultrasonically followed by DI water rinse
4. 5 minutes in boiling H_2SO_4:H_2O_2 (5:1) followed by DI water rinse
5. 2 minutes in boiling NH_4:H_2O_2:H_2O (1:1:4) followed by DI water rinse
6. 2 minutes in boiling HCl:H_2O_2:H_2O (1:1:4) followed by DI water rinse
7. 5 minutes Ultrasonic bath in DI water
8. Gas drying with N_2

Figure 3.4: Recipe for Diamond Etching - The above recipe is for the etching of diamond samples. It is performed entirely inside a chemical hood. This process removes surface impurities, metal, and residual graphite. It then attaches oxygen to surface dangling carbon bonds in preparation for the hydrogenation process.

3.3.2 Niobium preparation

Two washers are required for the capsule. One sample will be joined to diamond and sapphire layers, while the other will be attached to the opposing side of the sapphire. The washers are machined or EDMed from RRR Niobium. In the case of a 10mm diamond sample, they are identical in dimension. Each specimen has an outer diameter of 12.5 mm, an inner diameter of 7.9 mm, and a thickness of 1 mm. The dimensions required to join to a 5 mm diamond are slightly different.

Once the washers have been machined they are polished according to a previously established photocathode preparation procedure(included in supporting documents). The Nb washers are then subjected to a 20 minute ultrasonic bath in acetone instead of the called for hexane. The samples are then rinsed with ethyl alcohol and blown dry with dry nitrogen or a heat gun to avoid the formation of residues.

3.3.3 Sapphire washer preparation

A synthetic sapphire washer–manufactured by Swiss Jewel® acts as the electrical insulator between the capsules conducting plates. The sapphire, as delivered is polished on only one side. The cleaning process for the sapphire starts with wipe down with acetone, followed by a 20 minute ultrasonic bath in the same. It is then rinsed in Ethyl alcohol and blown dry with dry nitrogen or a heat gun to prevent residue formation.

3.3.4 Ticusil braze foil preparation (2 washers)

Ticusil is the braze material of choice, as it is specifically designed to join refractory metals and ceramic/diamond. The material comes in paste, foil, or preforms. Due to the varying size requirements of this project a 50 μm thick foil is selected. This will allow the volume to be controlled by changing the diameters of the washers. A Metallic 10 Tru Punch is used to separate washers from the foil. For a 10 mm diamond sample the ticusil washers has an ID of 8 mm and an OD of 8.5 mm. After many attempts this washer size was determined to have the appropriate volume for joining the Nb washers to both sapphire and diamond while eliminating excess flow outside of the joining region. After being punched, the washers are cleaned with acetone, then ethyl alcohol to remove oils and other contaminants. They are then blown dry with nitrogen or a heat-gun.

3.3.5 Brazing

Brazing is accomplished in two steps. Each step uses the same braze sample holder 3.5, which is a cylindrical multi-tiered stainless steel cup that accommodates the elements to be brazed along with the requisite Ticusil washers. The first step joins the sapphire washer and one of the niobium washers. The second step joins three layers; diamond, niobium washer, and sapphire washer. This step acts as a convenient example of the

Figure 3.5: Braze Sample Holder - This sample holder is used during the brazing process. It is machined from a single piece of 304ss, the BSH holds all components to be brazed; diamond, Nb, Sapphire, and Ticusil.

brazing process.

For the second step, five layers are loaded vertically into the braze sample holder in bottom-up order: diamond, small Ticusil washer, Nb washer, large Ticusil washer, and Sapphire washer. In this fashion only gravity is required to hold the elements in place. The loaded sample holder is placed on the furnace tongue which is then gently inserted into the furnace core to avoid vibrating the layers out of the sample holder. Once the sample is in the furnace core and the vacuum chamber is sealed, the chamber is pumped to 10^{-6}Torr and the braze program is started.

The braze program begins with a ramp to 870℃ over 4.25 hours. Once the furnace reaches the set point the system is allowed to equilibrate through a 2 hour

soak. After soaking the furnace is ramped to a core temperature of just over 900℃, which is the liquidus temperature of Ticusil, and quickly brought back down for the braze to solidify. The furnace is then ramped back down at a rate of 100℃/hr. The slow ramp allows the niobium washers to relax and absorb stresses thereby preventing cracking in the diamond and sapphire.

3.4 Post braze handling of DECA

Once brazing is completed on the DECA it is necessary to pressure check the whole assembly. This is accomplished with a Pfieffer Vacuum QualyTest helium leak checker. If no leaks are detected above the 10^{-9} background helium flow rate from a Viton seal, then the assembly is considered vacuum tight and it is cleaned in hexane to remove residual oils without leaving any residue. After cleaning, the DECA is subjected to Raman scattering and X-ray absorption spectroscopy. The results of these tests are compared to data from previous tests to ensure that no changes have occurred in the diamond or that any impurities have been introduced. Upon verification of the braze integrity and vacuum tightness, the DECA is stored under vacuum or inserted into the capsule assembly chamber for final testing.

3.5 Photocathode Preparation

As discussed above, the photocathode used in this experiment is made of oxygen free hard copper or OFHC. The copper photocathode is machined from a rod of this material and has a diameter of 12.5mm by height of 12.5mm. There is a threaded hole in the back face to accommodate mounting in the capsule assembly chamber. The photocathode has a raised central area that has a diameter of approximately 9mm surrounded by a 0.5mm deep by 1mm wide semicircular groove. The outer edge of the cathode is slightly lower than the central diameter to accommodate polishing.

After the copper is machined, it is cleaned with acetone to remove residual oils from the machining process. It is then submerged in a 5% acetic acid bath to remove oxides that have formed on the surface. The photocathode is removed from the bath once it has turned a lustrous pinkish color. The sample is then polished to a mirror finish according to a standard photocathode preparation recipe and finished in an ultrasonic hexane bath for 20 minutes. When it is removed from the hexane bath the photocathode is blown dry with pure nitrogen gas and loaded into the capsule assembly chamber or stored under vacuum, or in hexane, until called for.

3.6 In-situ Testing and Assembly of DAP Injector

Following assembly of the DECA and completion of photocathode preparation, both pieces are inserted into the Capsule Assembly Chamber. A variety of tests are performed to determine the overall performance of the diamond amplified photocahtode, as well as the performance of the individual constituent elements. First, cleaning of the photocathode to improve the quantum efficiency will be attempted. Then the number of electrons in a charge pulse emitted from the photocathode that make it across the accelerating potential to the metallization layer is measured. Finally, the secondary emission of the diamond sample is tested and the gain is calculated. The following procedure represents the likely steps that will be incorporated during the construction and testing of the capsule.

3.6.1 Surface Cleaning and Photocathode QE measurement

In order to obtain the best results from the photocathode, it is desirable to have the cleanest possible surface which will provide the best quantum efficiency. Therefore, we wish to examine two potential mechanisms available for cleaning the photocathode. As mentioned before, Palmer et. al. [8] reported that annealing the photocathode

will result in a clean high Q.E. surface. There is also sufficient light energy in the pulses generated by the Xe flash lamp, which will be used to stimulate emission, to clean the photocathode surface. Therefore, photocathodes will be subjected to both annealing and high intensity light from the flash lamp in order to test which of these methods will have the desired effect. The number of photoemitted electrons will be measured before and after each of these operations. If there is an increase in the QE, there will be an increase in the photoelectron yield. It should be noted that this test is flawed in that it will provide the magnitude of the increase in QE but not the actual value. It is, however, still possible to obtain a reasonable approximation of the photocathodes QE by taking as a basis earlier reported literature values.

3.6.2 Photoemission Measurement

Once the cleaning and QE measurements are completed the sample is inserted into the CAC and the system is pumped down to 10^{-9}Torr. At this point the CAC is configured for photocathode only operation with only the photocathode and wire mesh anode present in the system. For the purpose of measuring photoelectron yield, the anode is at ground and connected to the oscilloscope for data collection.

After the system is pumped down, the high voltage low current power supply is turned on and a positive voltage of up to 5 KV is applied to the anode. In this configuration the photocathode and the anode have a larger separation than that between the photocathode and the diamond metallization layer. Applying voltage to the anode ensures that all electrons will be extracted from the photocathode. The xenon flash lamp is then turned on and focused pulses are directed at the photocathode. The copper photocathode is stimulated to emit electrons by broad spectrum UV pulses that are incident on its surface. Electrons emitted by the photocathode are accelerated across the potential toward the anode where they are collected. Measurements of the photoemission are made at the photocathode to ensure all emitted charges are counted. The resulting pulse signal is passed to the oscilloscope where it

is recorded for later analysis.

3.6.3 Capsule Assembly and Testing

Upon the completion of photoemission measurements, the photocathode is retracted behind a gate valve and stored under 10^{-9} scale vacuum to preserve any QE enhancement that has been made. Once the photocathode is isolated, the remainder of the CAC is bled-up with dry nitrogen and opened to atmosphere, at which time the alignment guide is removed. The previously brazed DECA is placed into the alignment guide and all electrical contacts are checked. Then the alignment guide and relevant assembly is re-attached to the CAC. After the DECA is inserted into the CAC, the system is pumped by a Pfieffer TurboCube to 10^{-7} Torr then baked for 24hrs at $\sim$150℃. Once the system has cooled, the ion pump is turned on to bring the chamber down to low 10^{-10} scale before measurements are started.

To measure the amount of photoemission generated by UV transmitted through the diamond, a -5KV potential is applied to the photocathode. The diamond metallization layer is then held at ground so that it is effectively an anode relative to the photocathode. When the lamp is triggered, the resulting charge pulse is collected at the anode. The pulse signal is passed to an oscilloscope where it is recorded for later analysis calculation of the number of photoelectrons emitted.

To measure secondary emission, the electrical contacts on the Capsule Assembly Chamber are reconfigured such that the diamond metallization layer is at ground and a positive voltage in the range of 0-3.5KV is applied to a wire mesh anode outside the DAP. A positive voltage of 2.8KV sets-up an approximate 1 MeV/m field, depending on the thickness of the diamond. UV light pulses are directed through the assembly to generate photoelectrons. The resulting charge pulse is accelerated by a -5 KV potential, applied at the photocathode, toward the diamond metallization layer. Electrons in the charge pulse enter the diamond and lose their energy through scattering and the creation of many electron-hole pairs. The electron-hole pairs are

separated by the electric field in the diamond. Holes recombine with the current from the metallization layer. Electrons are induced to drift through the diamond by the field and pass through a hydrogen terminated surface into the vacuum.

The current from the metallization layer that recombined with the holes is converted to a voltage measured at the oscilloscope, and the number of electrons used in recombination is calculated. That number is compared to the original number of photoelectrons and the total gain is calculated.

After initial DAP testing the photocathode is lowered onto the diamond electrical contact assembly (DECA) and a seal is created between them by a thin indium wire, thus closing the capsule and creating a self contained vacuum apparatus. Once the capsule has been closed, the procedure specified in the paragraphs above is repeated to characterize the sealed DAP.

Chapter 4

Characterization of DAP Injector: Results and Analysis

The focus of this chapter will be the collection of information about the primary and secondary emission characteristics of a diamond amplified photo-injector capsule and the gain profile of this system. Several different characteristics of the CAC and the DAP injector are studied to ensure that the resulting signal from a closed capsule is, in fact, amplified secondary emission, with respect to primary emission from the photocathode.

To begin with, the emission profile of the unobscured photocathode is examined. This provides preliminary information about the functioning of the CAC and Xe flash lamp. Characterizing the yield from the photocathode allows quantification of background and EMI. It also allows determination of the effectiveness of proposed cleaning techniques.

Following the photocathode characterization the CAC is reconfigured for capsule assembly and measurement mode. This includes insertion of the DECA and 24hr bake-out of the system. With the CAC in assembly mode, initial measurements are made to quantify the diamond photoemission, secondary emission, gain, and to determine the magnitude of EMI effects in the capsule. From the resulting data, it is obvious that primary emission from the diamond is large and must be removed or reduced. Following these initial measurements, steps are taken to shield the system

from excess RF interference, and the remaining EMI is isolated to be subtracted from the the primary signal.

Finally, data is collected on secondary emission and the gain profile of a capsule. Multiple runs are conducted to identify the behavior of gain in the system as the anode voltage is increased. These results are discussed in detail and the capsule gain is shown to increase with the increasing field in the diamond.

4.1 Data Collection and Handling

During measurement the photoemission signal is routed through a circuit that contains a KΩ resistor to ground in parallel to an oscilloscopes internal resistance, which is set to 1MΩ. The resulting effective resistance, Eq. 4.1, of the circuit is approximately that of the smaller resistor, as it dominates in this configuration. The pulse is converted by the circuit into a voltage that can be recorded on the oscilloscope. The circuit is protected by a 70V Gas Discharge Tube that will short to ground if the voltage in the circuit becomes too large.

$$\frac{1}{R_{effective}} = \frac{1}{R_i} + \frac{1}{R_{scope}} \tag{4.1}$$

A Tek 3034 oscilloscope is triggered by the resulting pulses in the circuit. Noisiness in a single shot and small instabilities in the flash lamp necessitate that the scope be set to average the data over 16 pulses. The resulting waveforms are stored in a common format for import into analysis software.

In addition to stored data, approximate peak values for the voltage in each signal is recorded for quick examination of the system behavior. Peak gain calculated from these values is typically much larger than when the entire signal is taken into account. Still the peak values and related graphs provide a reasonable approximation of the systems behavior over a range of voltages or pulse energies.

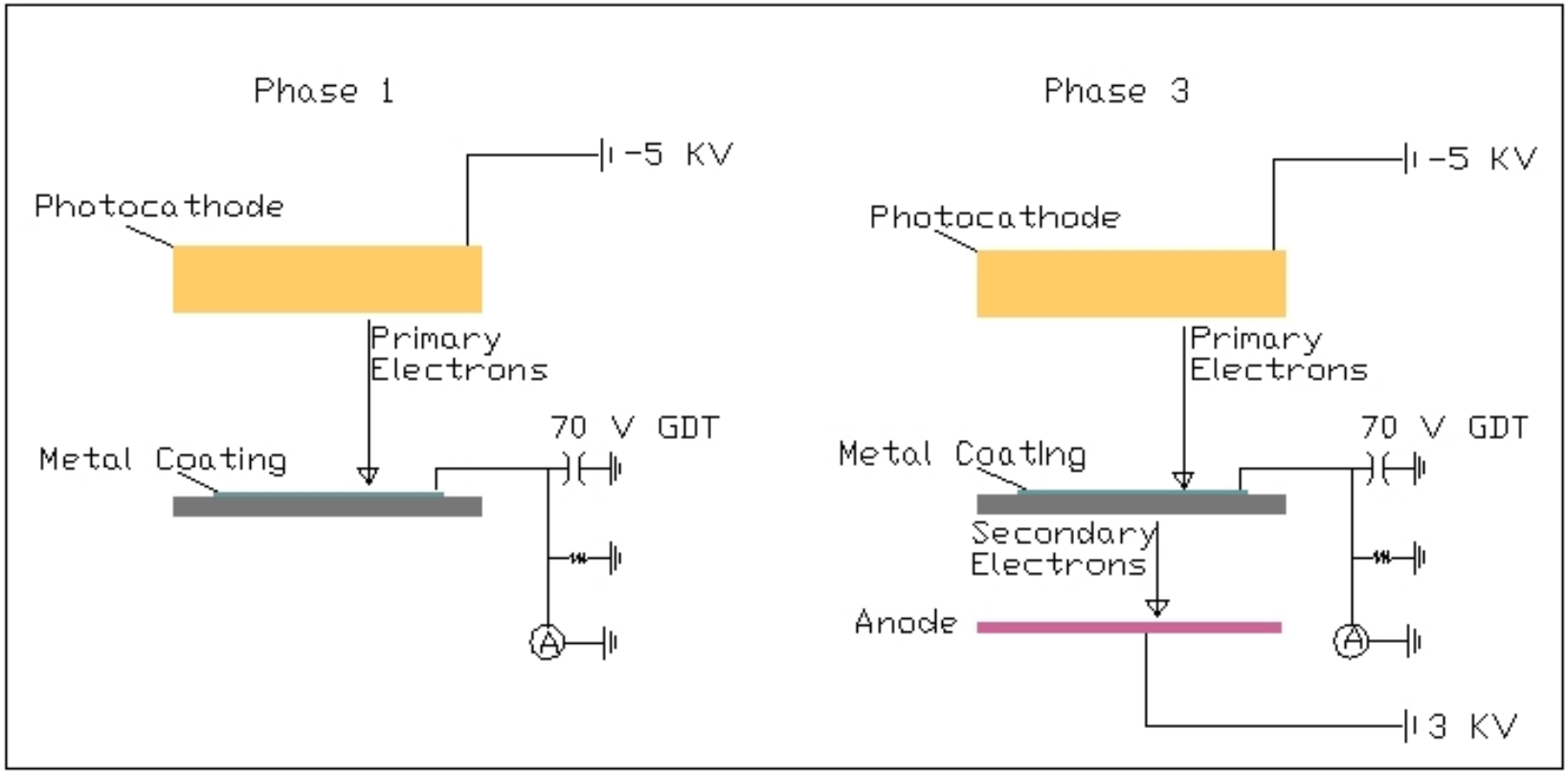

Figure 4.1: CAC Electrical Diagram - Displayed here is the electrical circuit for the CAC when configured for assembly. Both modes of operation are presented in the diagram. Primary electron measurement mode is detailed on the left, while secondary emission mode is on the right.

4.1.1 Integration and Conversion

The two pieces of information that can be derived from this experiment, that are of greatest interest, are the gain in secondary emission and the total charge in each pulse. The total charge in a pulse is based on the integrated pulse voltage and the pulse duration. These values are calculated in a slightly different fashion than the method used in section 2.7. The pulse charge(Q) is calculated from the integration of the photoemission signal over the pulse-duration(t), as seen in Eq. 4.2.

The amplification of the charge pulse through the diamond, or gain, is the result of dividing the amplified secondary signal from the diamond by the primary signal from the photocathode. This can be accomplished by dividing the pulse charges of each signal(Eq. 4.3), or more simply the integrated pulse voltages.

$$Q = \frac{V}{R_{effective}} t = \frac{1}{R_{effective}} \cdot t \cdot \sum_{t_i}^{t_f} v(t) \tag{4.2}$$

$$Gain = \frac{Q_{secondary}}{Q_{primary}} = \frac{V_{secondary}}{V_{primary}} \tag{4.3}$$

4.1.2 Smoothing and Noise Reduction

Even though the systemic noise in the waveforms has been reduced by averaging over multiple pulses, there still remains noise in the signal. While this is not a significant problem near large peaks, in the long tail, as the signal voltage approaches a minimum this can lead to a reduced or negative integral. This is especially important when gain is being calculated.

To combat the effect of noise and obtain a cleaner signal for calculations, smoothing must be applied to the waveforms. For this purpose the stored waveforms are imported into Seasolves' PeakFit software version 4.12. While this software is normally used to analyze data for spectroscopy and chromatography, it contains a smoothing function that is well suited to these purposes. The Savitzky-Golay algorithm, which

is used to smooth the data, employs a local area polynomial fit using a simplified least squares procedure [10]. The main benefit of this method is that it smooths the data without flattening any of the features or reducing peak heights. The result is a smooth curve with the important features preserved that will not result in improper reductions in signal voltage when it is integrated.

4.2 Dark Current and Background

Before proper measurement of the photoemission can occur, any systemic noise is identified so that it may be subtracted from later data. The dark current is examined in two ways. First, the signal inherent in the system is measured with both the light source and the voltage in the off position. The result is a signal that has an effective value of 0V. Next, the dark current with a voltage applied is recorded. During this measurement the light source is still in the off position. Applying a voltage of 5KV to the anode with the photocathode at ground results in a 100μV noise fluctuation about the 0V axis. As will be visible later this is approximately 0.005% of the photoemission for an 800mJ pulse and is therefore totally subsumed by the EMI background subtracted from the actual photoemission pulses.

4.3 Measuring The effect of EMI

The website for the Oriel Xe Flash Lamp makes note that the electro-magnetic interference(EMI) is a particular problem in this type of broad spectrum source that may effect measurement.

> Arc lamp ignition requires high voltage, high frequency pulses to break down the lamp, and a high current discharge to sustain the arc. Ignition creates significant electromagnetic energy, which may occasionally interfere with associated equipment. Even EMI proofed circuits may require extra attention to earthing, cable routing and EMI shielding, to avoid ig-

nition interference. Interference may be more problematic with a pulsed arc lamp system as each pulse requires lamp ignition.[9]

In order to both understand and negate the effects of EMI on the photoemission signal, it is necessary to characterize the EMI background of the system. This is accomplished by directing focused light into the chamber while the photocathode is backed away behind a gate valve. With the photocathode shielded and the voltage supply off, any emitted electrons will simply fly around in the vacuum until they collide with a surface and are reabsorbed.

The background signal registered at the photocathode electrical contact has two major components. The primary signal is the EMI generated by the flash lamp. The second, much smaller and less significant component of the signal, is the result of electrons liberated from other surfaces by the defocused and scattered light beam randomly striking the electrical contact. By isolating the EMI it is possible to identify the major characteristics that are present in the photoemission data.

The EMI is recorded across the full range of possible pulse energies(fig. 4.2). The amplitude of the waveform grows with increasing pulse energy. There appears to be an exponential decay envelope as the signal grows in the time domain.

The waveform that is generated by the EMI from the light source has a high frequency component, Fig. 4.3, that reaches peak value in 100-125ns and decays rapidly becoming indistinguishable from dark current in approximately 1μs. The large amplitude oscillations in this segment, with peaks in the tens to hundreds of mV, have a period of 32ns and exhibit an oscillating decaying envelope with a period of approximately 180ns. This indicates that for the high frequency noise the system rings down quickly after each pulse.

There is a large amount of variance in the HF-EMI peak voltage that does not correlate with pulse energy. This makes the high frequency noise difficult to subtract from signals. Fortunately, the smoothing algorithm mentioned above effectively removes most of the interference leaving only the low frequency EMI to subtract as

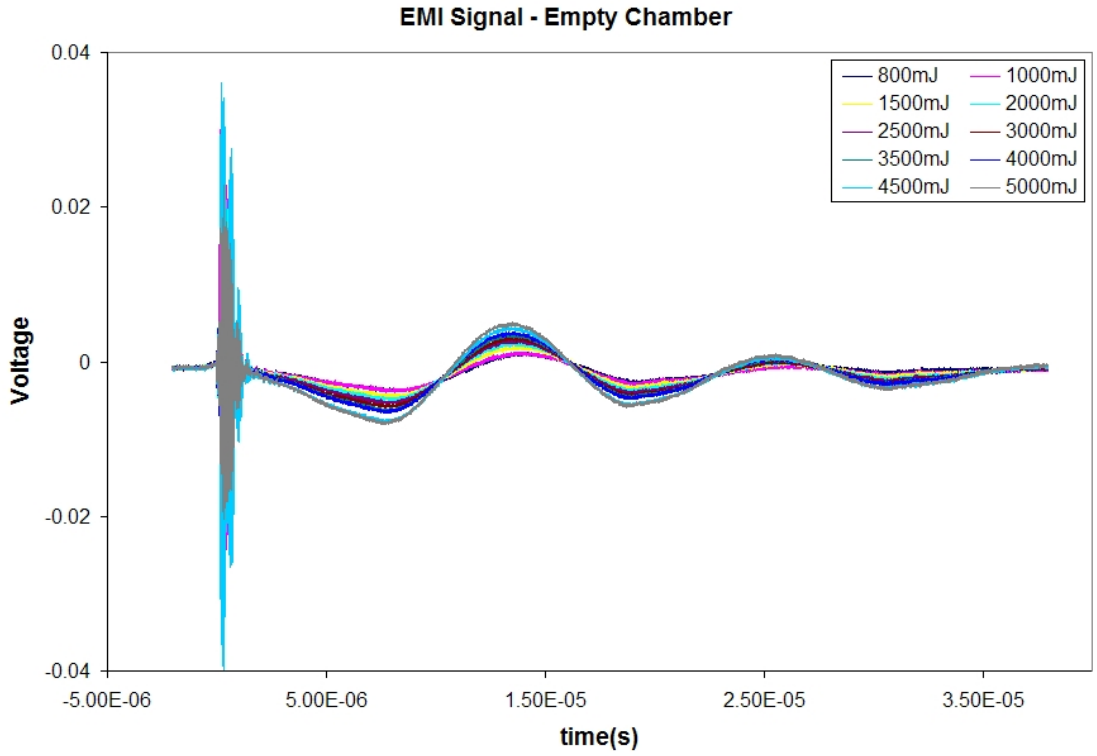

Figure 4.2: EMI Signal, No Shielding - The EMI signal is collected across the full range of possible pulse energies.

background.

The low frequency EMI, Fig. 4.4, has a considerably longer period of approximately 14ms. The peak amplitude for a 5 Joule pulse, which is the highest energy pulse, is approximately 7.5mV with a 5KΩ effective resistance on the circuit. These oscillations occur in the same temporal region as the photoemission pulses, and therefore can interfere directly with photoemission signals. For photocathode emission this is not a significant problem. The LF-EMI may simply be subtracted from the photoemission signal(§4.5) which is much larger than the interference.

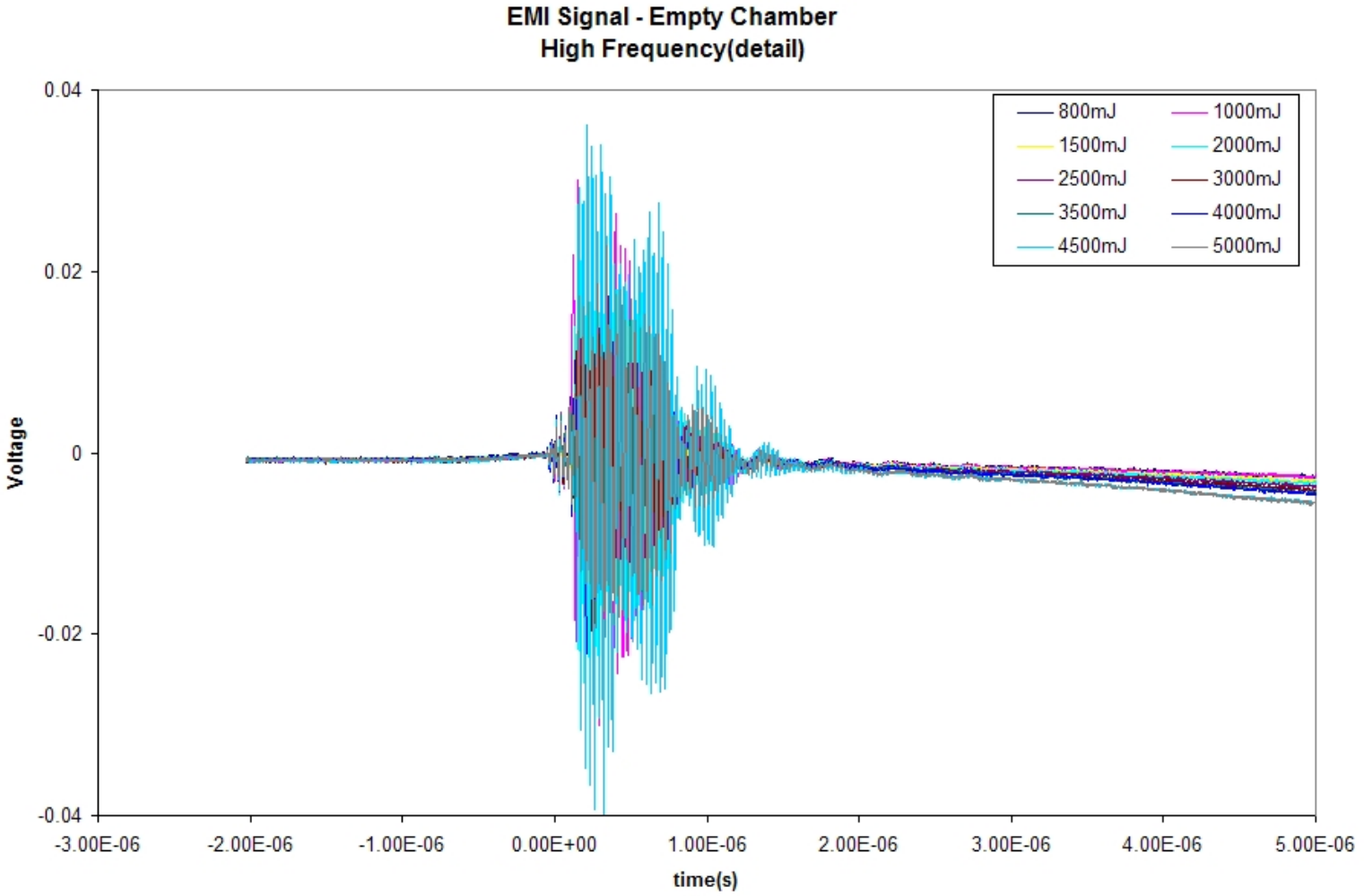

Figure 4.3: EMI Signal - No Shielding, HF Detail - This is the high frequency portion of the EMI signal showing high peaks, short period, and fast decay.

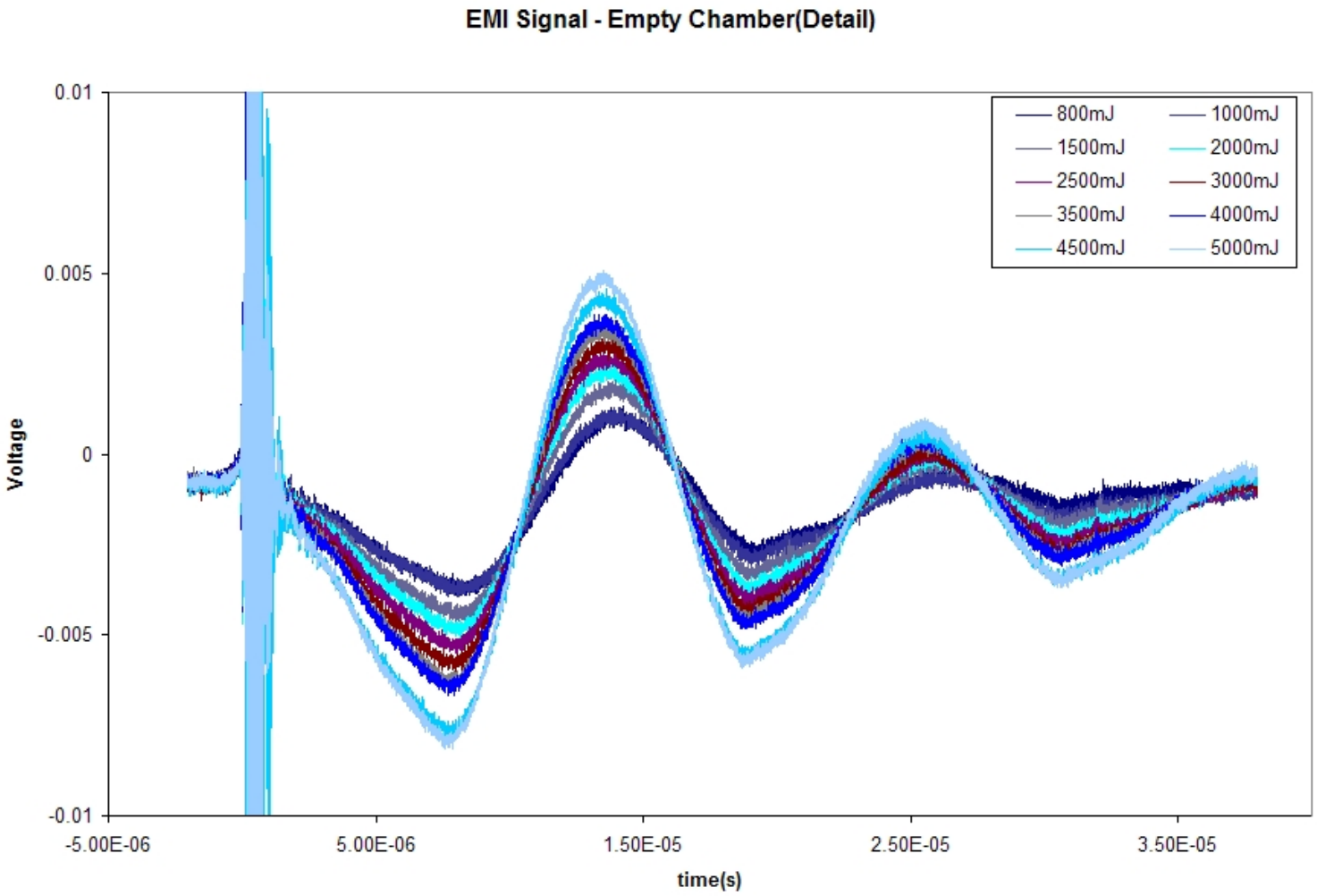

Figure 4.4: EMI Signal - No Shielding, detail - The EMI signal is expanded along the vertical axis to reveal how the waveform changes with increasing pulse energy.

4.3.1 The Necessity of RF Shielding

With the inclusion of a DECA in the beam-line, and the related reduction in light reaching the photocathode, the photo emission signal is significantly weaker. Consequently, to make the signal more easily observable, a larger effective resistance, $\sim$20KΩ, is required. This greatly increases the size and effect of the low frequency EMI as voltage read at the oscilloscope, which is proportional to $R_{effective}$ of the system. In actuality the EMI is unchanged, but the photoemission signal is smaller due to the decreased light throughput. The effect of the EMI in the unshielded system is visible in Fig. 4.5.

To negate or significantly reduce the impact of the EMI in the system, RF shielding is required. Shielding is accomplished by wrapping all cables with aluminum foil that is then connected to ground. The crumpled foil housing presents few surfaces that act as antennae to re-resonate the EMI frequencies and effectively reduces the interference. The most significant reduction is seen in the low frequencies(fig. 4.6).

It should be noted that the voltages in the two graphs result from different effective resistances. All other variables are the same. These two are presented to emphasize the effect of the EMI on the photoemission signal and how much cleaner the signal is when shielding is added to the system.

4.3.2 Remaining EMI After Shielding

Despite the reductions in EMI due to shielding, there may still be interference in the photoemission signals from the light source. To determine if there is residual EMI in the system that must be subtracted, a Schott glass filter is inserted into the beam line outside of the CAC. The filter used is a CVI Laser CG-OG-550. It effectively blocks all light below 550nm. Therefore, no UV light from the flash lamp is entering the CAC. The resulting signal, fig. 4.7, is generated solely by EMI. This background is subtracted from all data recorded after the system is shielded.

The remaining signal, after the system is shielded, is considerably smaller than

the those in Fig. 4.2. This is not obvious until the change in effective resistance is taken into account. The earlier measurements used a 5KΩ resistor, while the later uses a 50KΩ resistor. This makes the final post shielding EMI ten times smaller than it appears in the graph when compared to the unshielded EMI.

4.4 Pressure Increases in the CAC

During all measurements involving the injection of light pulses into the system, it was noted that significant increases in pressure occurred. This is especially true for early measurements of the photocathode and EMI. Measurements attempted for system pressures at or above a maximum value of $P_{max} = 1.0 \cdot 10^{-8}$Torr resulted in random voltage fluctuations as measured at the oscilloscope, indicating the systems inability to

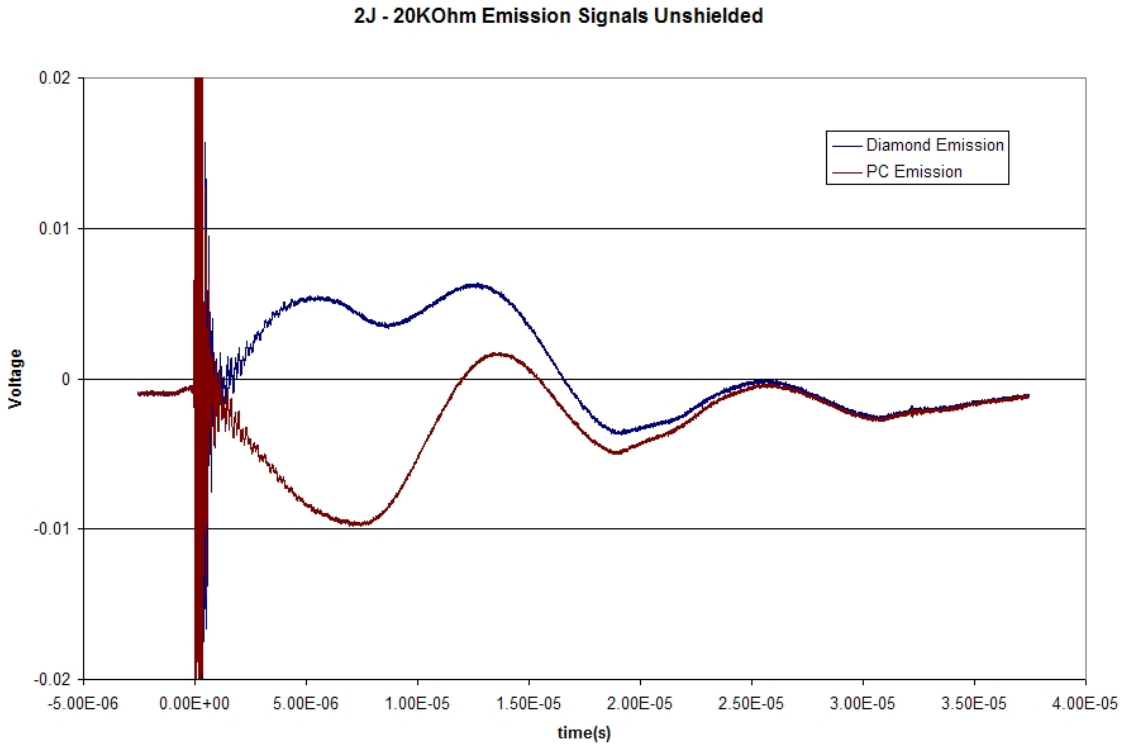

Figure 4.5: Raw Emission Signals from Photocathode and Diamond in an Unshielded System

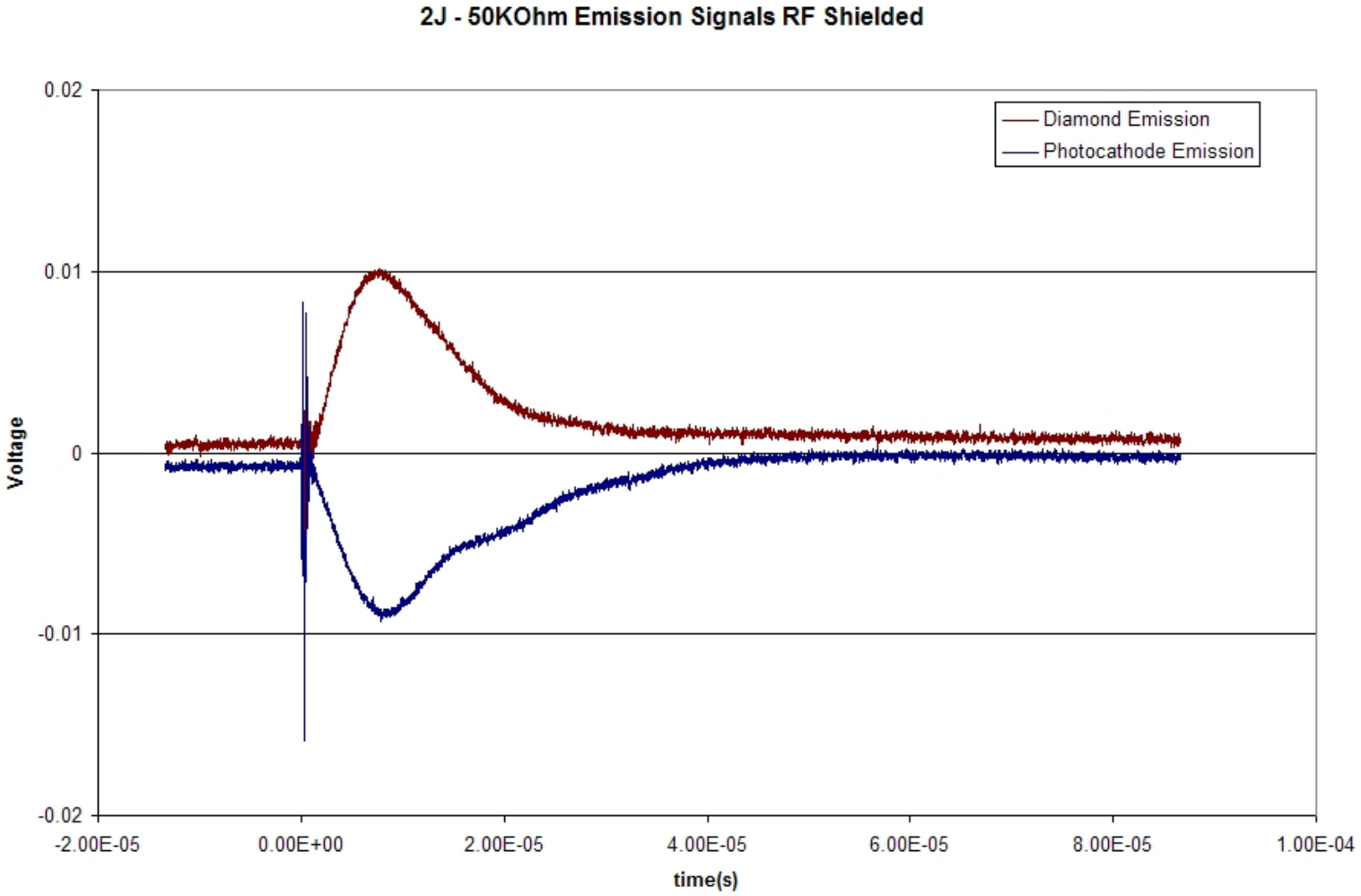

Figure 4.6: Raw Photocathode and Diamond Emission, RF Shielding on all Cables

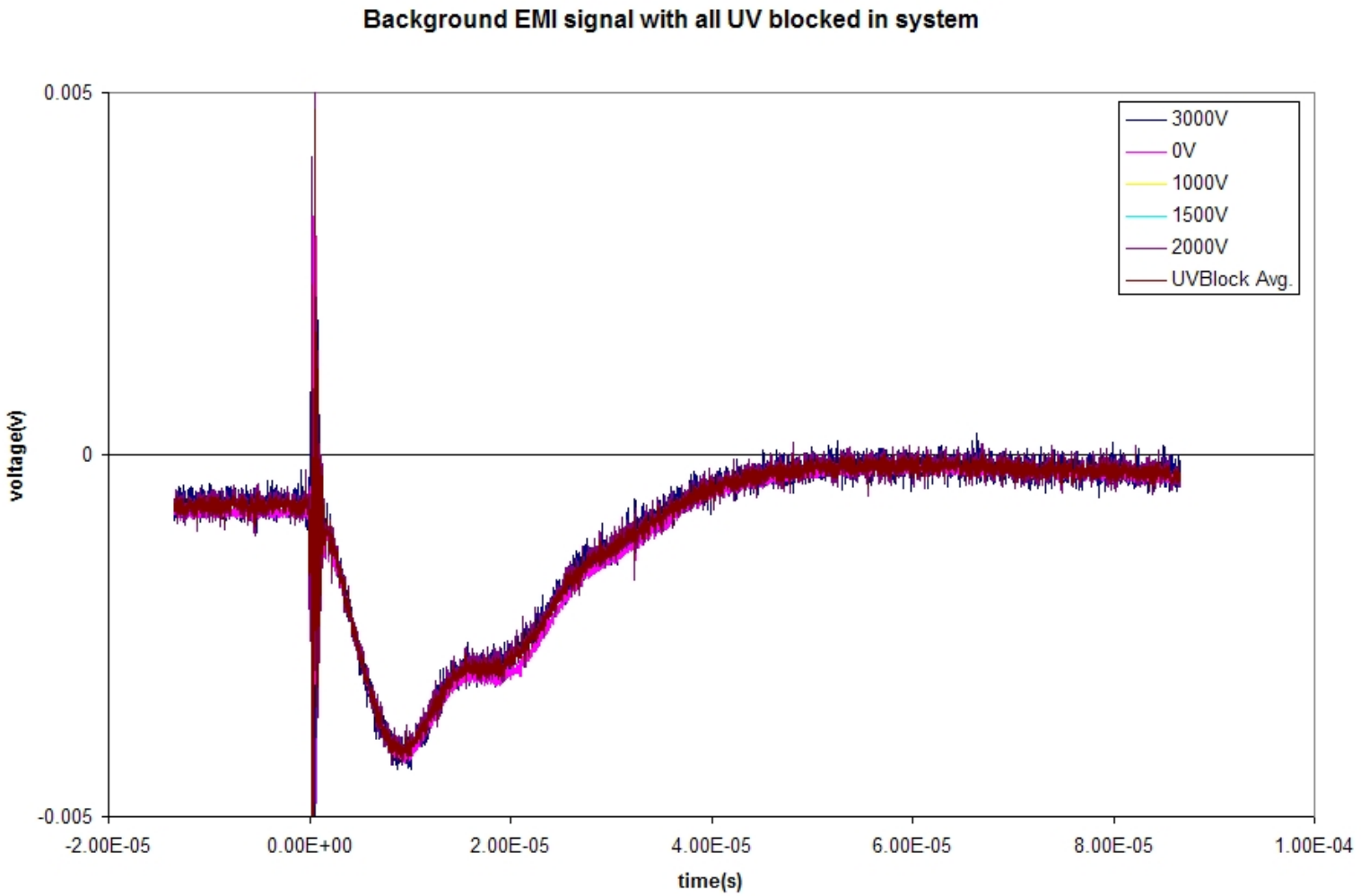

Figure 4.7: EMI Background with all UV Blocked - Remaining EMI background after insertion of a Schott glass filter that blocks all light below 550nm. This is the true EMI signal as all photoemission in the system has been blocked.

standoff the voltages required in this pressure range while the light source was active. However, once the light source was shut-off, voltage fluctuations ceased. When the system pressure was brought below P_{max} there were no such voltage fluctuations, even during light source operations. After an initial full system bake and approximately 24hrs pump-down, the base pressure in the CAC was $8.0{\cdot}10^{-10}$Torr. During the two initial successive runs to measure the EMI, the pressure was shown to increase by up to $\frac{1}{2}$ the next larger order of magnitude throughout an individual measurement, depending on pulse energy. In Fig. 4.8 we see the system pressure as related to pulse energy for three data series, collectively the earliest measurements made in the CAC. The pressure for each point is recorded after 16 pulses, by which time the pressure had reached a stable maxima. This was confirmed by allowing the light source to run until the maximum pressure stabilized for a given pulse energy. The vacuum was allowed to recover to base pressure between each of the measurements.

There are two possible explanations for the increase in pressure during light source operation that can be easily accounted for in this system. They both explain the increase in pressure. First, the light pulses are cleaning the surface of the photocathode(as well as other surfaces that light is incident on) and causing particulate emission – on top of electron emission – in the chamber. Second, the light pulses are causing heating in the gaseous particles in chamber, thereby raising the system pressure.

A simplistic approximation based on the Ideal Gas Law reveals that neither of these phenomena is likely the lone culprit responsible for the increase in pressure. If temperature is held constant and the pressure increase, which peaks at about $5.2{\cdot}10^{-9}$Torr for a 5J pulse, is due to surface particulate emission, then the number of particles ejected from surfaces is $\sim 3.3{\cdot}10^{14}$. This is about 1100 times the approximated number of electrons emitted for a 5J pulse(§2.7) or 0.13 monolayer ($1ML = 2.5 \cdot 10^{15} particles/cm^2$[16]) of particulates. If the number of particles is held constant and the pressure increase is due to a rise in temperature in the residual gas

in the chamber, then the necessary change in temperature would be a 1950K increase. Which, for the approximate number of particles in the system, would be equivalent to a systemic increase in the average kinetic energy of $frac32Nk_BT = \sim 2.0\mu$J. This is more than covered by the incident light energy (2.315mJ) in the chamber, but it is unlikely that such a large fraction of the light, 0.1%, will collide with free particles. Therefore, neither of these is the sole actor in the pressure increase. It must be a combination of both, coupled with other factors like heating in the photocathode, or electron induced gas desorption in the anode[16].

After additional bake-outs and continued operation, the system base pressure reached a minimum of $4.8{\cdot}10^{-10}$. In addition to this, during measurements where the base pressure was this low, it was normal to make a measurement and not have the system pressure exceed $9.0{\cdot}10^{-10}$. This occurred while the DECA was in situ. This may indicate that the photocathode was a large factor in the increasing pressure, since there is much less light making it to the photocathode. Assuming that photocathode ejected material was a large part of previously recorded pressure increases then there is a likelihood that there was an increase in the QE during this time.

4.5 Photoemission from an Unobscured Coper Photocathode

Before secondary emission and gain can be measured, primary emission from a unobscured, or bare photocathode, is measured. This measurement ensures that the CAC is operating properly and that the photocathode is emitting in a uniform manner. These measurements will serve as a metric by which to gauge the approximate UV throughput of the metalized diamond, and approximate the quantum efficiency of the photocathode.

In order to measure the photoemission from a copper photocathode, the CAC is arranged such that the wire mesh anode is held at a high positive potential, up to

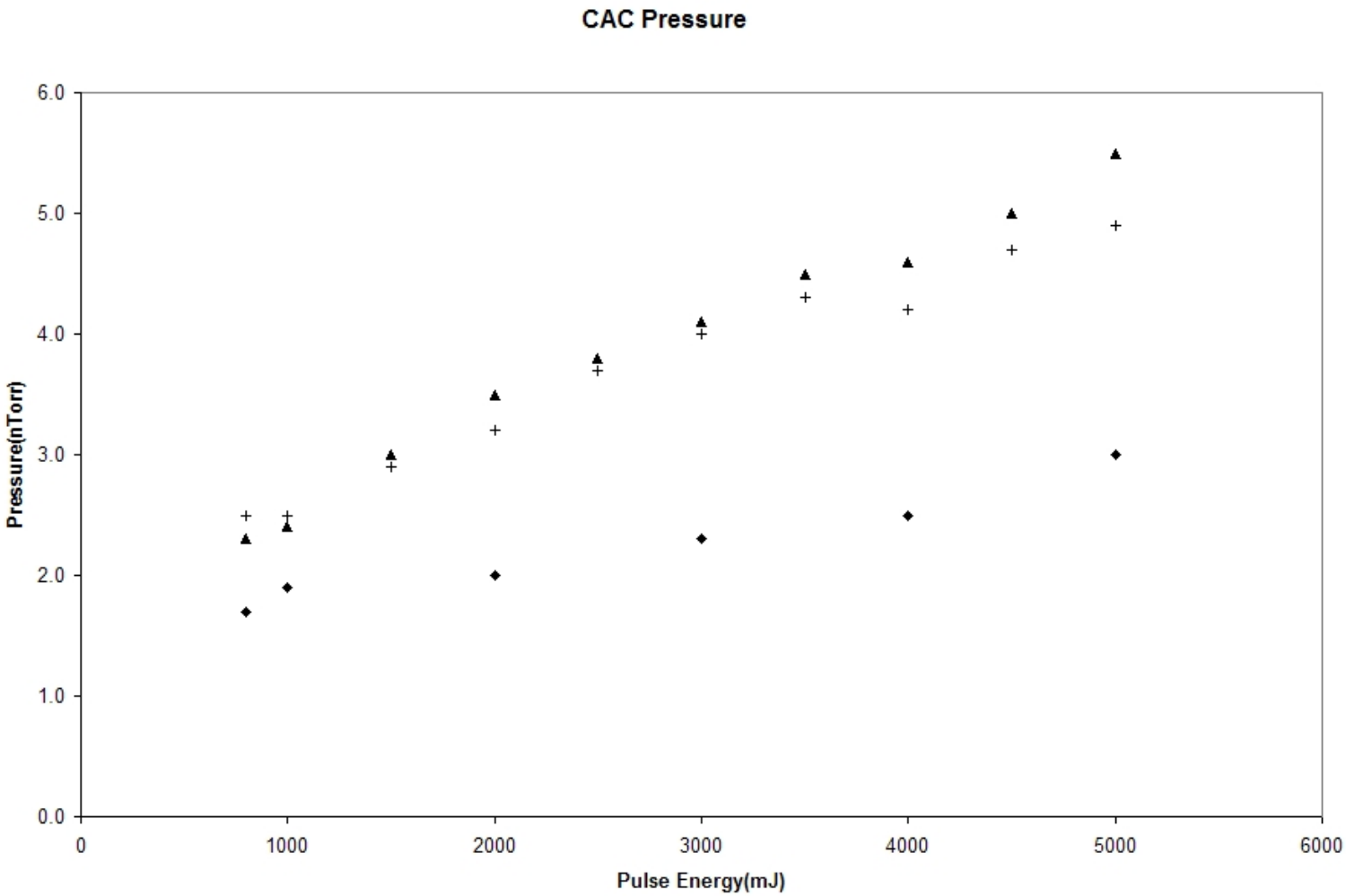

Figure 4.8: CAC Pressure vs. Increasing Pulse Energy - The pressure in the CAC is shown to increase linearly with pulse energy for three separate data sets.

+5KV, relative to the photocathode, which is at ground. The electrical configuration in photocathode-only-mode is similar to the diagram on the right in fig. 4.1. The primary difference is that since there is no diamond the voltage is applied to the anode. This requires that measurement of photoemission current take place through the photocathode, which ensures that all electrons emitted from the surface are extracted and counted.

Photoemission is sampled over the available range of pulse energies and anode voltages. For each run a particular anode voltage is set and a waveform and peak voltage is recorded for each stop as the pulse energy is increased from 800mJ to 5J. Waveforms are averaged over 16 pulses to reduce systemic noise. Data is collected in this fashion for anode voltages from 0-2KV in 500V increments and at 4.5KV and 5KV. To fill in the gaps in anode voltage data expediently, the peak voltage is recorded in data sets 2.5KV-4KV.

The graphical representations of data for these measurements are presented in Figures 4.9 and 4.10. A few important observations arise from these data. First, the magnitude of the photoemitted charge depends more on the pulse energy than on the anode voltage. This is demonstrated when the anode voltage is held constant while the pulse energy is raised. As the pulse energy increases the pulse charge and peak voltage both increase significantly. However, for anode voltages greater than zero the increase in emission across a particular voltage is small. Second, the photocathode, behaves in a uniform fashion. For given pulse energy the initial photoemision is small for anode voltage = 0V. When the anode voltage is increased there is an abrupt turn on and the photoemission appears to asymptotically approach a maximum value. The maximum photoemission increases in a regular fashion with pulse energy. Finally, the photoemission is larger than expected when compared to the approximation(§ 2.7, Table 2.4). Possible sources for this discrepancy include errors in the approximation, higher than expected UV transmission through the thin metal film deposited on the diamond, or multi-photon emission. In any case, this is not a problem, given the

consistent behavior of the photocathode. It will generate more primaries followed by more secondary emission in the diamond which will provide a larger signal to measure.

The larger than expected photoemission negates the need for increasing the QE of the photocathode. This is beneficial, since it will be difficult to determine without an accurate estimate of the incident beam energy. It may be possible to adjust the approximation after the DECA is in line and the UV transmission of the metalized diamond can be evaluated by a comparison of photoemission before and after insertion. However, it seems improbable that any further QE enhancement will be possible beyond what may have been achieved during the 24hr bake-out and initial bombardments that were performed after the photocathode was inserted into the chamber. This observation arises from the data collection order and duration of the data collection cycle.

If it is assumed that the total UV incident at the photocathode ranges from ∼0.5-2.88mJ (§ 2.7) and 163 measurements were performed with a minimum of 16 pulses each at 12Hz, then there should have been some QE enhancement in the ∼3.5 minute bombardment[11]. This would have been noticed in the data sets collected for anode voltages in the range from 2.5 to 4.0KV as they were collected immediately after the initial run to fill in gaps. Any enhancement would have produced a feature that stood out above the peak voltage vs. pulse energy curve in Fig. 4.9. The absence of such a feature indicates the lack of QE enhancement in the later photoemission data. Although, it is possible that some enhancement has occurred. There is also a not-insignificant number of early measurements where the data is considered suspect and discarded due to a lack of understanding of the system. It is possible that the bulk of enhancement could have occurred during these runs, as there were considerable increases in the system pressure as measurements were collected with light pulses injected into the system(see §4.4). Any increase in the QE that has occurred will be maintained as the photocathode is stored in 10^{-9} Torr vacuum during the reconfiguration of the CAC into capsule assembly mode.

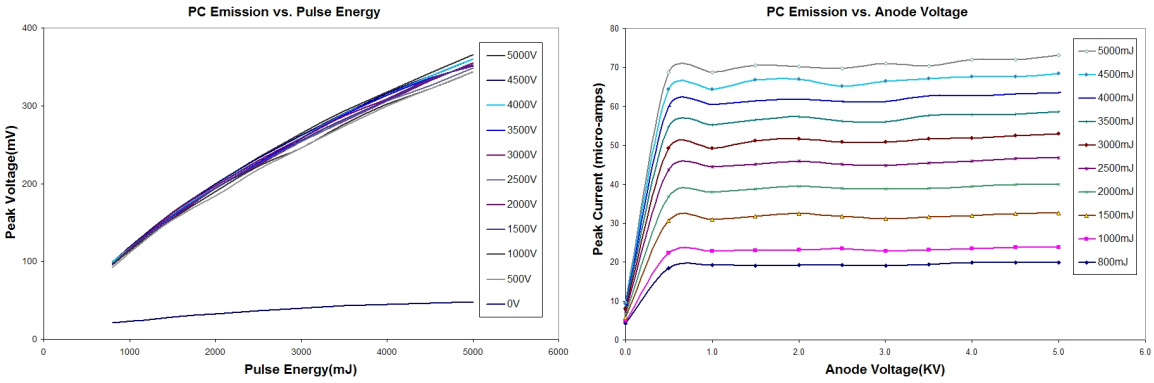

Figure 4.9: Peak Photoemission Voltage, Unobscured Photocathode - These graphs display data on the relationship between pulse energy, anode voltage and peak pulse voltage. Left - Peak voltage increases with pulse energy, anode voltage is held constant. Right - While pulse energy is held constant, peak voltage rapidly approaches a horizontal asymptote as anode voltage is increased.

4.6 DECA Preparation and Brazing

Simultaneously to the emission measurements of an unobscured photocathode, the preparation of a DECA sample was underway. A 300μm thick electronic grade diamond sample was etched according to the recipe described in §3.3.1. Following the etch, the diamond was sputtered with a film of TiPt in two steps(Fig. 4.11). The thickness of this film is unknown as the crystal monitor was not functioning during this deposition. It is, however, optically transparent. The metalized diamond is then inserted into the hydrogenation chamber, with the metalization layer protected by a cylindrical alumina standoff and a monolayer of hydrogen is implanted on the surface. After hydrogenation, the diamond sample and other elements that comprise the DECA are brazed according to the process described in §3.3.5.

Upon completion of the braze the DECA is removed from the furnace and leak-checked. The results show that the DECA is vacuum tight. The helium leak rate was $1.2 \cdot 10^{-9} \frac{Torr \cdot L}{s}$, which is consistent with the leak rate of the Viton ring that seals the test chamber. Visual inspection of the DECA shows that a the eutectic material used in the braze has flowed into the center aperture and is partially occulting

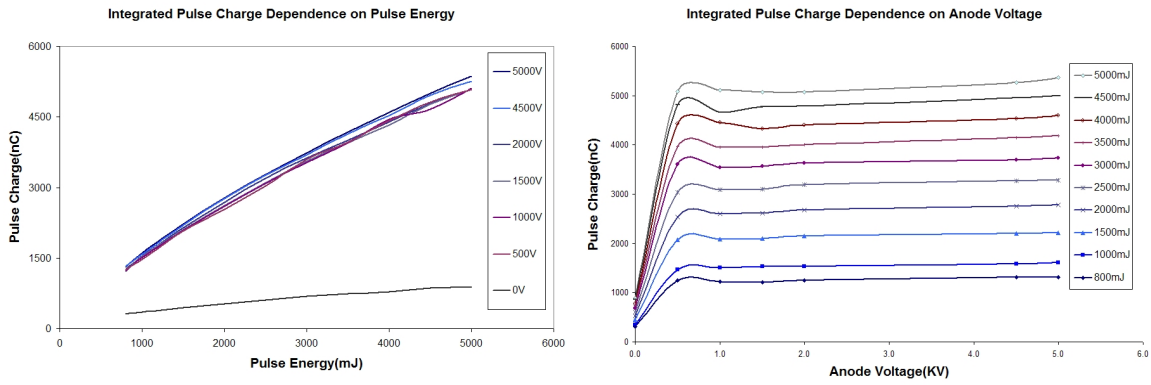

Figure 4.10: Integrated Pulse Charge for an Unobscured Photocathode - These graphs display data on the relationship between pulse energy, anode voltage and integrated pulse charge. Left - Integrated Charge increases with pulse energy while the anode voltage is held constant. Right - For a constant pulse energy the pulse charge asymptotically approaches a maximum value.

the metalization layer. Additionally, the metalization layer is substantially more transparent than it was before brazing. This is either a result of evaporative thinning or a chemical reaction, either of which could have occurred under the high temperature involved in the brazing process. There is good electrical contact between the diamond and Nb washer with a resistance of approximately 1.68KΩ. After these tests and observations the sample is loaded into the alignment guide(Fig. 4.12) and inserted into the CAC(Fig. 4.13). The CAC is baked to ∼150℃ for 24hrs, then pumped down to a base pressure of $\sim 4.8 \cdot 10^{-10}$ Torr before secondary emission measurements begin.

4.7 Reducing Diamond Photoemission

As was stated in §2.7, diamond is a primary emitter for photon energies above the band gap energy. In actuality the diamond begins to emit at around 290nm, but the photoemission is small at this wavelength and is still barely detectable at 260nm with QE of $\sim 10^{-8}$ [12]. Should the photoemission from diamond be large compared to the secondary emission, it could be completely obscured. To prevent this from occurring, the diamond photoemission must be reduced to the lowest possible level.

Figure 4.11: Metalized Diamond: Right - metalized diamond in the sample holder used during deposition. Left - The same diamond after metalization from a slightly higher angle. Near the center of the diamond the optical transparency is revealed by the visibility of a hole in the sample holder.

Isolation and measurement of diamond photoemission is accomplished by removing the electrical connections from the photocathode and biasing the anode with a high positive voltage relative to the metalization layer. 2000mJ pulses are introduced into the chamber and the photoemission signal is recorded, then an electronic grade diamond is inserted into the beam-line outside the chamber. The extra diamond window will block the majority of light with photon energies above the band gap energy, and effectively eliminate diamond photoemission. The photoemission signatures are presented in Fig. 4.14 along with the isolated signal. All measurements made after this point will include a diamond window in the beam line.

The addition of the diamond window is beneficial in that it blocks a significant portion of the diamond photoemission. However, it is problematic in that it also reduces the intensity of light that causes the photocathode to emit, thereby making the photoemission smaller. To counter this effect, the $R_{effective}$ of the system is increased to approximately 20KΩ. Increasing $R_{effective}$ will allow smaller signals to be measurable, with the caveat that it will simultaneously broaden the pulse width. Once the system resistance is changed it is necessary to investigate any remaining unidentified photoemission from the diamond.

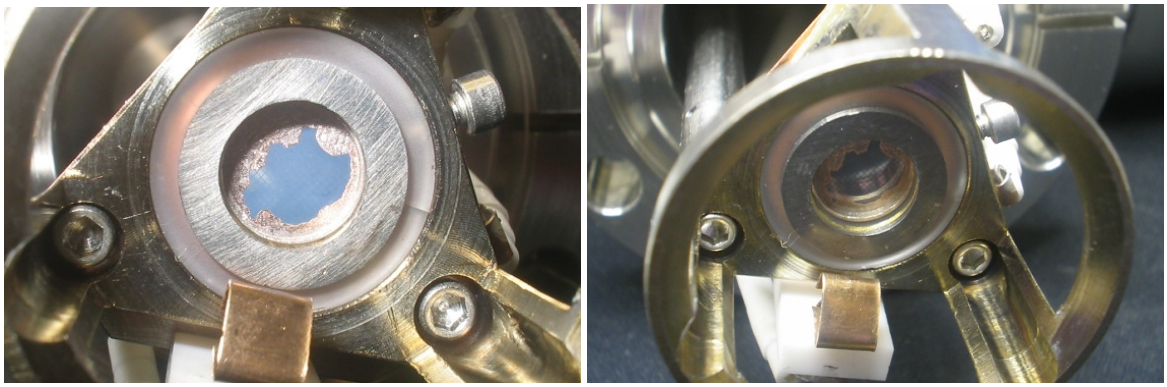

Figure 4.12: DECA in the Alignment Guide - Post Braze - DECA in the alignment guide awaiting insertion into the CAC as seen from two vantage points. The enhanced optical transparency after brazing is highlighted by the visibility of the wire mesh anode through the diamond in both images.

4.8 Residual DPE

Despite the addition of a diamond window there is a small residual diamond photoemission. This is most likely due to the flow of eutectic material around the edges of the central aperture of the DECA. The eutectic material contains Ti(ϕ=4.33eV), Cu(ϕ=4.53-5.10eV), and Ag(ϕ=4.64-4.74eV); all of which have work functions that make them primary emitters under these conditions. In addition to the eutectic material, the metalization layer contains Ti and Pt. Platinum will be largely occluded as its work function(ϕ=5.64eV)[13] is greater than the band gap energy of diamond.

The residual diamond photoemission is measured in the same fashion as in §4.7, with the exception that it is characterized over range of voltages for source light energy of 2000mJ. The resulting data is presented in Fig. 4.15 and Fig. 4.16. Both sets of graphs have the same layout. On the left is the is the signal voltage integrated over the pulse. On the right is the pulse charge calculated from the signal voltage. By the time this data has been recorded there has been a significant reduction in output

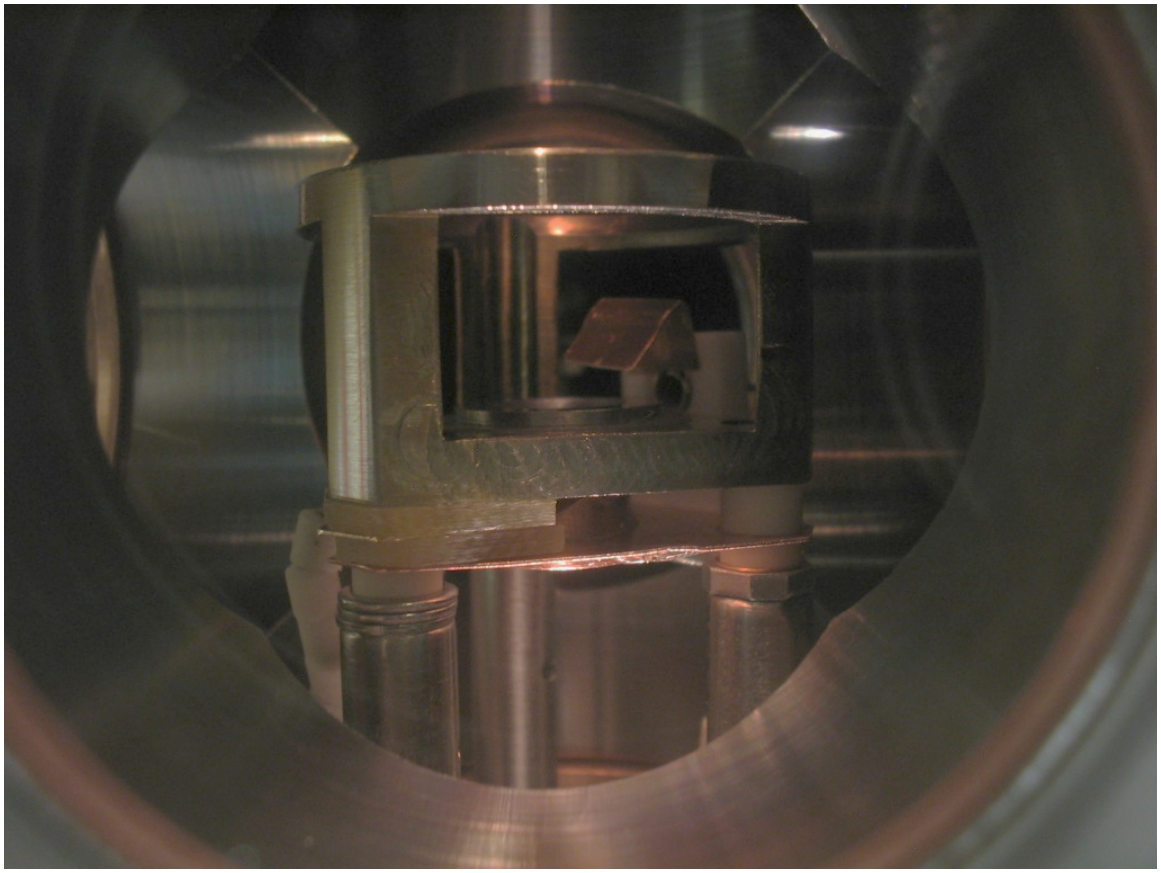

Figure 4.13: DECA and Alignment Guide in the CAC - DECA in the alignment guide ready for testing awaiting the completion of bake-out and pump-down.

from the diamond and the effective system resistance has been increased to ∼50KΩ.

From these graphs it is visible that the residual diamond photoemission, with a maximum value of ∼35nC is $\frac{1}{5}$ the size of the 190nC pulse charge recorded above. The result is an ∼80% reduction in photoemission from the diamond. Whatever the source of the residual photoemission, cutting it further with more filters will reduce the photocathode emission to a nearly unmeasurable level and make gain measurements exceedingly difficult. Therefore, the only way to deal with this photoemission is to measure and subtract it out. This will isolate the electron gain emission signal.

This residual diamond photoemission data also serves to reinforce the idea that the system is operating uniformly, and points to a possible explanation of the some of the

structural aspects of the photocathode emission reported earlier(§4.5). Comparing these graphs with those in Fig. 4.9, there is an obvious structure in the data recorded around 2.5KV anode voltage. This is interesting considering that the photocathode data was recorded in series of increasing pulse energy with the anode voltage held constant, while the diamond emission data is recorded by increasing anode voltage and holding the pulse energy constant. The existence of this structure in both data sets points to a systemic anomaly in the anode, as it is the only consistent factor. This is further supported by the enhancement generated when the photocathode is advanced into its forward position.

4.9 Secondary Emission Amplification from Diamond

Three signals are involved in the measurement of secondary emission and gain from the diamond. First, the raw primary photoemission is measured with a potential of

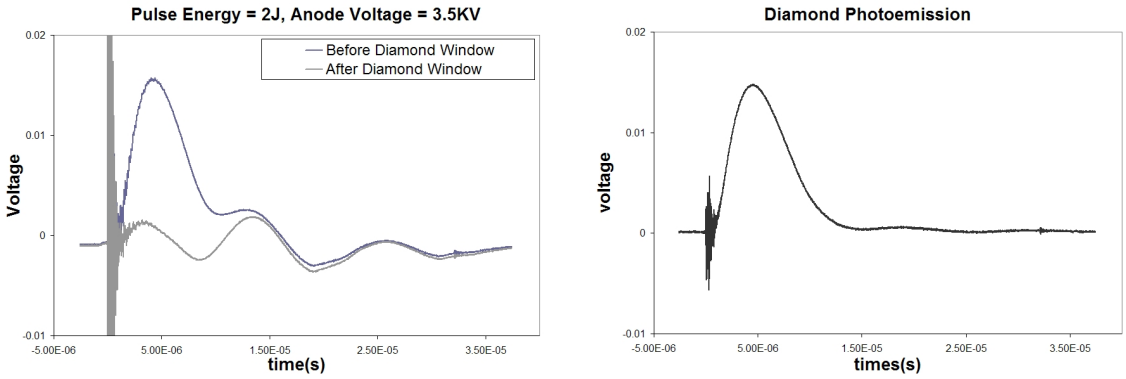

Figure 4.14: Isolation and Reduction of Diamond Photoemission - These graphs demonstrate the reduction of diamond photoemission through the inclusion of a diamond window in the beam-line external to the CAC. Left - photoemission signatures before and after insertion of diamond window. Right - isolated diamond photoemission, pulse charge = 190.16nC. These measurements were made prior to the implementation of RF shielding. R_{eff} for the system is $\sim$5KΩ.

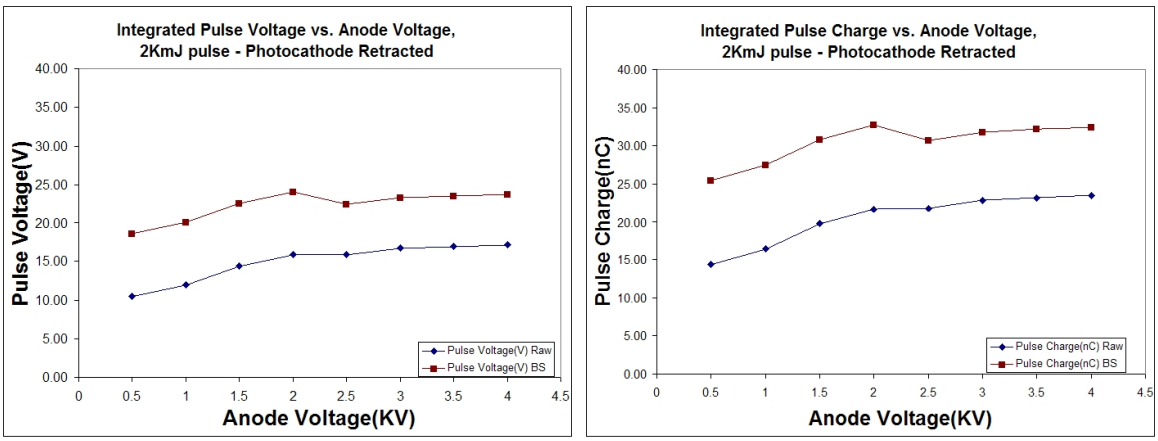

Figure 4.15: Diamond photoemission, Photocathode retracted - Residual diamond photoemission with a diamond window in the beam line to reduce the large diamond photoemission. The retracted photocathode does not contribute to the signal.

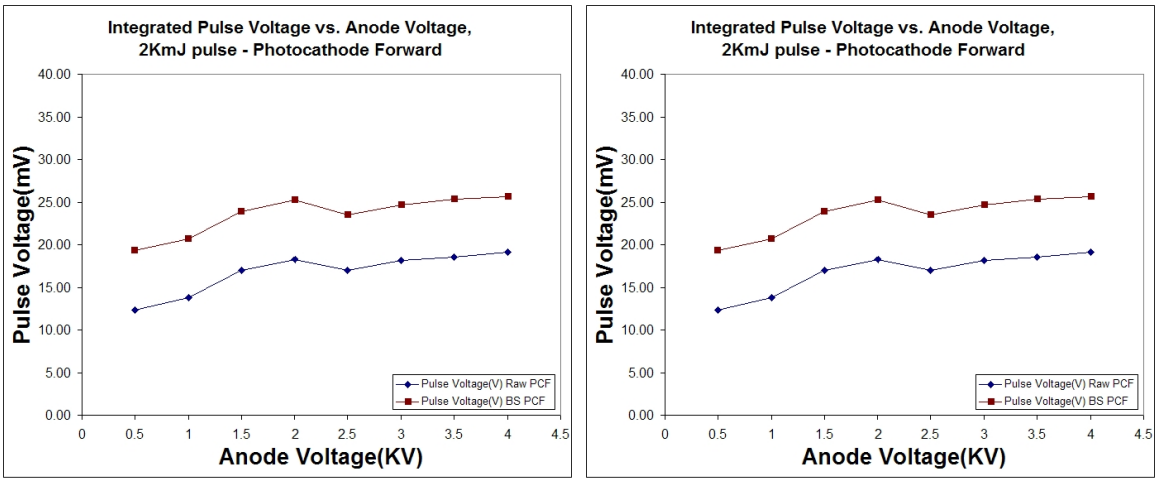

Figure 4.16: Diamond photoemission, Photocathode forward - Residual diamond photoemission with a diamond window in the beam line to reduce the large diamond photoemission. In this set the photocathode is forward and electrically connected. Its contribution to the signal is observable in comparison with fig. 4.15.

-5KV applied at the photocathode and zero voltage applied at the anode. The signal is collected at the metalization layer and has a negative value, as it is the result of the negative charge impinging upon the diamond metalization. Second, the photocathode voltage is set to 0V and the anode voltage is turned on to a positive value in the kilo-volt range and the background diamond emission is measured. The resulting signal is

positive, due to the photoelectrons being carried away through the diamond and emitted into vacuum. The actual measurement here is the replenishment current flowing into the metalization layer to recombine with holes that were created by background photoemission in the diamond. Third, the combined gain electron emission and diamond photoemission is measured. This measurement uses the high voltage settings applied to the photocathode and anode from the two previous measurements. The raw signals generated by a 2Joule pulse, with -5KV applied to the photocathode and 1.25KV at the anode, for each of the three measurements described are presented in Fig. 4.17. The emission signals analyzed here are representative samples of the other emission data collected in this run.

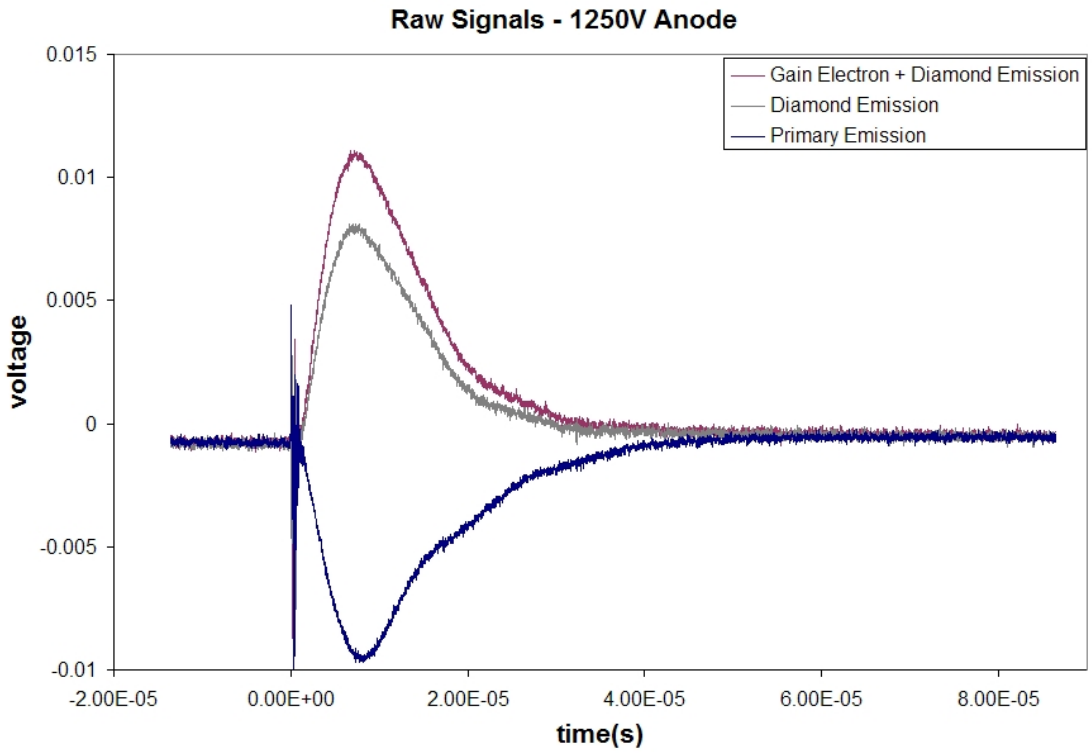

Figure 4.17: Raw Emission Signals from a Diamond Amplified Photocathode - This data is for a 2Joule flash lamp pulse. The cathode voltage is -5KV, and the anode voltage is 1.25KV. Each signal corresponds to one of three modes of operation. In order, from bottom up, they are cathode only, anode only, both anode and cathode.

To obtain a clean primary emission signal, the raw primary is smoothed using the method described in §4.1.2 and the previously smoothed version of the EMI background (Fig. 4.7) is subtracted. The resulting smooth primary is then inverted for later comparison with the secondary emission. Fig. 4.18 displays the results of the operations detailed above. The total primary charge is calculated by numerically integrating the pulse, dividing by the system resistance(50KΩ), and multiplying by the pulse duration as in Eq. 4.2. For this particular pulse the total primary charge is $\sim$12.13nC with peak current of 110nA.

Secondary emission is the amplified photoemission current emitted from the diamond into vacuum. By subtracting the raw diamond emission from the raw gain and emission signal, the gain electron signal is isolated. There is no need to subtract additional background from this result. Since each signal contains EMI, it is effectively removed by subtracting one from the other. The raw gain electron signal is then smoothed and the primary emission signal is added to yield the secondary emission signal. Both the electron gain and secondary emission are displayed in Fig. 4.19. As with the total primary charge, the total secondary charge is obtained by numerically integrating the pulse. The resulting charge is 18.80nC. The secondary emission pulse has a peak current of $\sim$170nA.

It is reasonable to construct the secondary emission signal in this fashion, because the primary electrons lose all of their energy to scattering, collisions, heating, and creation of electron/hole pairs. The incoming primary current is normally read as a negative pulse because the negative charge carriers, electrons incident at the diamond metalization, are measured. When the gain electron signal is measured, the primary pulse is entirely negated and a positive pulse signal is measured instead. This indicates that enough electron/hole pairs are being produced and separated that the incoming primary pulse is entirely subsumed in recombination with holes generated in the production of secondary electrons. The positive electron gain signal indicates that sufficient charge is being carried away from the recombination region by the field

in the diamond and emitted into vacuum to draw replenishment current from the measurement circuit. Therefore, the positive charge carriers, holes, are actually being measured.

Gain is calculated by dividing the total secondary emission charge by the total primary emission charge. This has the same result as using the integrated pulse voltages. For a 1250V anode and 5KV photocathode stimulated by light from 2J pulses, the gain is found to be $\frac{18.80nC}{12.13nC} = 1.55$. This equates to a 55% increase in the output due to secondary emission amplification, or an additional 41.6 billion electrons. While the gain is not as large as expected, it is none the less significant, since this is the first instance of an operating Diamond Amplified Photocathode.

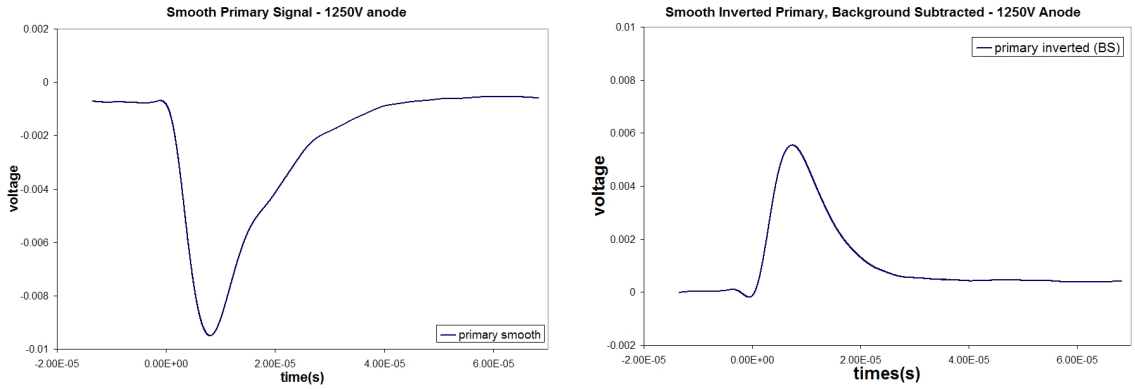

Figure 4.18: Smoothed and Inverted Primary Photoemission from DAP Left - smoothed primary photoemission in a diamond amplified photocathode. Right - Inverted smooth primary photoemission with background subtracted. For both the pulse energy is 2J, cathode voltage is -5KV, and anode voltage is 0V.

4.10 Gain vs. Field in Diamond

Three separate runs of data were collected in order to characterize the secondary emission amplification of the DAP against the field in the diamond. These sets all have light source pulse energy of 2Joules to deliver constant primary electron energy, and were measured using the same technique as in §4.9. The three runs are presented

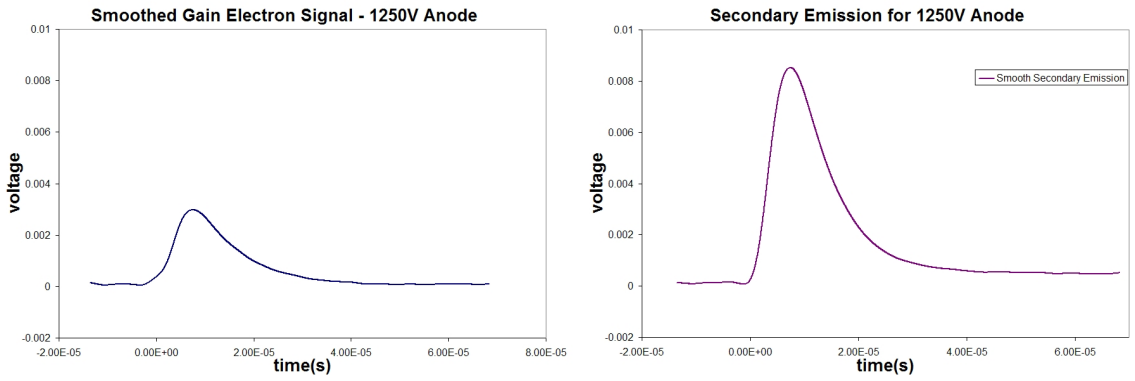

Figure 4.19: Gain Electron and Secondary Emission from DAP; Left - gain electron signal comprised of secondary electrons. Right - secondary emission signal, which is the sum of the primary emission and gain electron signals. Pulse energy is 2J, cathode voltage is -5KV, and anode voltage is 1.25KV.

together in Fig. 4.21 – plotted against voltage, and in Fig. 4.22 – plotted against field, with related error bars. From these graphs there appears to be an initial linear enhancement in the secondary emission amplification. As the anode voltage is raised, the slope levels off to asymptotically approach a maximum value. This is similar to previous results reported by this group[14] on the behavior of secondary amplification with increasing voltage for a similar diamond. However, the previous results indicate that the increase in gain should be much larger than is seen here, and the asymptotic approach to a maximum value occurs at a much higher field. Therefore, the gain should be linearly increasing in this field range.

It should be noted that throughout the collection of data for each run, the system pressure was increasing above the base pressure of $4.8 \cdot 10^{-10}$Torr. In some cases the pressure rose as high as $\sim 5.0 \cdot 10^{-9}$Torr. While the vacuum was allowed to recover between each measurement, after the first few pulse chains the base pressure was no longer attainable in a reasonable amount of time. Consequently, most of the measurements were made for a range of vacuum pressures from base to $\sim 9.0 \cdot 10^{-10}$Torr. This certainly had an effect on the measurements, although to what extent is unknown. To allow for the cleanest possible data samples the CAC was allowed to cool off and

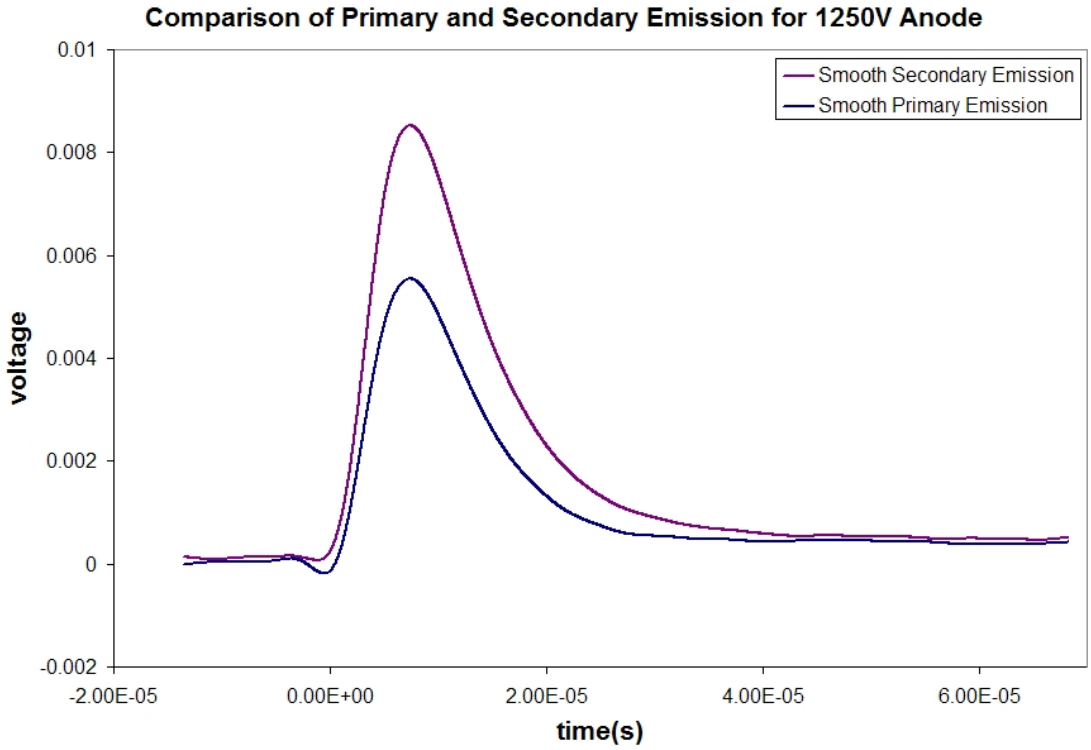

Figure 4.20: Primary and Secondary Emission from DAP - Here is seen a comparison of primary and secondary emission from a diamond amplified photocathode. Secondary emission amplification is clearly visible. Pulse energy is 2J, cathode voltage is -5KV, and anode voltage is 1.25KV. The primary charge is 12.13nC, and the secondary charge is 18.80nC. The resulting gain is $\sim$1.55 indicating an increase in secondary emission of 41.6 billion electrons.

pump down overnight.

The first data set is taken with a 20KΩ effective resistance in the measurement circuit. At this point the RF shielding has been applied to the CAC and an additional diamond window has been placed in the beam line to block DPE. Three sets of pulses were recorded at equivalent intervals for anode voltages from 1.5KV to 2.5KV in order to get a large scale picture of the gain over this range. After calculating the gain for each set of pulses,the result is plotted against the electric field in the diamond, as seen in Fig. 4.25. The uncertainty in gain is $\pm$6%, owing to uncertainties of $\pm$3% in both the primary and secondary charge. The three points in this series are fit to a line

with a slope of 0.389m/MV. For this linear fit, $\chi^2/\nu = 1.344 \cdot 10^{-3}$ with better than a 99% probability of exceeding this value[15]. Thus the gain is increasing linearly over this range in this data set.

After the initial run, it was decided that the second series would start at a lower voltage and smaller steps would be used to provide greater resolution. In addition to this change in technique, the primary and secondary emission signals suddenly appeared smaller than had previously been observed. In order to increase the measureable voltage, the system resistance was changed to 50KΩ. This series of data begins with an anode voltage of 101V and continues to 2KV. This corresponds to a final field in the diamond of approximately 0.7MV/m for diamond to anode separation of 500μm. This series is not nearly as coherent as the first run of data. To investigate the linearity of this set, a solid line was fit. The resulting least squares fit has a slope of 0.897m/MV, but $\chi^2 \cong 13$ which is significantly larger than the desired value of $\chi^2 \cong (N - m) = 8$, based on the number of degrees of freedom. It is obvious from Fig. 4.24 that this is not the best fit to the data. Still, this does show a basically linear increase in gain with increasing field. That only 50% of the measurements in this series are within the range of uncertainty for this linear fit indicates that the system is not behaving as intended. It is possible that the behavior seen here is due to the same phenomena that produced the fluctuations visible in Fig. 4.16 and in Fig. 4.10 around 2KV, only shifted due to some property of the diamond.

The final set was recorded after the system had been allowed to rest over night and return to base pressure. Also, the residual diamond background was characterized just before this set, during which time the DAP was exposed to a large number of 2Joule pulses. This set was recorded to fill out the last portion of the 2Joule gain vs. field series. A linear fit is applied to this data. The resulting fit has a slope of 0.477m/MV with a $\chi^2/\nu = 0.549$ corresponding to a 66% probability of a higher χ^2 value. Therefore, the values for gain collected in this electric field range rise linearly, but more data is needed to find the true rate of increase.

It is visible from the graphical data that each of the individual sets shows increasing gain as a function of anode voltage. While all of the data sets exhibit some linearity, only the first set has a good solid line fit to data, although this could be random when compared to the other data. The other sets exhibit fluctuations and spikes, but generally have a bulk increase in gain as the diamond electric field increases. Taken as a whole, the gain measurement over the entire range also exhibits this bulk increase. This demonstrates that gain grows as a function of field. The total number of measurements is taken as verification that amplification is occurring and that a functioning DAP has been produced.

4.11 Measurement of Closed Capsule

One of the goals of this experiment has been to demonstrate the closed capsule operation of a diamond amplified photocathode. Originally, the intent was to have a ring of indium wire attached to the DECA with which to seal the DAP injector. During the testing of photocathode emission, it was observed that the vacuum pressure rose by up to an order of magnitude throughout measurement(§4.8). A significant increase in pressure was also noted during diamond photoemission and gain measurements, although not as large as during photocathode-only operation. In early testing it was noted that photoemission output, especially for the photocathode, was highly dependent on chamber pressure. Should the system pressure increase too much, the photoemission is unmeasurable. In addition to the increases in pressure there is a strong possibility that electron induced gas desorption[16] from the metalization layer could poison the photocathode in a closed capsule. Desorption could also increase the intracapsule pressure to such a degree that now further measurements would be possible. Therefore, it was decided that sealing the capsule with indium wire would not be an optimal solution at this time. Leaving the capsule unsealed allows it to be reopened and pumped back down between measurements.

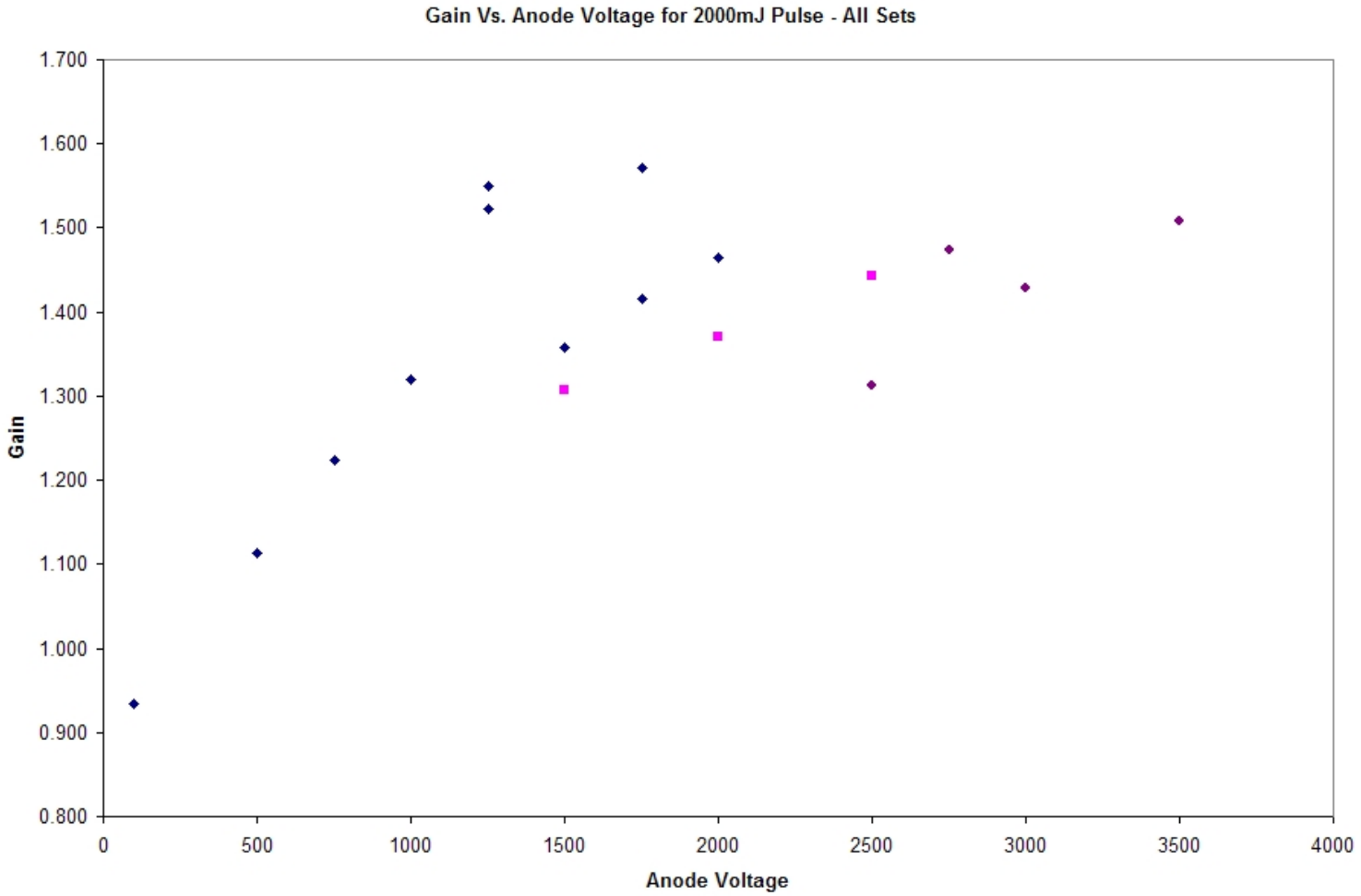

Figure 4.21: Gain vs. Anode Voltage for 2000mJ Pulse Energy - There is a clear trend, despite local fluctuations, toward increasing gain as the anode voltage increases.

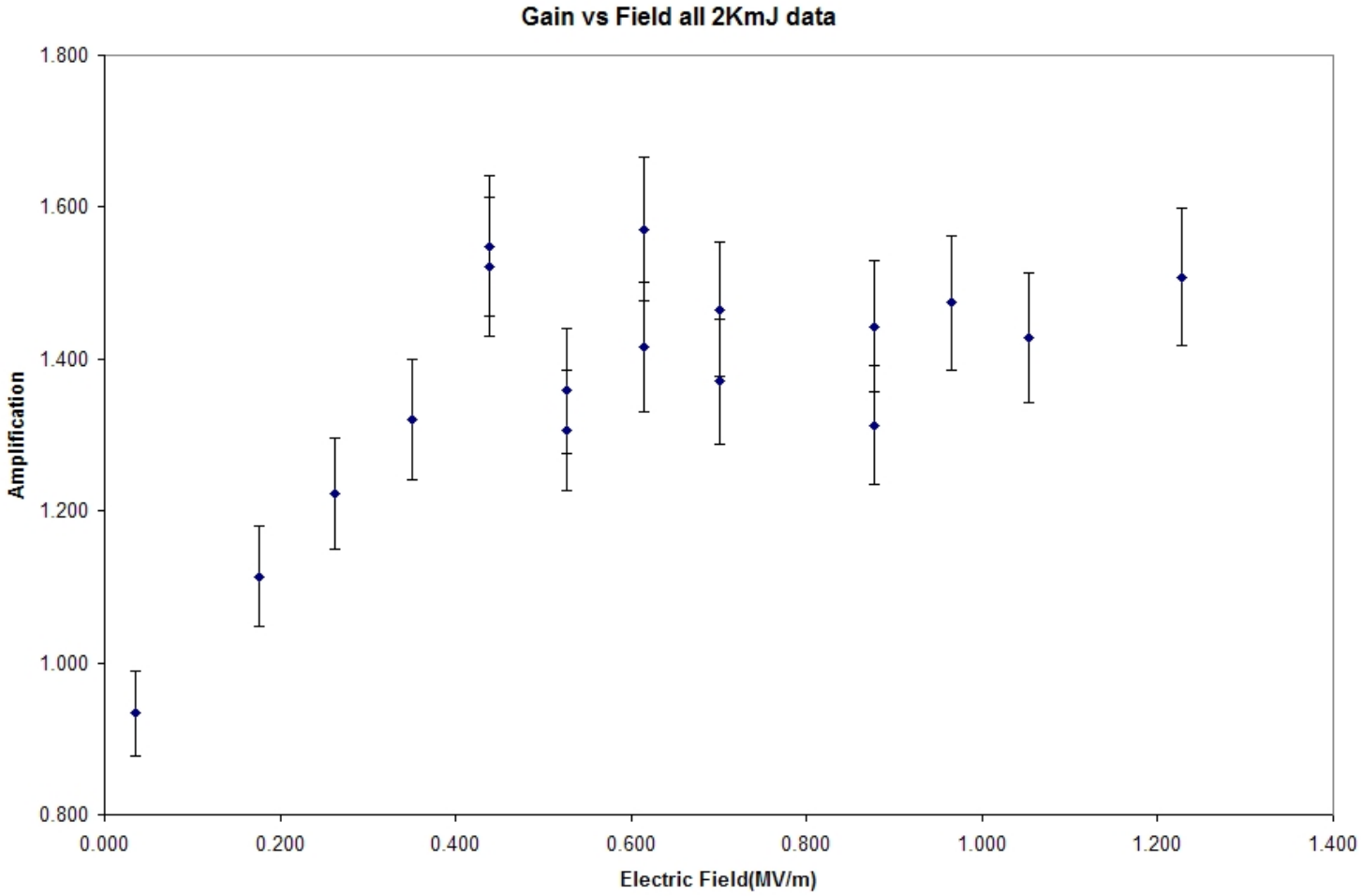

Figure 4.22: Gain vs. Electric Field in the Diamond for 2000mJ Pulse Energy - There is a clear trend, despite local fluctuations, toward increasing gain as the electric field in diamond increases. The error bars detail the $\pm 6\%$ uncertainty in calculated gain as propogated from measurements.

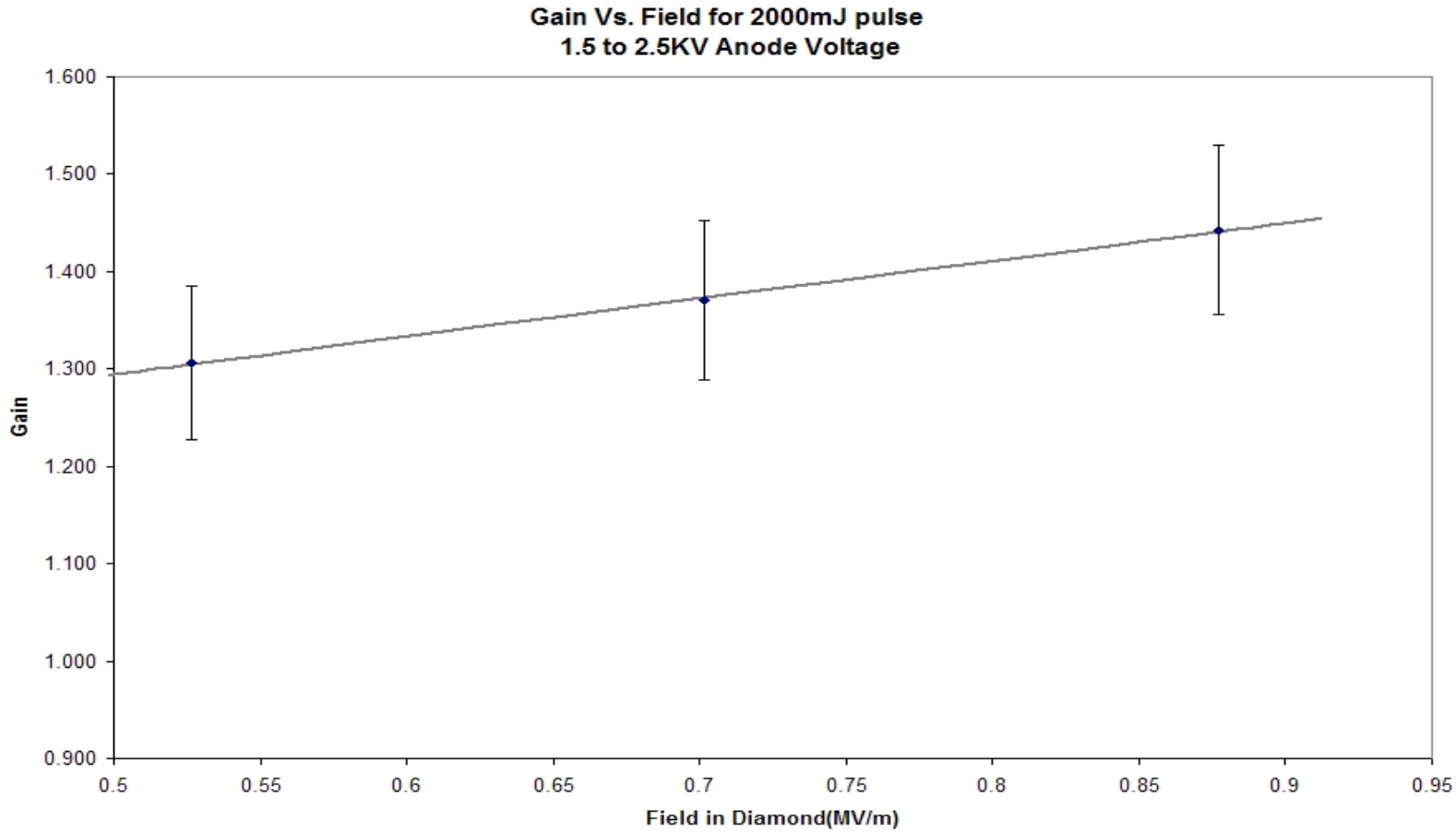

Figure 4.23: Gain vs. Field, Second Set - Gain vs. field for 2000mJ pulse energy. There is a marked trend of increasing gain as the field in diamond increases. This data set is the first recorded. It was measured using a 20KΩ effective resistance and consequently had to be converted for comparison of pulse charge. The resulting pulse charges for these measurements are significantly larger than the other data, but this has no effect on the gain calculation.

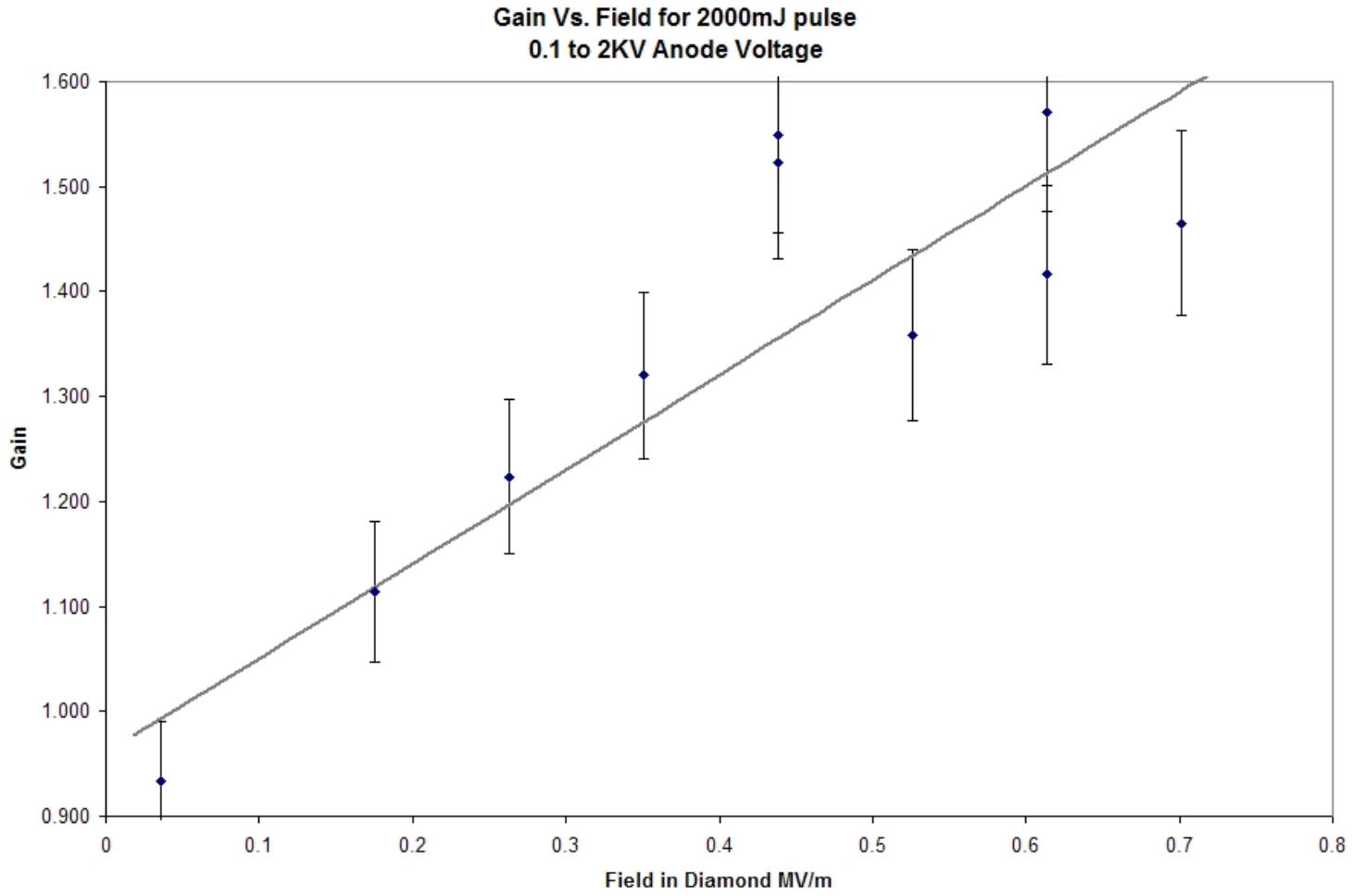

Figure 4.24: Gain vs. Field, First Set - Gain vs. field for 2000mJ pulse energy. This is the main data set. There is a marked trend of increasing gain as the field in diamond increases.

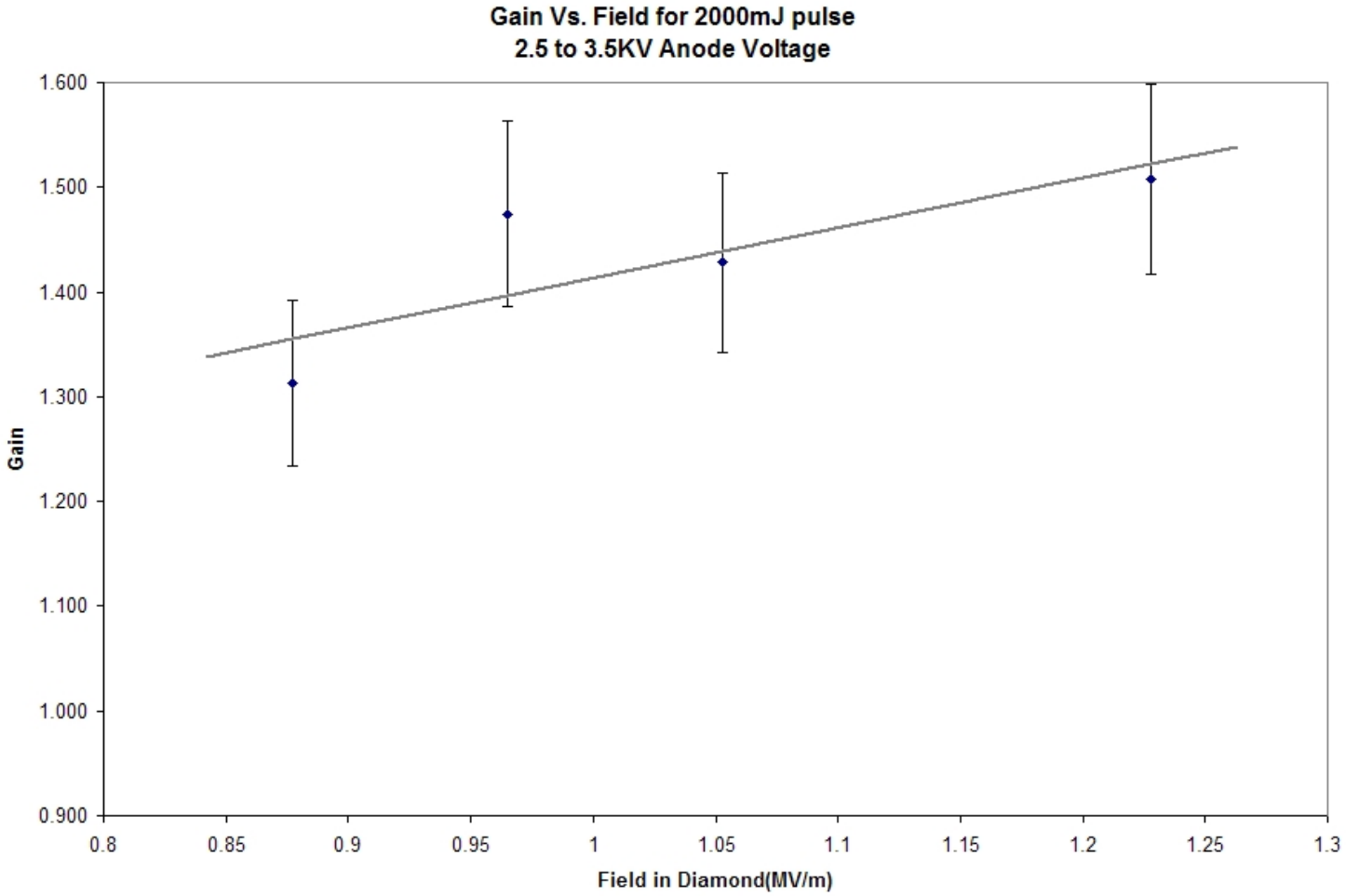

Figure 4.25: Gain vs. Field, Third Set - Gain vs. field for 2000mJ pulse energy. There is a marked trend of increasing gain as the field in diamond increases. The data in this set was recorded after the main data set with the system operated for other data collection tasks and allowed to idle over night.

To make a measurement with the closed capsule, the photocathode was lowered until it was in contact with the DECA as in Fig. 4.26. Once in this position, voltages were applied to the photocathode and anode. The anode was set to 1.25KV, since the best gain was obtained at that voltage during previous measurements(§4.10). The photocathode was set to 2.5KV to reduce the possibility of spontaneous arcing. The standard set of measurements, as in §4.9, with the light source set to deliver 3000mJ per pulse.

The results of this measurement are presented in Fig. 4.27. The capsule appears to be operating appropriately, as the signal has the same profile as other measurements. Clearly there is gain recorded in this measurement. The primary emission pulse charge in closed configuration is 12.80nC which produces a secondary amplified charge of 19.99nC. Therefore, the gain is $\frac{19.99}{12.80} = 1.56$.

Unfortunately, only one closed capsule measurement could be made before a malfunction caused the DAP to cease operation. After this point the DAP was no longer able to standoff the photocathode voltage required to energize the primary photoelectrons sufficiently to generate secondaries. Thus endeth the capsule measurements.

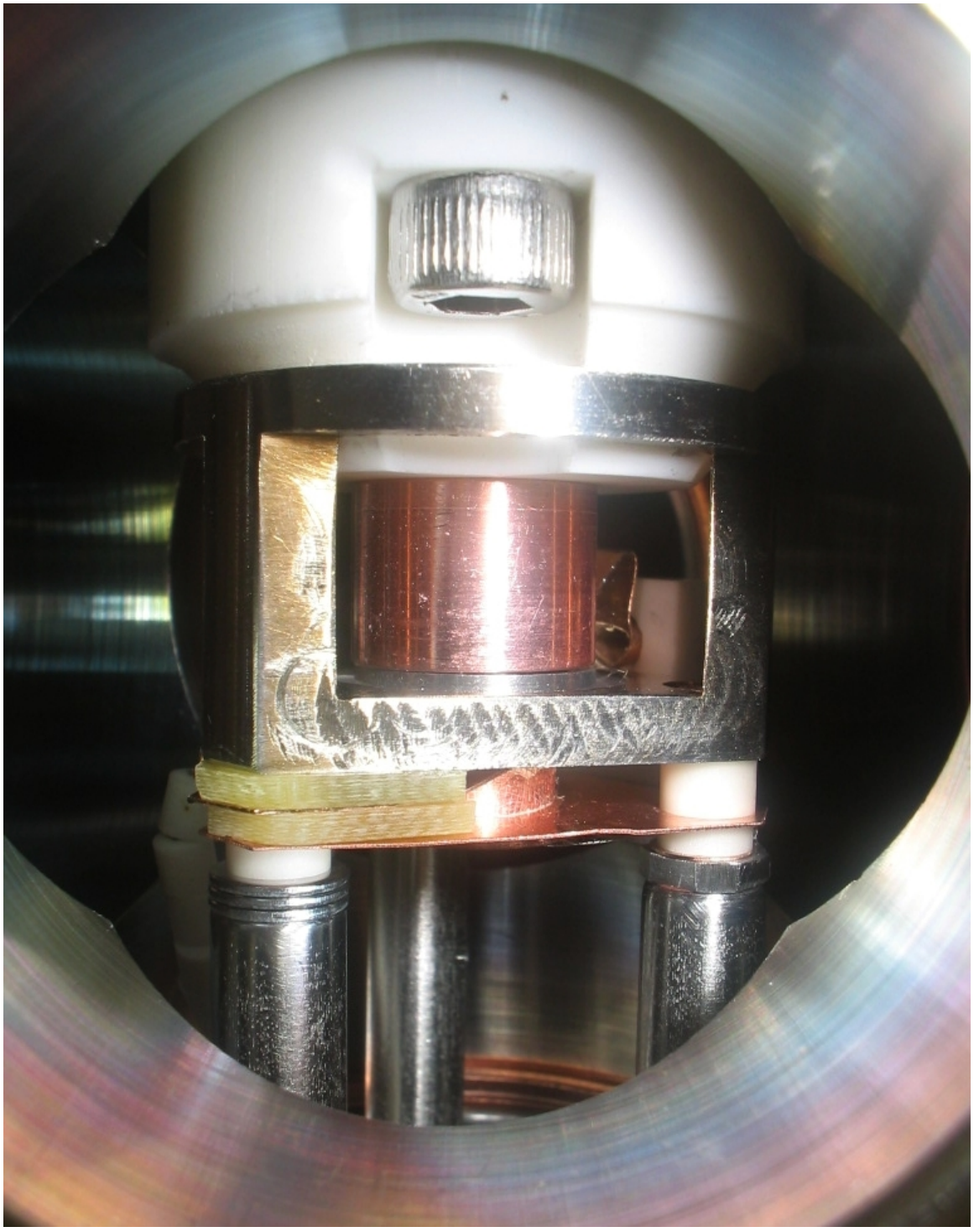

Figure 4.26: The DAP Injector Capsule in Closed Position - In this configuration the capsule is ready for measurement of secondary emission amplification.

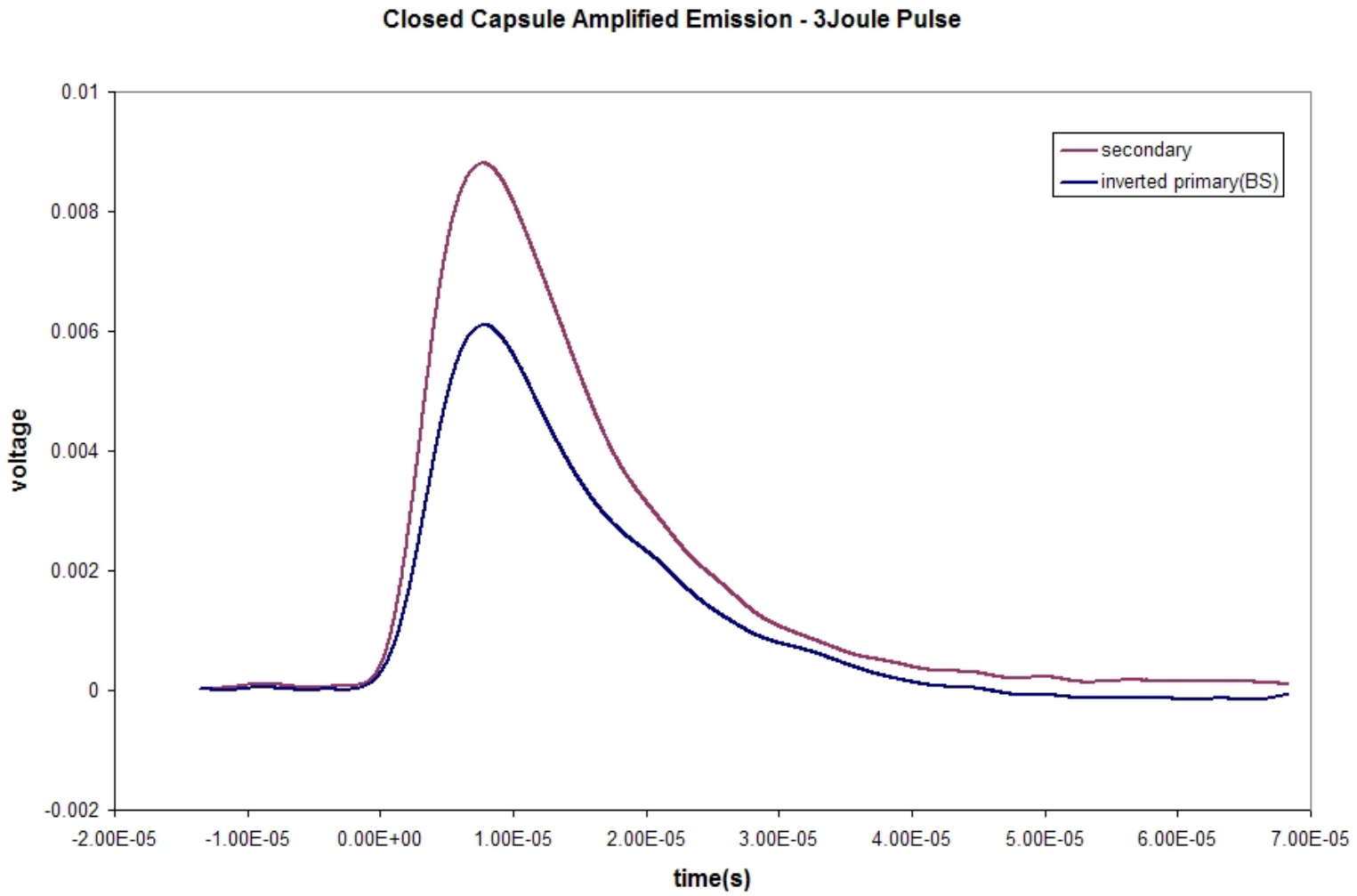

Figure 4.27: DAP Injector Capsule Closed-Emission - Here is a comparison of primary and secondary emission in a closed capsule. There is clearly amplification measured in the closed DAP Injector Capsule.

Chapter 5

Conclusion

The goal of this investigation has been the successful construction and operation of a prototype diamond amplified photocathode. This report details this accomplishment and the many steps required to reach this result. The primary focus of this chapter will be discussion of successful gain measurements and how the DAP may be improved in future investigations, as well as some possible sources of error in this work.

5.1 Gain from a DAP

As stated in §4.9, this is the first instance of the successful operation of a diamond amplified photocathode. A number of steps are taken to isolate the gain due to secondary emission. First, the primary photoemission from the photocathode is measured. Next, the diamond photoemission (DPE) and gain emission signal are measured. The signals recorded are the average over 16 pulses. Each of these signals is processed using a Savitzky-Golay algorithm to reduce the system noise without removing any of the pulse features. After smoothing, the EMI background is subtracted from the primary photoemission.

To isolate the gain electron signal, the DPE is subtracted from the gain emission signal. The secondary emission signal is constructed by adding the primary photoemission to the gain electron signal. The pulse charge for each of these signals is

then calculated from the integrated pulse voltage. The gain is found by dividing the secondary pulse charge(18.80nC) by the primary pulse charge(12.13nC). The resulting gain in the DAP from incident 5KeV primaries for a 1.25KV applied anode voltage is 1.55.

While the reported gain is smaller than expected, it is definitely large enough to be measurable above the system noise. It should also be noted that, since the signals used are the average over 16 pulses, the DAP is essentially operating in steady state condition. This is important because later iterations of the capsule will have to operate for long durations over many pulses.

5.1.1 Diamond Photoemission

While reductions in diamond photoemission have been achieved, the residual photoemission has a negative impact on secondary emission. With a voltage applied at the anode, and thereby an electric field in the diamond, the e-h pairs produced by the relevant UV in the light pulse are separated. The charges then drift toward their respective poles, all the while reducing the field in the diamond. This is a complicated, time evolving field reduction, but the bulk effect is to decrease the total secondary emission. To prevent this from occurring, all UV that causes photoemission in the diamond must be eradicated.

5.2 Increasing Gain with Anode Voltage

To show that the capsule is operating as desired, the gain is measured against increasing anode voltage, and thereby increasing field in the diamond. This is demonstrated in §4.10. From the aggregate data in this section we see that there is a bulk increase in the gain as the electric field increases. It is somewhat problematic that there appears to be a flattening in the gain once the anode voltage passes beyond approximately 1.5KV. However, this is not entirely unexpected.

In previous results by this group[14] the gain has been shown to asymptotically approach a maximum value. While those results demonstrate a steeper slope on the increasing gain and a higher maximum, they are for a thinner electronic diamond sample that has not been subjected to the same processing as this 300μm thick sample. Additionally, a more homogeneous energy spread is used in the incident electron beam.

A similar flattening has been reported by Isberg et al.[17] on a similar 160μm thick electronic grade sample operating in transmission mode. Their data is fit using the Hecht model, Eq. 5.1 to describe the charge transmitted through a biased semiconductor. While it appears that this may provide an explanation for behavior observed in the DAP as the electric field is increased, further analysis is required before this model can be accepted.

$$Q = N_0 e \frac{\mu\tau V}{D^2}[1 - \exp - \frac{D^2}{\mu\tau V}] \tag{5.1}$$

Although the shape of this curve is somewhat suspect, these measurements provide for some interesting observations about the operation of the DAP. The fact that gain is reported across the range of voltages demonstrates that the capsule is functioning in a repeatable fashion. The linearity in gain for anode potential less than 1000V indicates that there is a minimum field $\sim$0.095MV/m before amplification is observed. This suggests the magnitude of external applied field required to overcome any internal fields present in the diamond. Finally, the data suggests that a significant amount of charge collection is occurring. Were this not the case the gain would continue to increase well beyond the values reported. So we see that despite any issues with the shape of the gain vs. field data, the results of this measurement are informative.

5.3 Gain in a Closed Capsule

The final measurement of the DAP is intended to test the capsule operation in closed configuration. This is handled in the same fashion as all other measurements with the exception that the photocathode is in contact with the DECA. In this formation a primary pulse charge of 12.80nC is measured. The resulting secondary emission charge is 19.99nC. Therefore, we see a gain of 1.56 for the closed capsule.

This is, unfortunately, the only result for the closed capsule, as it ceased functioning after this measurement. The reasons for this failure are uncertain, but given the successful operation of the photocathode in other modes, further investigation along this line is unnecessary. This result will only further obviate the necessity of pumping internal to the capsule, a line of thought that was already growing in our group near the end of this exercise. This being the case, all other measurements demonstrate the successful operation of a DAP with the CAC taking the role of the self pumping capsule.

5.3.1 Anomalies in Closed capsule operation

Referring back to §4.11, the emission seen here is an interesting result because the photocathode voltage is only -2.5KV. Previous measurements of DAP secondary emission utilized -5KV photocathode voltage. Therefore, the primaries in this measurement only have 2.5KeV energy as opposed to 5KeV. The primary pulse charge of 12.80 is very close in value to those previously recorded, but the light pulse generating this photoemission is 50% larger than earlier measurements(§4.9 and §4.10). So the 2.5KeV primaries produce a gain of 1.56 that yields a 19.99nC secondary pulse. This means that, in this case the energy cost $\sim$1.6KeV per secondary, whereas in previous measurements it cost on the order of 3.3KeV per secondary.

The reason for this reduction in primary energy cost per secondary electron may have roots in surface electron trapping and photo-stimulated release of the trapped

electrons. Comparing primary and diamond emission for this measurement with those in §4.9, the ratio of 3J primaries to 2J primaries is ∼1.054 while the ratio of 3J to 2J diamond emission is ∼1.132. This accounts for only around 18% more photoemission when there are 50% more photons.

It is also possible that the QE of the photocathode has changed significantly over these few measurements. As demonstrated in §4.4 there were significant pressure increases during preliminary photoemission measurements. Should pressures of the magnitude reported, or greater, be trapped inside the capsule, the photocathodes QE would quickly be reduced to a base level. There is also more than anecdotal evidence for the occurrence of electron induced gas desorption in metals[16]. Any positive ions generated would be accelerated toward the photocathode and rapidly poison the QE.

5.4 Improvements

While the DAP has been shown to function, it is obvious from the data that these results are not commensurate with either predictions[1] or previous results[14]. This is largely due to the fact that the diamond used in this experiment has been subjected to much more extreme conditions than similar samples have seen, e.g. brazing. There are five immediate areas in which improvements would be of significant benefit. Three of these pertain directly to the capsule, the remaining two are with regard to the capsule assembly chamber.

In order to improve the secondary emission yield the order of assembly could be rearranged. In the current capsule the sample was etched, metalized, hydrogenated, and finally brazed. In §4.6 it was reported that the metalization layer had thinned during the braze. While this was beneficial to this experiment, it may not be in others. One suggested process would be to braze the sample, then metalize and hydrogenate. To test the efficacy of specific methods, identical samples should be manufactured using a different order of assembly for each. The resulting secondary

emission signatures would establish the best order of assembly.

Another method to improve secondary emission would be to refresh the hydrogenation after assembly. This would effectively replace hydrogen that has been desorped from the surface. Refreshing or reactivating is a simple procedure that is accomplished by repeating the hydrogenation step. This has proven effective in previous work[12]. A simple measurement of the sample's secondary emission pre- and post-reactivation would demonstrate the effect of this technique.

Perhaps the most visible defect in this capsule happens during the brazing step, Fig. 4.12. It is obvious that braze foil and metalization layer are incompatible. Or perhaps the problem is that they are too compatible. To reduce the braze flow–which is a problem new to this capsule–either the braze volume must be reduced or the ring dimensions must be changed. Both of these solutions should be effective, but the simpler to implement is the dimensional change. If the inner diameter of the ring were increased to 9mm while maintaining the relative outer diameter, all flow would be relegated to the space between the diamond and the Nb washer. Improvements to the braze flow would be visible to the naked eye when the sample emerged from the furnace.

As noted above, the remaining improvements pertain to the chamber itself. When comparing the data from this experiment to that presented in earlier work of this group[14], it is visible that higher fields in the diamond are needed to produce the desired magnitude of secondary emission. This is accomplished by repositioning the anode so that it is closer to the diamond. A reduction of separation to 100μm between the diamond and anode would lead to a 5x increase in the intra-diamond electric field. This would effectively bring these measurements in line with the previous data and and allow them to be used as a comparator.

Further improvements to the CAC would necessitate a complete redesign of the chamber. Some of the general elements that should be included are improved EMI shielding and grounding, enhanced electrical insulation, and improved wiring and

electrical contacts. Extra attention should be paid to photoemission from the anode-plate and other surfaces, including wires. If these improvements are implemented a significant increase in secondary emission should be noticed.

5.5 Further Research

There are many interesting questions that have arisen during this investigation. Two of which are of primary interest and should be investigated further. A brief discussion of each follows.

It has been suggested that electrons trapped in the diamond will be liberated by light of the appropriate wavelength. The result of this would be an increase in gain with increased pulse energy from the light source. While there is existing data on secondary emission with increasing pulse energy, there is no data on the associated diamond photoemission. It is possible to approximate the DPE based on other photoemission data. The better solution is to repeat the experiment and measure all the relevant parameters to determine whether or not secondary emission is enhanced by light incident on the diamond.

As mentioned in §5.2 the Hecht model may be a good fit to the recorded data. This should be investigated, not only for this data, but for multiple samples. If the Hecht model fits it may be possible to generate a model that allows for comparison of diamond amplified photocathodes based on charge collection distance. This would also allow for an in-line diagnostic to determine if the diamond is the source of failure in an inoperative capsule.

5.6 Closing

To conclude this report, the construction of a prototype diamond amplified photocathode has been demonstrated. This prototype has been successfully operated and gain has been measured repeatedly over a range of anode voltages. The nature of

these measurements demonstrates DC operation in a steady state for an extended period over a large number of pulses. Additionally, the total output of the DAP is in the range of many tens of nanoCoulombs per pulse, which is an order of magnitude larger than required for future applications. The device resulting from this investigation is clearly the first instance of a functioning diamond amplified photocathode.

Bibliography

[1] Diamond Amplifier For Photocathodes Rao, T., Ben-Zvi, I., Burrill, A., Chang, X.et al. AIP Conf. Proc. 737, pp. 178-190 (2004)

[2] Study of Secondary Emission Enhanced Photoinjector, X.Y. Chang, I. Ben-Zvi, A. Burrill, P.D.J. Johnson, J. Kewisch, T. Rao, Z. Segalov, Y. Zhao, Proceedings PAC05, 2711 - 2713, May 16-20 2005

[3] Measurement of the Secondary Emission Yield of a Thin Diamond Window in Transmission Mode, X.Y. Chang, I. Ben-Zvi, A. Burrill, S. Hulbert, P.D.J. Johnson, J. Kewisch, T. Rao, Z. Segalov, J. Smedley, Y. Zhao, Proceedings PAC05, 2251 - 2253, May 16-20 2005

[4] Diamond to Nb Brazing in a Vacuum Furnace - MSI Minor Project, Grimes, J. Stony Brook University (2006)

[5] Negative-electron-affinity effects on the diamond (100) surface, van der Weide, J., Zhang, Z., Baumann, P. K., Wensell, M. G., Bernholc, J., & Nemanich, R. J., Phys. Rev. B, 50, 5803 (1994)

[6] Space-charge-limited current density as a function of electron flow duration in an emissive diode, Girardeau-Montaut, J.-P., & Girardeau-Montaut, Journal of Applied Physics, 65, 2889 (1989)

[7] Insulator Seal Website, Copyright©2004 Insulator Seal
http://www.insulatorseal.com/searchs/doc/sapphireintro.htm

[8] Quantum efficiency and topography of heated and plasma-cleaned copper photocathode surfaces; Palmer, D., et. al. SLAC-PUB-11355 (2005)

[9] Newport Oriel Website, Copyright©1996-2007 Newport Corporation
http://www.newport.com/store

[10] Smoothing and Differentiation of Data by Simplified Least Squares Procedures. Savitzky, Abraham and Golay, M. J. E. Anal. Chem., 36, 8, 1627 - 1639, (1964)

[11] A Review of Photocathode Research, Palmer, D. ARDB Technical Notes Volume 4, SLAC-TN-05-080 (2004)

[12] Applications of Diamond Films to Photocathode Electron Guns and Accelerators Beetz, C. P. et. al. IEEE PAC 1991 ,1981

[13] CRC Handbook of Chemistry and Physics, (87th Edition), David R. Lide, ed., Taylor and Francis, Boca Raton, FL. (2007)

[14] Electron Amplification in Diamond J. Smedley, I. Ben-Zvi, A. Burrill, X. Chang, J. Grimes, T. Rao, Z. Segalov, and Q. Wu, AIP Conf. Proc. 877, 672 (2006)

[15] Bevington, P., Robinson K., Data Reduction and Error Analysis for the Physical Sciences - 3rd. Ed., McGraw-Hill, c. 2003

[16] Temperature dependence of the electron induced gas desorption yields on stainless steel, copper, and aluminum J. Gomez-Goni and A. G. Mathewson, J. Vac. Sci. Technol. A 15, 3093 (1997)

[17] Charge collection distance measurements in single and polycrystalline CVD diamond, Isberg J., Hammersberg J., Bernhoff H., Twitchen D.J., Whitehead A.J., Diamond and Related Materials, 13 (4-8), pp. 872-875. (2004)

Appendix A

List of Abbreviations

BSH	–	Braze Sample Holder
CAC	–	Capsule Assembly Chamber
DAP	–	Diamond Amplified Photocathode
DECA	–	Diamond Electrical Contact Assembly
DPE	–	Diamond Photo-Emission
EMI	–	Electro-Magnetic Interference
HF	–	High Frequency
HV	–	High Vacuum
OFC/OFHC	–	Oxygen Free Hard Copper
PC	–	Photo-Cathode
QE	–	Quantum Efficiency
RF	–	Radio Frequency
SCL	–	Space Charge Limit
UHV	–	Ultra-High Vacuum
UV	–	Ultra-Violet

Appendix B

Procedures for building DAP

Brazing

1. Braze sample holder.

    - A single cylindrical piece of 304 Stainless Steel that has a multi-tiered cup inside to accommodate all five elements of the braze process.

2. Sample loading.

    - The five elements are inserted into the sample holder in bottom up order: diamond, small Ticusil washer, Nb washer, Large Ticusil washer, Sapphire washer. Gravity holds everything in place.

    - Place the loaded sample holder on the furnace tongue and slide it gently into the furnace core.

3. Pump the furnace down to 10-8 (see brazing procedure sheet) and Run program 1 on the Mellen MT1300 furnace. Braze occurs at 900℃. –Program 1 consists of the following; an 4.25 h ramp to 870℃, a soak at 870℃ for 2 hours to allow the system to equilibrate, ramp to 935℃ for braze followed by 100℃/hr ramp to ambient temp.

Post Braze handling of DECA

The steps in this process are summarized below:

A. DECA characterized (Raman, x-ray)

B. DECA is inserted into etch sample holder and a gentle pressure of less than 1 psi is applied. Etch sample holder defends Nb, Sapphire, braze joints, and metalization layer during etch process.

C. Diamond surface is etched according to SOP.

D. Diamond surface hydrogenated.

E. DECA re-characterized (Raman,x-ray).

F. DECA stored under vacuum or Inserted into CAC.

Photocathode Recipe:

A. Machine OFC Copper according to drawing specifications.
The Cu Photocathode has a raised central diameter of approximately 9mm in diameter surrounded by a 0.5mm deep by 1mm wide semicircular groove. The outer edge of the cathode is slightly lower than the central diameter.

B. Clean copper with Acetic acid 5% to remove oxides

C. Polish copper photocathode according to Nb cathode preparation procedure.

D. Ultrasonically clean copper photocathode in Hexane for 20 minutes.

E. Blow-dry with dry nitrogen.

F. Alternate preparations
– Cover the central diameter with a mask and sputter gold into the groove.
or
– Clean polished Photocathode with Acetic acid 5% to remove oxides.

G. Apply indium wire -previously cleaned in 5-10% hydrochloric acid-to groove.

H. Heat cathode and indium assembly to indium melting point under 10^{-6} scale pressure in vacuum furnace. Anneal for two hours to allow for wetting and adhesion. (Note: metalization of Cu with Pt might increase adherence and decrease migration and resulting brittleness between Cu and In)

I. Attach photocathode to insulator on linear translator and quickly close system and start pumping down.

Capsule Assembly and Testing

Required Equipment:

Xenon Flash Lamp: Lamp and its power supply are commercial equipment.

UV rated quartz optics: for bringing light into vacuum chamber.

Vacuum Chamber: UHV chamber comprised of standard flange ports and standard ion pump. The standard power supply for the ion pump is 5kV.

Oscilloscope: Standard oscilloscope for signal measurement.

Cathode Charging: DC high voltage power supply for anode: standard 5kV, 5mA DC power supply which is commercially purchased.

Anode Charging: DC high voltage power supply for anode: standard 5kV, 5mA DC power supply which is commercially purchased.

Procedure:
Start-up: Make sure to use PPE where appropriate; UV goggles, long sleeve shirt, pants.

1. Load photocathode and DECA samples onto appropriate holders and insert into chamber.
2. Check all seals. Make sure system has appropriate electrical grounding.
3. Pump down Capsule Assembly Chamber: Make sure all valves are open and start turbo pump.
4. Bake Chamber (if needed): Turn on Variacs. Make sure temperature does not exceed 150℃. Allow system to cool before proceeding.
5. Start Ion Pump: Check to make sure pressure at turbo is less than 10 micro-Torr. Close all-metal valve to isolate CAC. Turn on cold cathode gauge. Wait for system to reach minimum 10 nano-Torr pressure or better before proceeding.
6. Adjust photocathode position to within 0.5mm of DECA.
7. Turn on DC power supply to Cathode: Check cables and connections. Watch vacuum levels.
8. Turn on Xenon flash lamp: Set pulse energy and repetition rate on lamp power supply.
9. Collect data from the oscilloscope.

10. Close capsule: Stop flash lamp. Reduce DC voltage to cathode before creating seal then return it to previous level.

11. Turn on DC power supply to Anode: Check cables and connections. Watch vacuum levels. Restart flash lamp.

12. Collect data from the oscilloscope.

Shut-down:

1. Turn off flash lamp.

2. Reduce voltages to zero on anode and cathode and turn off power supplies.

3. Turn off oscilloscope.

4. Clean up experimental area.

Opening system:

1. Make sure complete shut-down procedure has been performed.

2. Disconnect all electrical cables except grounding cables.

3. Turn off Cold Cathode Gauge

4. Turn off Ion pump.

5. Open all-metal valve to turbo pump: Make sure turbo pump is on and system is under vacuum on other side of valve.

6. Connect dry nitrogen hose.

7. Open nitrogen cylinder: Adjust regulator flow until 1 psi pop-it valve is barely rattling.

8. Turn off turbo pump.

9. Close nitrogen cylinder once system is purged.

Appendix C

Surface Preparation of Niobium/Copper for High Photoelectron Yield

Super conducting RF injectors are highly sought after for high brightness, high duty factor electron sources to be used in Free Electron Lasers and for electron cooling of ions. The major hurdle in its development is the lack of a suitable photocathode that has high quantum efficiency, long life time and compatible with the superconductivity of the injector. Cs_2Te and Nb have been the materials tested for this application. So far the quantum efficiency (QE) of Nb was found to be too low to be used in this application. They have invented a surface preparation technique that has increased the QE from 10-6 to 10-3. This makes the construction of superconducting RF injectors with Nb as the photocathode material highly feasible. Surface Preparation: This procedure is highly suitable for flat surfaces and can be modified for curved surfaces. The following procedure will assume a flat surface for illustration.

1. Nb surface is chemically etched and cleaned as per the surface preparation for superconducting Nb (prior technology)

2. Any deviation from the flat surface, caused by the etching process is corrected using Buehler Microcut 800 grit abrasive paper (# 30-5528-800-100) on a Buehler Ecomet 5 polisher/grinder at a speed of 120 rpm and a pressure of 4 lb. for 2 min

3. Fine scratches on the surface are removed and surface flatness ensured by the following procedure:

    a The cathode was mounted on a chuck that holds it in a three point design, with other two points formed by flat " diameter stainless steel rods.

    b The three points are adjusted so that all the three surfaces are accurately leveled.

    c Surface scratches are removed by polishing the Nb surface using Buehler Microcut 600 grit paper (part number 30-5519-600-100) and Buehler Metadi fluid polishing extender (part number 40-6032)

4. The rest of the surface preparation is done using a double platen, Buehler Ecomet 5 polisher/Grinder (part No. 49-1785-160) with Automet 2 power head (Part No. 60-1950-160) and Buehler Mastertex (part No. 40-7738) polishing cloth. One of the platens and associated work station is reserved for the final polishing with 1 micron diamond polishing compound and hence kept covered to avoid contamination, while the other platen and the workstation was used for 9 and 6 micron polishing compound. The polishing cloth is attached to the platen rotating at 120 rpm. Buehler Metadi 9 micron diamond suspension (part no. 40-6543 oil base) is sprayed on the polishing cloth to soak it so that liquid is pooled on the cloth. The Automet 2 is set for a polishing time to 90 sec and pressure of 3 lb. The cathode in its chuck fixture is attached to the Automet and lowered on to the platens. The Automet will automatically lift itself off the platen at the end of the set time.

5. Rinse the cathode and the fixture using Hexane. Wipe the polishing machine and other parts with an all-surface cleaner and rinse them off with water.

6. Repeat steps 4 and 5 with Buehler Metadi 6 micron diamond suspension (part no. 40-6542).

7. Switch over to the other head and work station.

8. Repeat step 4 using Buehler Metadi 1 micron diamond suspension (part no. 40-6540), but reduce the polishing time to 60 sec. Inspect the surface and repeat if necessary. Over polishing may introduce peeling of the surface.

9. Rinse the cathode completely with hexane.

10. Remove the cathode quickly from the fixture and immerse it in 100 ml of hexane in a small beaker.

11. Place the beaker in an ultrasonic cleaner for 20 minutes to remove embedded polishing material.

12. Remove the cathode from hexane, blow the surface with high purity nitrogen at 60 psig.

13. Transfer the cathode to vacuum chamber and pump the system. The time lapse between blowing the surface with nitrogen and starting the pump down should be kept minimum ($<$ 2 minutes)

14. When the background pressure is in low 10-7 to 10-8 bake the system at 100 C for 8-12 hours.

15. Irradiate the cathode with the laser for 45 minutes. The laser energy = 0.6 mJ, wavelength = 266 nm, pulse duration = 12 ps, spot size on the cathode 1 mm diameter 16. The laser energy and spot size will have to be adjusted to yield the high QE without damaging the surface.